

---

Masters Theses

Student Theses and Dissertations

---

Summer 2013

## Effect of mix parameters on longevity of bituminous mixtures

Clayton Reichle

Follow this and additional works at: [https://scholarsmine.mst.edu/masters\\_theses](https://scholarsmine.mst.edu/masters_theses)



Part of the [Civil Engineering Commons](#)

Department:

---

### Recommended Citation

Reichle, Clayton, "Effect of mix parameters on longevity of bituminous mixtures" (2013). *Masters Theses*. 5393.

[https://scholarsmine.mst.edu/masters\\_theses/5393](https://scholarsmine.mst.edu/masters_theses/5393)

This thesis is brought to you by Scholars' Mine, a service of the Missouri S&T Library and Learning Resources. This work is protected by U. S. Copyright Law. Unauthorized use including reproduction for redistribution requires the permission of the copyright holder. For more information, please contact [scholarsmine@mst.edu](mailto:scholarsmine@mst.edu).



EFFECT OF MIX PARAMETERS ON

LONGEVITY OF BITUMINOUS MIXTURES

by

CLAYTON MATTHEW REICHLE

A THESIS

Presented to the Faculty of the Graduate School of the  
MISSOURI UNIVERSITY OF SCIENCE AND TECHNOLOGY

In Partial Fulfillment of the Requirements for the Degree

MASTER OF SCIENCE IN CIVIL ENGINEERING

2013

Approved by

David N. Richardson, Advisor  
Jeffery S. Volz  
Demitri Feys



## ABSTRACT

This study was performed to evaluate the effects of varying aggregate sources, aggregate gradations on the stripping and rutting potential of bituminous based plant mixes specified by the Missouri Department of Transportation. The different aggregate combinations included two different aggregate sources (Potosi Dolomite and Jefferson City Dolomite) including two variations for the Jefferson City Dolomite mix to simulate a marginally in-specification mix and an out-of-specification but in-field tolerance mix. The “field” mix simulated the marginal mix where field tolerance of high dust and low binder content were maximized. All three mixes were evaluated for stripping susceptibility using the Tensile Strength Ratio (TSR) test and the Hamburg Wheel Tracking Device (HWTB). The mix characteristics (unit weight, effective binder content, and air voids) were used for a Level 3 analysis in the Mechanistic-Empirical Pavement Design Guide (MEPDG) to determine long term pavement distress conditions such as fatigue cracking, rutting, and IRI (smoothness).

The Potosi mix exhibited the best resistance to rutting and stripping during both the TSR testing as well as the Hamburg testing. The Jefferson City In-Spec and Out-of-Spec mixes showed less resistance to rutting and stripping in order, respectively. This was expected for the Jefferson City mixes where the aggregate was of lower quality (higher Los Angeles Abrasion, Micro Deval loss, absorption, and deleterious materials). Also, in the case of the Jefferson City Out-of-Spec mix, the binder content was lower. Upon evaluating the mixes using the MEPDG software, it was shown that mix characteristics such as air voids, VMA, and VFA influenced the fatigue cracking, rutting, and IRI predictions to a minor degree.

## ACKNOWLEDGMENTS

Thanks to the staff in the civil engineering building for solving some technical issues with the laboratory equipment.

Thanks to my fellow civil graduate students that kept me sane when testing in the laboratory wasn't always going the way I hoped.

Thanks to Brittany Coppedge and Brandon Wolk for their helping hands when extra material needed to be shaken during a time crunch.

Thanks to Mike Lusher for always answering any questions I had, whether they were big or small, and for the wealth of knowledge when it came to test procedures.

Thanks to Dr. Richardson for giving me the opportunity to have a deeper understanding of asphalt mixtures, for taking the time to ponder my dilemmas in the lab, analyzing my data, and most importantly, taking the time to read and edit this thesis.

Thanks to Dr. Volz and Dr. Feys for serving on the research committee for this research.

Finally, thanks to my family who has always been there to support me and encourage throughout my entire college career.

## TABLE OF CONTENTS

	Page
ABSTRACT.....	iii
ACKNOWLEDGMENTS .....	iv
LIST OF ILLUSTRATIONS.....	ix
LIST OF TABLES.....	xii
<b>SECTION</b>	
1. INTRODUCTION.....	1
1.1. STATEMENT OF PROBLEM.....	1
1.2. OBJECTIVES.....	1
1.3. SCOPE OF INVESTIGATION .....	1
2. REVIEW OF LITERATURE.....	3
2.1. RUTTING.....	3
2.1.1. Causes of Rutting. ....	3
2.1.2. Rutting Prediction.....	3
2.1.2.1 APA.....	4
2.1.2.2 Hamburg. ....	5
2.1.2.3 MEPDG.....	6
2.2. STRIPPING .....	7
2.2.1. Causes of Stripping. ....	7
2.2.2. Stripping Prediction.....	8
2.2.2.1 TSR. ....	9
2.2.2.2 Hamburg. . .	9

2.3. MEPDG.....	11
2.3.1. General. ....	11
2.3.2. Rutting Prediction.....	13
2.3.3. Fatigue Cracking Prediction. ....	17
2.3.4. IRI Prediction.. ....	20
2.4. LITERATURE REVIEW SUMMARIES.....	22
3. LABORATORY INVESTIGATION.....	24
3.1. EXPERIMENTAL DESIGN .....	24
3.1.1. Mix Design. ....	24
3.1.2. Specimen Preparation.....	25
3.1.3. Replicates. ....	25
3.2. EQUIPMENT .....	26
3.2.1. Washing of the Aggregate.....	26
3.2.2. Drying Oven. ....	26
3.2.3. Aggregate Specific Gravity and Absorption. ....	27
3.2.4. Mix Specific Gravity.....	29
3.2.5. Gradation. ....	32
3.2.6. Gyrotory Compaction. ....	32
3.2.7. Marshall Compaction. ....	33
3.2.8. Tensile Strength Ratio.....	35
3.2.9. Specimen Coring. ....	36
3.2.10. Specimen Sawing. ....	37
3.2.11. APA.....	38



3.2.12. AMPT.....	40
3.3. MATERIALS.....	44
3.3.1. Aggregate. ....	44
3.3.2. Binder. ....	50
3.4. TEST PROCEDURES .....	51
3.4.1. Aggregate Preparation.....	51
3.4.2. Aggregate Specific Gravity and Absorption. ....	51
3.4.3. Mix Specific Gravity. ....	53
3.4.4. Gyratory Compaction. ....	57
3.4.5. Marshall Compaction. ....	59
3.4.6. Tensile Strength Ratio. ....	62
3.4.7. Specimen Coring. ....	65
3.4.8. Specimen Sawing.. ....	65
3.4.9. APA – Hamburg.....	65
3.4.10. AMPT.....	69
4. RESULTS AND DISCUSSION .....	74
4.1. MIX DEVELOPMENT.....	74
4.2. MIX DESIGN.....	75
4.3. SPECIMEN PAIRING.....	77
4.4. RUTTING.....	78
4.5. STRIPPING.....	81
4.6. MEPDG.....	90
4.7. AMPT.....	97

5. SUMMARY AND CONCLUSIONS.....	102
5.1. SUMMARY .....	102
5.2. CONCLUSIONS.....	102
5.2.1. Hamburg.....	102
5.2.2. TSR. ....	103
5.2.3. MEPDG.....	104
5.2.4. AMPT.....	105
5.2.5. Correlations. ....	105
6. RECOMMENDATIONS .....	107
7. FUTURE RESEARCH.....	108
APPENDICES	
A. MIX DEVELOPMENT TABLES.....	109
B. TEST PROCEDURES.....	113
BIBLIOGRAPHY.....	199
VITA.....	203

## LIST OF ILLUSTRATIONS

	Page
Figure 3.1 - Aggregate Washing Table.....	26
Figure 3.2 - Grieve Oven .....	27
Figure 3.3 - Fine Aggregate Specific Gravity and Absorption Setup.....	28
Figure 3.4 - Coarse Aggregate Specific Gravity and Absorption Setup.....	28
Figure 3.5 - Pycnometer; Cooling Pan and Fan .....	29
Figure 3.6 - Vacuum Setup .....	29
Figure 3.7 - Specific Gravity Weigh-Below Setup.....	30
Figure 3.8 - Corelok Vacuum Chamber.....	31
Figure 3.9 - CoreDry Rapid Vacuum Drying Machine .....	31
Figure 3.10 - Standard 12 in. Sieves .....	32
Figure 3.11 - Pine Gyrotory Compactor .....	33
Figure 3.12 - Marshall Bottom Plate, Forming Mold, and Top Collar.....	34
Figure 3.13 - Marshall 10 lb Hammer and Heating Plate .....	34
Figure 3.14 - Marshall Puck Extruder.....	35
Figure 3.15 - Indirect Tensile Strength Apparatus.....	36
Figure 3.16 - Milwaukee Dymodrill Coring Drill .....	37
Figure 3.17 - Specimen Wet Saw .....	37
Figure 3.18 - Custom Built Cored Specimen Holder.....	38
Figure 3.19 - Asphalt Pavement Analyzer (APA) .....	39
Figure 3.20 - APA Rut Test Setup .....	40
Figure 3.21 - APA Hamburg Test Setup.....	40
Figure 3.22 - AMPT Test Chamber with Verification Apparatus .....	41
Figure 3.23 - Latex Wrapped Specimen for Flow Number Test .....	42
Figure 3.24 - Conditioning Chambers for AMPT Specimens .....	43
Figure 3.25 - Sper Scientific 4 Channel Data Logging Thermometer .....	43
Figure 3.26 - Potosi Dolomite Mix Gradation .....	48
Figure 3.27 - Jefferson City Dolomite In-Spec Mix Gradation .....	49
Figure 3.28 - Jefferson City Dolomite Out-of-Spec Mix Gradation.....	49

Figure 3.29 - Temperature-Viscosity Plot .....	50
Figure 3.30 - Standard 12 in Sieves .....	52
Figure 3.31 - Standard Roto-Sifter.....	52
Figure 3.32 - Vacuum System .....	53
Figure 3.33 - Specific Gravity Weigh-Below System .....	54
Figure 3.34 - CoreDry Vacuum Chamber.....	55
Figure 3.35 - CoreLok Vacuum Chamber .....	56
Figure 3.36 - Pine Gyrotory Compactor .....	59
Figure 3.37 - Marshall Bottom Plate, Forming Mold, and Top Collar .....	60
Figure 3.38 - Marshall Compaction Pedestal with Mold Secured in Place .....	60
Figure 3.39 - Marshall Compaction Hammer and Heating Plate.....	61
Figure 3.40 - Marshall Puck Extruder.....	62
Figure 3.41 - Vacuum Saturation Setup.....	63
Figure 3.42 - Water Bath for Conditioned Pucks .....	63
Figure 3.43 - Indirect Tensile Testing Apparatus .....	64
Figure 3.44 - APA Hamburg Test Specimens .....	66
Figure 3.45 - Hamburg Mold Plan View and Dimensions .....	66
Figure 3.46 - APA Hamburg Specimens on Sliding Tray .....	68
Figure 3.47 - APA Hamburg Specimens Submerged in Water .....	68
Figure 3.48 - APA Hamburg Results Chart .....	69
Figure 3.49 – Gauge Points Attached on Specimen Side .....	70
Figure 3.50 - Specimen Loaded Into Test Chamber with LVDTs Attached .....	70
Figure 3.51 - AMPT Dynamic Modulus Results Plot .....	71
Figure 3.52 - Specimen with Platens and Vacuum Collar with Latex Membrane .....	72
Figure 3.53 - Latex Membrane Installed Over Specimen and Platens .....	72
Figure 3.54 - AMPT Flow Number Results Plot .....	73
Figure 4.1 - PD-5 Hamburg Rutting Plot.....	79
Figure 4.2 – JCD-7 Hamburg Rutting Plot.....	80
Figure 4.3 – JCD-12 Hamburg Rutting Plot.....	81
Figure 4.4 - Typical Hamburg Plot with Labels .....	82
Figure 4.5 – PD-5 Hamburg SIP Plot .....	83

Figure 4.6 – JCD-7 Hamburg SIP Plot .....	83
Figure 4.7 – JCD-12 Hamburg SIP Plot - No SIP Present.....	85
Figure 4.8 – PD-5 Unconditioned Top/Conditioned Bottom.....	86
Figure 4.9 – JCD-7 Unconditioned Top/Conditioned Bottom.....	87
Figure 4.10 – JCD-12 Unconditioned Top/Conditioned Bottom.....	88
Figure 4.11 - TSR/Hamburg Data Correlation .....	89
Figure 4.12 - Fatigue Cracking - Years vs. VFA.....	91
Figure 4.13 - Fatigue Cracking - Years vs. % Va.....	92
Figure 4.14 - Rutting - Years vs. VFA.....	94
Figure 4.15 - Rutting - Witczak E vs. Years.....	94
Figure 4.16 - IRI - Years vs. VFA .....	96
Figure 4.17 - IRI - Years vs. % Va .....	96
Figure 4.18 – PD-5 - 4°C .....	98
Figure 4.19 – PD-5 - 20°C .....	99
Figure 4.20 – PD-5 - 40°C .....	100
Figure 4.21 – PD-5 AMPT Summary Plot.....	101

## LIST OF TABLES

	Page
Table 3.1 - Specific Gravity and Absorption Data .....	44
Table 3.2 - Jefferson City Dolomite Gradations .....	45
Table 3.3 - Potosi Dolomite Gradations .....	45
Table 3.4 - Potosi Dolomite Mix Gradation (PD-5) .....	47
Table 3.5 - Jeff City Dolomite In-Spec Gradation (JCD-7).....	47
Table 3.6 - Jeff City Dolomite Out-of-Spec Gradation (JCD-12) .....	48
Table 3.7- AMPT Dynamic Modulus Test Temps and Frequencies .....	71
Table 3.8 - AMPT Flow Number Recommended Parameters .....	73
Table 4.1 – Final Mix Properties .....	77
Table 4.2 - Hamburg Rutting Summary Data.....	81
Table 4.3 - Hamburg SIP Summary Data .....	85
Table 4.4 - TSR Summary Data.....	89
Table 4.5 - MEPDG Sensitivity Summary .....	97
Table 4.6 - AMPT Summary Data .....	97

# 1. INTRODUCTION

## 1.1. STATEMENT OF PROBLEM

Testing asphalt mixes for rutting and moisture susceptibility is done to evaluate the mix properties for short term and long term performance. Data from physical testing, such as Tensile Strength Ratio and Hamburg Wheel Tracking testing, and mix characteristics are used in the Mechanistic-Empirical Pavement Design Guide (MEPDG) software to evaluate long term characteristics of a mix. The outputs generated by the software can show distress values, types, and approximate the life cycle of the pavement.

## 1.2. OBJECTIVES

The Missouri University of Science and Technology (MS&T) has contracted with the Missouri Department of Transportation (MoDOT) to create methods of selecting appropriate maintenance and rehabilitation treatments of distressed pavements. As part of this study, various maintenance hot mixes are to be evaluated to determine their mix characteristics. The objective of this study is to examine the rutting and moisture susceptibility of BP-1 mixes at several levels of quality. Using mix parameters generated during mix design, and results of Asphalt Mixture Performance Tester (AMPT), the long term predictions generated by the MEPDG software are to be evaluated.

## 1.3. SCOPE OF INVESTIGATION

This project will evaluate the rutting and stripping susceptibility of three MoDOT BP mixes and the long term predictions of distresses using the MEPDG software. The high quality mix, meeting MoDOT Section 401 and 1004 specifications, will be the Potosi In-Spec mix. The lower quality mix that barely meets the MoDOT Section 401 and 1004 specifications will be the Jefferson City In-Spec mix. The Jefferson City Out-of-Spec mix will be the lowest quality mix that does not meet MoDOT Section 401 design mix specifications but does meet in-field tolerances. For both Jefferson City mixes, shale will added to some fractions of the mix gradation (See Section 3.4.4). What constitutes an Out-of-Spec mix will be the excessive levels of dust along with the addition on montmorillonite clay to the dust fraction.

With the mix designs complete, specimens will be made for testing in the Hamburg Wheel Tracking Device to simulate accelerated load testing and induce rutting and stripping stripping of the mixes. Along with Hamburg testing, Tensile Strength Ratio (TSR) specimens will be made to simulate accelerated moisture exposure to the mix and evaluate the loss of strength due to stripping.

The three mixes will also be evaluated for long term performance using the MEPDG software. With the mix parameters entered into the software, the base and subbase selected, the location selected, ADTT estimated, and the design life selected, the three mixes will be evaluated for fatigue cracking, rutting, and smoothness (IRI) over their selected design lives.

Also, the Asphalt Mixture Performance Tester (AMPT) was to be used to determine the dynamic modulus for all three mixes. By applying loads at different frequencies and temperatures, the dynamic modulus can be computed. This mix specific property can then be entered into the MEPDG software to make long term distress predictions of the mixes. However, due to the unavailability of the AMPT equipment from equipment failure issues, AMPT testing was not completed.



## 2. REVIEW OF LITERATURE

### 2.1. RUTTING

Rutting is defined as the permanent deformation of the HMA and/or the underlying base or subbase caused by repeated traffic loads (Brown et al., 2009). Rutting can be classified into two types; plastic and consolidation rutting. With excessive rutting, the expected life of the pavement will decrease and the overall roughness of the pavement increases.

**2.1.1. Causes of Rutting.** With both plastic and consolidation rutting identified, it is important to understand the causes of both types. Plastic rutting can be caused by high traffic loads, slow moving traffic, low speeds, or excessively high temperatures. Plastic rutting can also be caused by over-asphalting mix. By over-asphalting the mix, the traffic loads are supported by the asphalt cement rather than the aggregate. With the excessive amount of cement, the internal friction is lost and lateral plastic flow results. With the potential of plastic rutting due to high temperatures, the stiffness of the asphalt cement is very important. Choosing the correct upper performance graded (PG) number, along with correct air void system, and avoiding the hump in the gradation curve around the #30 sieve can help prevent plastic rutting. Unlike plastic rutting, consolidation rutting is generally caused by a combination of excessively high air voids after compaction. When excessively high air voids are combined with traffic loads, the kneading action of the wheels cause the mix to consolidate. Another factor in contributing to both types of rutting is the shape of the aggregate in the HMA mix. If the amount of rounded aggregate used is excessive, the locking interaction of the aggregate is reduced, transferring more of the traffic load to the asphalt cement.

**2.1.2. Rutting Prediction.** Many studies have been performed to identify methods to predict the rutting potential of HMA mixes accurately and easily. Through these studies the methods have been both software based, such as the Mechanistic-Empirical Pavement Design Guide (MEPDG), and laboratory based, such as the Asphalt

Pavement Analyzer (APA), French Rutting Tester (FRT), and the Hamburg Wheel Tracking Device (HWDT).

**2.1.2.1 APA.** With any HMA design, steps are taken to eliminate rutting issues. Many of these steps are taken before the pavement has been physically developed and created. With the advent of new testing equipment, such as the APA, researchers and engineers have begun to rely on allowable design thresholds and laboratory testing to predict field performance of HMA pavements. Kandhal and Mallick (1999) evaluated the potential of the APA to predict rutting of HMA. Three different aggregates along with three different gradations for each aggregate were tested to see if APA rutting results would correlate with field performance and if the APA results were sensitive to aggregate type and gradation. The three aggregates tested were limestone, granite, and gravel with gradations passing above, through, and below the restricted zone (abbreviated ARZ, TRZ, and BRZ, respectively). With the variance in gradations, the stability of the mix was altered. With these factors in mind, the study was able to distinguish that the APA results would be sensitive to these variations. It was found that in most cases, the mixes with the BRZ gradation showed the least amount of rutting, whereas mixes with ARZ gradation showed the highest amount of rutting; mixes with TRZ gradation showed either higher or similar rutting as mixes with gradation BRZ. After reviewing the APA and field results, it was concluded that the APA could correlate with field performance but further testing would be required due to the varying age of field test sections, which allowed the test sections to be subjected to different amounts of ESALs.

According to Choubane et al. (1998), laboratory results were compared to field performance of previously constructed roadways with known levels of rutting. Both the gyratory and beam specimens accurately ranked the mixes according to their field performance. The variability of test results within the three test locations and two test samples for each location in the APA machine was also evaluated. After testing both gyratory and beam samples, it was concluded that variability in tests results was present, not only in the three test locations in the APA (left, center, and right) but also within the two different test locations (gyratory samples; front and back positions). A paired-

difference experiment was conducted to further determine the significance level of the observed differences among the testing locations and test samples. The results from this experiment indicated that the variability of test results was significant and that the APA testing setup may not be completely effective. Further testing would need to be done to isolate the cause of variability, whether it is mix related or machine loading related (Choubane et al., 1998).

Goh and You (2009) evaluated a mix containing 15% RAP for rutting potential using the APA; results were compared to a control mix containing no RAP. It was concluded that mixes containing 15% RAP significantly reduced the rut depth by 24%, on average, when compared to the control mix. This was expected due to the higher mix stiffness achieved using RAP, which contains aged binder.

**2.1.2.2 Hamburg.** The Hamburg Wheel Tracking Device (HWT), originally developed in the 1970s by Esso A.G. of Hamburg Germany, measures the combined effects of moisture and rutting damage by rolling a steel wheel across a compacted asphalt specimen submerged in hot water (Hamburg, 2011). Beginning in the 1970s improvements have been made to the original HWT device, and even Pavement Technology Incorporated (PTI) has also incorporated its own HWT system into the APA. Not all test methods produce results that correlate with field performance of a HMA mix. With the use of HWT becoming more popular, research into the comparison of test results to field performance of mixes has increased. In a project conducted in cooperation with the Texas Department of Transportation and the Federal Highway Administration, the correlation of field performance to HWT testing results was evaluated (Yildirim et al., 2006). Three mix designs and three separate mixes were evaluated in the laboratory through HWT testing and a road test section. Samples for all nine combinations were tested using the HWT and the results indicated no stripping inflection point (SIP) present. This indicates that all mixes should not be prone to rutting throughout the pavement life. Next the road test sections were constructed and observed over throughout the duration of the project. Over a period of three years, no significant rutting was visually detected or detected by the profilometer. In all test sections, the

rutting measured less than 2.5 mm, despite the high traffic load applied to the pavement. With no significant rutting present in both laboratory specimens and field sections tested, it was concluded that the HWTD can accurately predict field performance of HMA pavements.

**2.1.2.3 MEPDG.** The Mechanistic-Empirical Pavement Design Guide is software that is used in the design and analysis of new and rehabilitated pavement structures. Predictions of pavement behavior are estimated through calculations of pavement responses (stresses, strains, deflections) and the software uses those responses to compute incremental damage over time (MEPDG manual, 2008). However, it is important to compare the outputs from the MEPDG software, in the case of rutting, to the results from field performance of the mix being used. In one particular study by Azari et al. (2008), specimens were made and tested in an Accelerated Loading Facility (ALF) as part of a FHWA experiment. This consisted of constructing asphalt pavement lanes containing different HMA mixes as well as different thicknesses and testing them for rutting. Loose mix from the lanes was also collected, compacted, and tested for flow number and dynamic modulus of the mix. The dynamic modulus and flow number values were later used as Level 1 inputs (mix specific inputs generated by physical laboratory testing) for the MEPDG software. With these values, both a Level 1 and Level 3 (mix inputs automatically generated by global data models) analysis was performed to predict rutting in the HMA pavements. With prediction of rutting estimates available, the estimates could be compared to actual rutting measurements recorded from the field pavements. It was found that rutting predictions by Level 3 analysis with the software were generally higher than rutting measured on the ALF lanes but were not drastically different. However, rutting predictions by Level 1 analysis were significantly higher than both rutting measured on the ALF lanes and Level 3 predictions. It was determined that the cause of this drastic over-prediction was the stiffness prediction equation used in the Level 3 analysis by the software. Also, the over-prediction from the Level 1 analysis was due to the software using the NCHRP 1-37A permanent deformation model rather than using the dynamic modulus ( $E^*$ ) values found during the initial phase of loose mix testing.

Goh and You (2009) studied thirteen mixes with varying asphalt binder PG numbers. The mixes were tested for dynamic modulus values which were to be used as Level 1 inputs in the MEPDG software. The software was then used to predict rutting of pavements incorporating the thirteen different mixes over a period of two years. These predictions were then compared to field rutting performance data obtained by the Michigan Department of Transportation for each mix tested. The comparison showed that the MEPDG software over-predicted the rutting potential of each mix. However, the ranking values assigned based on field rutting and assigned by the MEPDG software were comparable. This indicated that the MEPDG software could in fact be applicable for use as a basic pavement design tool. It was concluded that further local calibration of the MEPDG software would be needed to obtain a more reliable prediction of rutting.

## 2.2. STRIPPING

Among many types of damage to flexible pavement, stripping is another common problem. Stripping can be defined as the weakening or eventual loss of the adhesive bond between the aggregate surface and the asphalt cement in the HMA mixture, usually in the presence of moisture (Brown et al., 2009). Stripping is an issue that is found throughout the entire nation (Transportation, 2003). Understanding the causes of stripping allow mix designers to predict future stripping issues and incorporate techniques to prevent stripping of new pavements.

**2.2.1. Causes of Stripping.** As the name implies, the asphalt cement film is literally stripped from the aggregate. However, this may be the at the point of ultimate failure of the pavement. Other signs of distress, in the form of rutting, shoving, and/or raveling, usually occur first as an indication of an underlying cause (Putnam, 2006). The weakening of the aggregate/asphalt cement bond is usually gradual but it can be immediate depending on the severity of the available moisture at the pavement, type and use of the mix, asphalt cement properties, characteristics of the aggregate, traffic levels, construction practices, and the use of anti-strip additives. The particular climate the pavement is exposed to can greatly affect the potential of stripping. For example, in a Northwestern climate such as the state of Washington where the environment is typically

wet throughout the year, the stripping potential solely based on climate is greater than in an environment found in Arizona. This issue can be alleviated through the type of mix used and the construction practices used. Developing a mix design that is not prone to stripping is done in several ways. The major factor is the type of aggregate chosen (mineralogy), which includes the use of good quality aggregates. Aggregates that do not have clay or dust coating on the surface provide a cleaner surface and promote the bond between the aggregate and the binder, thus providing more stability in the mix. During pavement design and construction, allowing a way for surface water to be removed from the pavement provides important protection to the pavement structure from water intrusion. However, subsurface moisture can also cause damage. By adding permeable bases on subbases, trapped moisture under the pavement can be removed before stripping effects can begin. A construction practice that plays an important role in stripping prevention is compaction of the asphalt mix. If the specified compaction is not achieved, this could result in a high percentage of air voids in the pavement structure. With high air voids, capillary voids are interconnected, allowing water to penetrate from the surface and from the bottom of the pavement. Over time the constant movement of water through the pavement structure weakens the bond due to hydraulic scouring and the constant changes in pore pressure. Along with proper mix design, pavement design, and construction techniques, anti-stripping agents can provide another method of prevention. By adding hydrated lime or liquid anti-stripping agents, the bond between the aggregate and binder is chemically improved by reducing the surface tension between the aggregate and the binder (Putnam, 2006).

**2.2.2. Stripping Prediction.** Many studies have been performed to identify methods to predict the stripping potential of HMA mixes accurately and easily. Through these studies the most common methods have been the Tensile Strength Ratio (TSR) test, the Hamburg Wheel Tracking Device (HWTD), Saturation and Freeze-Thaw Cycling testing, and Boiling Water Test. Both the TSR and HWTD have been thoroughly tested for both repeatability of results and the effectiveness of predicting the stripping potential of HMA mixes in the field.

**2.2.2.1 TSR.** The Tensile Strength Ratio test is a common way to evaluate the change in tensile strength of an HMA mix resulting from the effects of saturation and accelerated conditioning (Hunter and Ksaibati, 2002). In this particular test, a set of HMA pucks are compacted to 7 +/- 1.0 percent air voids using a gyratory compactor, usually with a set equaling six specimens. Of the six specimens, three are grouped as non-conditioned specimens and are tested in the indirect tensile strength testing load frame. The other three specimens are vacuum saturated and conditioned through at least one freeze thaw cycle, more if specified, thawed in water at an elevated temperature, and then tested in the indirect tensile strength load frame. The average results from the conditioned and non-conditioned specimens are used to calculate the tensile strength ratio (0-100), which expresses the resistance of the HMA mix to the detrimental effect of water to the original strength of the mix. Many agencies use the TSR results as an effective way of evaluating the stripping potential of an HMA mix. It is important to note that there are factors than can affect the results of the TSR test. Some of these factors include aggregate type and asphalt additives. Through the research performed by Hunter and Ksaibati, the use of limestone and granite provided varying results when using a standard AC-10 binder. Different variations of the binder was also tested for both limestone and granite mixes, which included AC-10, aged AC-10, AC-10 with lime added, and AC-10 with a model compound. When the results were compiled, the limestone mixes showed a slight improvement in the TSR ratio when compared to the mixes using granite aggregate. As noted previously, the addition of lime improves the bond by reducing the surface tension between the aggregate and the binder. It was also noted that the mixes that reached the 70 percent failure set-point in the least amount of freeze-thaw cycles were the mixes that used plain AC-10 binder. The number of freeze-thaw cycles allowed before the set-point was reached was increased in the respective order of binder used; AC-10 with model compound, AC-10 aged, and AC-10 with lime (Hunter and Ksaibati, 2002).

**2.2.2.2 Hamburg.** Using the Hamburg Wheel-Track Device (HWTB), HMA can be evaluated for moisture susceptibility. Hot mixes that exhibit tendencies towards moisture susceptibility are likely to encounter stripping issues during the life cycle of the

pavement. Analyzing the data results of a moisture susceptible mix from a Hamburg test, the observer may notice four distinct things: the post-compaction consolidation, creep slope, stripping inflection point (SIP), and stripping slope. Hamburg post-compaction consolidation is the densification of the HMA test specimens during the first 1000 passes of the steel wheels. The creep slope is accumulation of the deformation due to other factors besides moisture and is used to describe rutting susceptibility. The SIP and stripping slope are the key indicators of moisture damage in the test specimens. The SIP is noted as the point at which the creep slope and the stripping slope intersect and indicates the point at which moisture damage begins. Lastly, the stripping slope is the accumulation of permanent deformation due to moisture (Hamburg, 2011).

A commonly used Superpave HMA by the Arkansas DOT was evaluated by use of a Hamburg Wheel-Track Device. With a wheel track device constructed to the specifications of the original wheel track device, a Superpave field mix sampled from I-30 near Little Rock, Arkansas was evaluated for rutting and stripping susceptibility. The mix was compacted using the gyratory compactor to 7 +/- 1% air and the face was cut to ensure good contact between the test specimens. Cores from the existing roadway were also taken and tested in the wheel track device to compare in place results with lab compacted results. When evaluating the results, Hall and Williams (1999) found that the average air voids from the field compacted specimens differed significantly when compared to lab compacted specimens. Although this could potentially affect Hamburg test results, Hamburg testing of the mix showed an HMA not susceptible to rutting or stripping. It was noted that the rut depths measured during testing were larger for field compacted specimens when compared to gyratory compacted specimens, but overall the depths were not significant. It was recommended that more HMA mixes used by the Arkansas DOT be tested for to produce a larger data base of rutting and stripping results.

Starting in 2000, the Texas Department of Transportation (Rand, 2006), began compiling Hamburg test data from its commonly used mixes containing PG 76-xx, PG 70-xx, and PG 64-xx binder. TxDOT evaluated the rut depths and stripping potential and set forth specifications that the mixes should not exceed 12.5 mm of rut depth at 20,000



cycles, 15,000 cycles, and 10,000 cycles for their mixes containing PG 76-xx, PG 70-xx, and PG 64-xx binder, respectively. It was found with these specifications that at least 80% of the mixes were able to pass the test. In 2006, a technical advisory was released with updated results and trends. The expanded database showed that adjustments to the specifications needed alteration. The expanded results showed that nearly 50% of the PG 64-xx mixes tested did not meet the 10,000 cycle minimum limit. It was concluded that the mixes did not vary much from the original database; rather the database was now much larger and better represented the mixes used by TxDOT. It was suggested that the limit be reduced to 10,000 cycles and 5,000 cycles for mixes containing PG 70-xx and PG 64-xx binder, respectively. Options were also suggested to contractor to improve their Hamburg test results. These suggestions included the use of anti-stripping agent such as hydrated lime or liquid anti-strip, the use of higher quality aggregates, the use of cleaner aggregates, incorporate recycled asphalt pavement (RAP), or use a higher binder PG grade (PG 70-xx vs. PG 64-xx, etc.) (Rand, 2006).

### 2.3. MEPDG

**2.3.1. General.** As with most state departments of transportation, typical pavement mix designs were developed using some form of the American Association of State Highway and Transportation Officials (AASHTO) Guide for Design of Pavement Structures. This empirically-based design methodology was developed through the AASHTO Road Test in the 1950s. Because this methodology is strictly empirically based, all pavements, new or rehabilitated, designed are based on regression equations developed from pavement behavior of one type of climate, traffic loading, HMA, base, subbase, and subgrade. With pavement materials evolving, climates varying from state to state, and traffic loading conditions changing, a mechanistic approach to mix design was needed. In 2004, the National Cooperative Highway Research Program (NCHRP) Project 1-37A was formed to develop the new design guide based on mechanistic principles. In 2007, after several revisions, the NCHRP 1-40D Project approved the new design approach which is now referred to as the Mechanistic-Empirical Pavement Design Guide (MEPDG) (Mallela, 2009). Unlike the original AASHTO Road Test, the MEPDG uses distress prediction algorithms to predict field performance of a pavement structure.

This is based on several concepts. First, user inputs from laboratory testing can be entered into the software to further refine the distress prediction algorithms to produce more accurate prediction of distresses, such as rutting, IRI, and cracking of the specific pavement being designed. User inputs are separated by levels based on quality of data available and importance of the project. The three levels are Level 1, 2, and 3, with level of quality in decreasing order, respectively. Level 1 requires laboratory measured material properties such as dynamic modulus for the asphalt binder, resilient modulus for unbound materials, and project specific traffic data. Level 2 inputs are obtained through empirical correlations with other parameters such as resilient modulus estimated from CBR data. Lastly, Level 3 inputs are selected from national or regional databases using default values for type or highway class to determine variables such as soil classification, resilient modulus, and traffic classifications (Schwartz and Carvalho). Also, the distress prediction algorithms were derived from field performance data from several hundred experimental flexible in-service pavements located throughout the United States and contained in the Long-Term Pavement Performance (LTPP) database, as well as other national databases (Mallela, 2009). However, these prediction models were nationally calibrated and did not always accurately predict pavement distresses for all specific locations within a state, traffic loading, or materials used in the HMA pavement. State agencies began additional research to determine whether local calibration was needed to further refine the prediction models used in the MEPDG software. By mechanistically calculating the structural responses (stresses, strains, and deflections) based on material properties, environmental conditions, and loading characteristics, and entering these responses as inputs for the empirical models to compute distress performance, the software generates more accurate distress predictions when compared to previous design methods (Schwartz and Carvalho).

**2.3.2. Rutting Prediction.** As mentioned before, rutting is the permanent vertical deformation of the HMA, base/subbase, and/or subgrade of the pavement structure. In the MEPDG software, the prediction of rutting is done by incrementally calculating the plastic vertical strain found in each layer of the pavement structure due to repeated traffic loading. To further summarize, the sum of all plastic vertical strain at the midpoint of all pavement layers over a given period of time is rutting. However, the accumulation of rutting is not a linear relationship over time. The rate of layer plastic deformation can vary based on pavement layer properties (HMA, unbound aggregate, or subgrade), temperature changes throughout the calendar year (summer vs. winter), changes in moisture (wet vs. dry), and changes in applied traffic loads (Mallela, 2009). The model used in the MEPDG software to calculate total rutting is based on the “strain hardening” relationship developed from data generated by repeated load permanent deformation triaxial tests of HMA, unbound aggregate, and subgrade soils in the laboratory. With these derived relationships, they were then calibrated to match rut depths found in roadways in the field. The MEPDG field-calibrated relationship is shown in equations 1-4. In a study performed by the Missouri Department of Transportation (MoDOT), the distress models that predict total rut depth were evaluated to determine if revisions were needed for the calibration coefficients used in the software algorithms. Using data from LTPP and selected MoDOT pavement sections, a sensitivity analysis of the distress models was performed. For rutting, the MEPDG model was inadequate and predicted rutting poorly. MoDOT concluded that recalibration using local data to adjust all three rutting sub-models (HMA, base, and subgrade) was required to use the model for routine design use.

$$\Delta_{p(HMA)} = \varepsilon_{p(HMA)} h_{HMA} = \beta_{1r} k_z \varepsilon_r(HMA) 10^{k_{1r} n} n^{k_{2r} \beta_{2r}} T^{k_{3r} \beta_{3r}} \quad (1)$$

where:

$\Delta_{p(HMA)}$  = Accumulated permanent or plastic vertical deformation in the HMA layer/sublayer, in.

$\varepsilon_{p(HMA)}$  = Accumulated permanent or plastic axial strain in the HMA layer/sublayer, in/in.

$\epsilon_{r(HMA)}$  = Resilient or elastic strain calculated by the structural response model at the mid-depth of each HMA sublayer, in/in.

$h_{(HMA)}$  = Thickness of HMA layer/sublayer, in.

$n$  = Number of axle-load repetitions

$T$  = Mix or pavement temperature, °F

$k_z$  = Depth confinement factor

$k_{1r,2r,3r}$  = Global field calibration parameters (from the NCHRP 1-40D recalibration;  $k_{1r} = -3.35412$ ,  $k_{2r} = 0.4791$ ,  $k_{3r} = 1.5606$ )

$\beta_{1r,2r,3r}$  = Local or mixture field calibration constants; for the global calibration, these constants are all set to 1.0

$$k_z = (C_1 + C_2 D) 0.328196^D \quad (2)$$

$$C_1 = -0.1039(H_{HMA})^2 + 2.4868H_{HMA} - 17.342 \quad (3)$$

$$C_2 = 0.0172(H_{HMA})^2 - 1.7331H_{HMA} + 27.428 \quad (4)$$

$D$  = Depth below the surface, in.

$H_{HMA}$  = Total HMA thickness, in.

Equation 5 below is the field-calibrated equation used to calculate the plastic vertical deformation within all unbound pavement sublayers and the foundation or embankment soil:

$$\Delta_{p(soil)} = \beta_{s1} k_{s1} \epsilon_v h_{soil} \left( \frac{\epsilon_o}{\epsilon_r} \right) e^{-\left( \frac{\rho}{n} \right)^\beta} \quad (5)$$

Where:

$\Delta_{p(soil)}$  = Permanent or plastic deformation for the layer/sublayer, in.

$n$  = Number of axle load applications

$\epsilon_o$  = Intercept determined from laboratory repeated load permanent deformation tests, in/in

$\epsilon_r$  = Resilient strain imposed in laboratory test to obtain material properties  $\epsilon_o$ ,  $\beta$ , and  $\rho$ , in/in

$\epsilon_v$  = Average vertical resilient or elastic strain in the layer/sublayer and calculated by the structural response model, in/in

$h_{soil}$  = Thickness of the unbound layer/sublayer, in.

$k_{s1}$  = Global calibration coefficients;  $k_{s1}=1.673$  for granular materials and 1.35 for fine-grained materials

$\beta_{s1}$  = Local calibration constant for the rutting in the unbound layers; the local calibration constant was set to 1.0 for the global calibration effort

$$\text{Log}\beta = -0.61119 - 0.017638(W_c) \quad (6)$$

$$\rho = 10^9 \left( \frac{C_o}{(1-(10^9)\beta)} \right)^{\frac{1}{\beta}} \quad (7)$$

$$C_o = \text{Ln} \left( \frac{a_1 M_r^{b_1}}{a_9 M_r^{b_9}} \right) = 0.0075 \quad (8)$$

$W_c$  = Water content, percent

$M_r$  = Resilient modulus of the unbound layer or sublayer, psi

$a_{1,9}$  = Regression constants;  $a_1=0.15$  and  $a_9=20.0$

$b_{1,9}$  = Regression constants;  $b_1=0.0$  and  $b_9=0.0$

Unlike the original AASHTO design guide, the MEPDG software predictions rely on asphalt variables such as air voids, binder percentage, and binder PG number for pavement analysis. In a study by Tarefder and Sumeer (2011), a one-to-one sensitivity analysis was performed to identify how variability of inputs into the MEPDG software affects the outputs generated by the software. In this particular study, AC rutting, along with other distresses, were evaluated. By providing a range of values for air void content, binder percentage, PG number, and % passing the #200 sieve, the sensitivity analysis was completed. It was shown that PG grade, binder content, and air voids affect AC rutting significantly (Tarefder and Sumeer, 2011). In another study performed by Tashman and Elangovan (2012), seven mixes used by the Washington State Department of Transportation with variations in dynamic modulus were tested. In this study it was found that rutting varied based on whether Level 1 or Level 3 inputs were used. This is expected due to Level 3 using default values incorporated into the software for rutting

prediction. In contrast, Level 1 uses specific mix inputs entered by the user, such as dynamic modulus. Using mix specific inputs rather than default values, the software provides a better prediction of pavement performance. This was shown in the rutting predictions generated in this study. Level 3 over-predicted rut depths by an average of 60% whereas Level 1 under-predicted rut depths by an average of 40%. The trend of predicted rut depths agreed well with the dynamic modulus trend of lower rut depths with higher dynamic modulus values. This is expected since higher dynamic modulus values of a mix associate with a stiffer pavement mix. This higher stiffness provides better resistance to lateral flow of the mix, or plastic rutting.

Goh and You (2009) evaluated MEPDG rutting predictions of mixes containing 15% RAP. Dynamic modulus testing of the RAP mix initially completed in the study indicated an increase in mix stiffness and a lower rutting potential based on the results of the  $E^*$  test. Both specimens, compacted to 4% and 7% air voids, were evaluated in the MEPDG software. Goh and You concluded that both RAP mixes showed a significant reduction in rut depth based on a pair t-test statistical analysis, but did not affect rut prediction in a Level 1 design significantly, with the largest reduction of rut depth at 13% for the 4% air void mix and less for the 7% air void mix.

Chehab and Daniel (2006) predicted field performance of RAP mixtures using MEPDG Level 3 inputs. Evaluation of mixes containing 15%, 25%, and 40% in the MEPDG software was compared to data from existing LTPP pavement sections. It was found that Level 3 analysis was difficult due to the uncertainty associated with the effective binder grade of the RAP mixture, since the Level 3 function of the software uses predictive equations to generate mixture properties rather than using laboratory data (Chehab and Daniel, 2006). Upon evaluating all three RAP mixtures, there was a slight increase in rutting with mixtures containing 15%-25%, with the 25% RAP mix exhibiting higher rutting than the 15% RAP mix. This is expected due to the increase in binder content of the mixes, even though the overall stiffness of the mix is increased. However, it was found that the mix containing 40% RAP did decrease the predicted rutting. This is

expected due to the additional increase of stiffness to the mix compared to the lower percentage RAP mixes.

Cooper et al. (2012) evaluated a control HMA mix, a mix containing 15% RAP, and mixes with other sustainable materials for rutting prediction using the MEPDG software and rutting potential using laboratory testing of the physical mixtures. For the software, each mix was evaluated for a 20 year design life and at three different traffic levels (low, medium, and high). It was shown through the software that the performance predicted by the software was improved through the use of sustainable materials in the mix, most notably the mixes containing RAP. Out of all of the RAP mixes, the mix containing 40% RAP exhibited the most favorable predicted performance. However, when comparing the software predictions with test results from physical testing using the Hamburg Loaded Wheel Tester, the rutting predictions differed. Cooper et al. concluded this was due to the rutting models in the MEPDG that use  $E^*$  as the main factor in describing the mix mechanistic properties in a Level 1 analysis.

**2.3.3. Fatigue Cracking Prediction.** In a study performed by the Missouri Department of Transportation (MoDOT), the distress models that predict alligator cracking, and smoothness (IRI) were evaluated to determine if revisions were needed for the calibration coefficients used in the software algorithms. Using data from LTPP and selected MoDOT pavement sections, a sensitivity analysis of the distress models was performed. For alligator cracking, the MoDOT pavement sections observed in the field exhibited little to no cracking. Similarly, the outputs generated by the MEPDG software predicted little to no cracking in the pavement structure. With this known, MoDOT concluded that the nationally calibrated models were acceptable for routine design use, although further evaluation should be performed once highly fatigued pavements become available. The equations below show the process the MEPDG software uses to predict fatigue cracking based on user inputs such as traffic classifications, climate, and HMA mix properties such as effective asphalt, air voids, and dynamic modulus.

$$DI = \sum(\Delta DI)_{j,m,l,p,T} = \sum \left( \frac{n}{N_{f-HMA}} \right)_{j,m,l,p,T} \quad (9)$$

where:

- $n$  = Actual number of axle load applications within a specific time period  
 $j$  = Axle load interval  
 $m$  = Axle load type (single, tandem, tridem, quad, or special configuration)  
 $l$  = Truck type using the truck classification groups included in the MEPDG  
 $p$  = Month  
 $T$  = Median temperature for the five temperature intervals or quintiles used to subdivide each month, °F  
 $N_{f-HMA}$  = Allowable number of axle load applications for a flexible pavement and HMA overlays

The allowable number of axle load applications needed for the incremental damage index computation is shown in equation 10 below (MEPDG, 2008):

$$N_{f-HMA} = k_{f1}(C)(C_H)\beta_{f1}(\varepsilon_t)^{k_{f2}\beta_{f2}}(E_{HMA})^{k_{f3}\beta_{f3}} \quad (10)$$

$N_{f-HMA}$  = Allowable number of axle load applications for flexible pavement and overlays

$\varepsilon_t$  = Tensile strain at critical locations and calculated by the structural response model, in/in.

$E_{HMA}$  = Dynamic modulus of the HMA measured in compression, psi

$k_{f1}, k_{f2}, k_{f3}$  = Global field calibration parameters (from NCHRP 1-40D re-calibration;  $k_{f1}=0.007566, k_{f2}=-3.9492, k_{f3}=-1.281$ )

$\beta_{f1}, \beta_{f2}, \beta_{f3}$  = Local or mixture specific field calibration constants; for the global calibration effort, these constants were set at 1.0

$$C = 10^M \quad (11)$$

$$M = 4.84 \left( \frac{V_{be}}{V_a + V_{be}} - 0.69 \right) \quad (12)$$



- $V_{be}$  = Effective asphalt cement by volume, percent  
 $V_a$  = Percent air voids in the HMA mixture  
 $C_H$  = Thickness correction term as follows:

$$C_H = \frac{1}{0.000398 + \frac{0.003602}{1 + e^{(11.02 - 3.49H_{HMA})}}} \quad (13)$$

$H_{HMA}$  = Total HMA thickness, in.

$$FC_{Bottom} = \left(\frac{1}{60}\right) \left(\frac{C_4}{1 + e^{(C_1 C_1 + C_2 C_2 \text{Log}(DI_{Bottom}))}}\right) \quad (14)$$

where:

$FC_{Bottom}$  = Area of alligator cracking that initiates at the bottom of the HMA layers, percent of total lane area

$DI_{Bottom}$  = Cumulative damage index at the bottom of the HMA layers

$C_{1,2,4}$  = Transfer function regression constants;  $C_4=6,000$ ;  $C_1=1.0$  and  $C_2=1.0$

$$C_1 = -2C_2 \quad (15)$$

$$C_2 = -2.40874 - 39.748(1 + H_{HMA})^{-2.856} \quad (16)$$

In a study performed by Tashman and Elangovan (2012), it was found that the MEPDG software generally over-predicted longitudinal cracking for both Level 1 and Level 3 inputs. However, in both cases, cracking was predicted to be virtually zero. This agreed with field cracking observed for projects already in use with the mixes tested in their study. It was noted that the choice of level input used for alligator cracking did not significantly affect the prediction results. In another study performed by Schwartz and Carvalho (2007), fatigue cracking estimated by the MEPDG software was compared to current Maryland pavement structures already in service. The software predicted little to no cracking in any of the proposed mix designs. This agreed with the field observations, which was expected because significant cracking is not frequently observed in the field for these particular Maryland mix designs.

Tarefder and Sumeer (2011) conducted a one-to-one sensitivity analysis to identify how variability of inputs into the MEPDG software affects the outputs generated by the software. Alligator cracking, along with other distresses, were evaluated. By providing a range of values for air void content, binder percentage, PG number, and % passing the #200 sieve, the sensitivity analysis was completed. It was shown that fatigue cracking was sensitive to air voids and binder content. In another study performed by Cooper et. al (2012), a control HMA mix, HMA mix containing 15% RAP, and other sustainable materials were evaluated for alligator cracking prediction using the MEPDG software. It was found that % alligator cracking predicted by the MEPDG software were very low for all mixes tested and minimal improvement was recorded when compared to conventional mixes.

**2.3.4. IRI Prediction.** The equations for IRI prediction are shown below:

$$IRI = IRI_o + 0.0150(SF) + 0.400(FC_{Total}) \quad (17)$$

where:

$IRI_o$  = Initial IRI after construction, inches/mile

$SF$  = Site factor, refer to equation 18

$FC_{Total}$  = Area of fatigue cracking (combined alligator, longitudinal, and reflection cracking in wheel path), percent of total lane area. All load related cracks are combined on an area basis – length of cracks is multiplied by 1 foot to convert length into an area basis

$TC$  = Length of transverse cracking (including the reflection of transverse cracks in existing HMA pavements), feet/mile

$RD$  = Average rut depth, inches

The site factor (SF) is calculated using the following equation:

$$SF = Age(0.02003(PI + 1) + 0.007947(Precip + 1) + 0.000636(FI + 1)) \quad (18)$$

where:

- Age* = Pavement age, years  
*PI* = Percent plasticity index of the soil  
*FI* = Average annual freezing index, degree F days  
*Precip* = Average annual precipitation or rainfall, inches

In MoDOTs MEPDG calibration study, the distress models that predict smoothness (IRI) were evaluated to determine if revisions were needed for the calibration coefficients used in the software algorithms. Using data from LTPP and selected MoDOT pavement sections, a sensitivity analysis of the distress models was performed. For IRI, both new HMA and overlaid HMA pavements, the nationally calibrated models were inadequate in predicting IRI. MoDOT concluded that the models should be re-calibrated for local Missouri conditions to make it more applicable in routine design use.

According to Tashman and Elangovan (2012), IRI predicted by Level 1 and Level 3 agreed with each other fairly well, however, the software over-predicted the IRI by an average of 80% when compared to field observations. It was noted that the selection of level input used for IRI did not significantly affect the prediction results, and did not accurately predict the distress due to over-prediction. In another study by Tarefder and Sumee (2011), a one-to-one sensitivity analysis was performed to identify how variability of inputs into the MEPDG software affects the outputs generated by the software. In this particular study, IRI, along with other distresses were evaluated. By providing a range of values for air void content, binder percentage, PG number, and % passing the #200 sieve, the sensitivity analysis was completed. It was shown by Tarefder and Sumee that IRI was not sensitive to these mix design variables.

Chehab and Daniel (2006) compared predicted IRI values from the MEPDG software for mixes containing 15%, 25%, and 40% RAP were to each other. It was found that for all mixes initial and terminal IRI values, 100 in/mi. and 175 in/mi. respectively, were exceeded before the end of the design life. When compared to each other, it was concluded that RAP content did not significantly affect the IRI values throughout the design life. It was noted that the lack of sensitivity of IRI to RAP content could possibly

be due to the fact that the IRI values computed in the study are not heavily impacted by bottom-up cracking because minimal alligator cracking was predicted (Chehab and Daniel, 2006). In another study performed by Cooper et al. (2012), a control HMA mix, HMA mix containing 15% RAP, and other sustainable materials were evaluated for IRI prediction using the MEPDG software. It was found that the use of RAP improved the IRI prediction the most for all traffic levels when compared to all mixes evaluated.

#### **2.4. LITERATURE REVIEW SUMMARIES**

During previous research, laboratory results from APA rutting specimens were compared to field performance of actual pavement test sections. Kandhal and Mallick (1999) showed that laboratory results could correlate with field results, however, the age of the field specimens could affect that correlation. Choubane et al. (1998) performed a similar study but found that the location of the laboratory specimens within the APA testing tray could also affect the rutting data produced during testing. Hamburg testing can also show rutting characteristics of mixes. The Texas Department of Transportation (TxDOT) found that its extensive laboratory testing of Hamburg specimens agreed with the field performance of its pavement test sections with the same mix. Long term rutting performance of a mix is difficult to predict with laboratory testing. With the development of the MEPDG software, long term rutting could be estimated. However, based on the type of input level selected, the software generally over-predicts the rutting potential of the pavement when compared to field performance.

Stripping susceptibility can be measured through TSR and Hamburg testing. Hunter and Ksaibati (2002) found that the selection of binder and gradation can affect the stripping potential of the mix. Through their testing, they found that unmodified binders performed less favorably than mixes that had the addition of lime or the binder was aged. The addition of lime chemically improved the adhesion of the binder to the aggregate surface therefor increasing the resistance of the binder from being pulled, or stripped, off of the aggregate surface during freeze/thaw cycles. However, it has been noted in previous research that the TSR test does not always provide a good correlation with the field performance of mixes. In some cases a mix that is deemed stripping susceptible

through TSR testing does not exhibit signs of stripping in the field. With the inconsistency of TSR testing, the Hamburg test was developed to provide an alternate testing method. Through extensive testing, TxDOT showed that Hamburg testing could provide valuable insight on the stripping potential of their commonly used mixes. By compiling large volumes of data, TxDOT developed rut depth limits for their mixes based on the grade of binder selected and expected Hamburg performance based on that selection.

Along with rutting and IRI, fatigue cracking is another distress prediction generated by the MEPDG software. Based on research from Tashman and Elangoven (2012), as well as Schwartz and Carvalho (2007), it was shown that the fatigue cracking predicted by the MEPDG software correlated well with field performance of pavements. However, Tarefder and Sumeer (2011) took a different approach to their research. Their analysis studied the variables that affected the fatigue cracking prediction generated by the MEPDG software. They found that fatigue cracking prediction was sensitive to the air voids and binder content of the mix being evaluated. This makes sense as the fatigue cracking equation is a function of air void and binder content. As these variables change, the stiffness of the mix changes, which ultimately affects the number of allowable loadings the pavement can experience before fatigue cracking becomes present.

### 3. LABORATORY INVESTIGATION

#### 3.1. EXPERIMENTAL DESIGN

**3.1.1. Mix Design.** In order to evaluate MoDOT Section 401 plant mixes for longevity, three levels of quality were chosen. The asphalt mix designs for this study were based on MoDOT specification requirements outlined in Sections 401 and 1004. The objective of studying the three mixes was to simulate: 1) a high quality mix, 2) a marginal quality mix, barely meeting the 401 specifications for mix design acceptance, and 3) a poorly inspected production mix where the amount of screenings and natural sand might increase and the binder content might decrease, resulting in poor volumetrics. The higher-quality mix containing tough, low absorption aggregate, no deleterious materials and percent passing the #200 at the low end of the 5-12% by mass range set by MoDOT. The mid-quality mix containing less tough, higher absorption aggregate, with deleterious material contents at the maximum allowable set by Section 1004 of the MoDOT specifications, a lower effective binder content, and the amount of percent passing the #200 in the middle of the 5-12% by mass range set by MoDOT. The low-quality mix containing the same aggregate as the mid-quality mix, with the same deleterious material contents as the mid-quality mix, a lower effective binder content, and the amount of percent passing the #200 at the upper end of the 5-12% by mass range set by MoDOT). The higher-quality mix contained Potosi Dolomite which has a lower absorption (1.4% coarse fraction and 2.1% fine fraction on average) than the Jefferson City Dolomite (3.4% coarse fraction and 4.2% fine fraction on average). The Potosi Dolomite was tougher (MD = 9.5, LAA = 26) compared to the Jefferson City Dolomite (MD = 21.5 and LAA = 30). Although both aggregates met the 1004 LAA limit of 55, MoDOT considers aggregates with LAA values greater than 30 to be inferior and values less than 30 to be good. For the Jefferson City In-Spec mix (mid-quality mix), the percent passing the #200 was set at 7%. For the Jefferson City Out-of-Spec mix, the % passing the #200 was set at 12%, which is the upper end of the limit set by MoDOT Section 401.3. This was to simulate the worst case scenario and to simulate what the effect of excessive total dust may have on physical lab testing and distress predictions. For both Jefferson City mixes, shale and clay dust was added to some of the gradation

fractions to simulate a poor quality quarry operation. The deleterious materials content was set at the maximum allowable (section 1004) for the mid-quality mix in order to give a range of behavior during the performance testing (TSR and Hamburg) for 401-acceptable mixes. For the poor quality mix, the deleterious material contents remained the same as the mid-quality mix. Montmorillonite clay was combined with the minus #200 fraction for both Jefferson City mixes to also simulate the influence of clay that had broken down into dust. The amount of shale was set at 2% of the plus #4 sieve total aggregate and the clay dust content was set at 3% of the total aggregate by mass. The poor quality mix contained 0.3% less total binder content by mass as allowed during production. Thus the binder content was out-of specification for design acceptance, but within the allowable field production tolerance. The gradation requirements in section 401.3 were followed for both the Potosi Dolomite and Jefferson City Dolomite BP-1 mix designs. Using the Marshall method, two Marshall pucks were made along with an maximum theoretical specific gravity specimen to determine trial mix design volumetrics such as maximum specific gravity (G<sub>mm</sub>), bulk specific gravity (G<sub>mb</sub>), % air, voids filled with asphalt (VFA), void in the mineral aggregate (VMA), and percent binder effective (P<sub>b</sub>e). Trial mix designs were evaluated for all three types of mixes (Potosi, Jefferson City In-Spec, and Jefferson City Out-of-Spec) until the design % air of 3.5% was reached along with the VMA of 13% (MoDOT Section 401.4.4.1). The mix gradations can be found in Section 3.3 of this study.

**3.1.2. Specimen Preparation.** With the volumetrics of the mix in order, tensile strength ratio (TSR) and Hamburg pucks were made. This was done by using the design G<sub>mm</sub> and G<sub>mb</sub> to estimate puck volumes for a specific height and a % air of 7 +/- 0.5%. Several trials were completed to fine tune the exact weights of mix needed to obtain the target % air for each type of test specimen. See Appendix B for procedure.

**3.1.3. Replicates.** For this study, three sets of specimens were made for each mix design for Hamburg testing. Only one set is required to run a full Hamburg test, but since there was room for three sets, three were made and tested. For TSR testing, the number of conditioned/unconditioned specimens was set at six for each mix design.

## 3.2. EQUIPMENT

**3.2.1. Washing of the Aggregate.** For all aggregates tested in this study, washing of the aggregates was completed using deep stainless steel pans and a wash table as seen in Figure 3.1 below. The wash table consists of six overhead spray nozzles and a large open table with wood boards spaced out to allow water to flow to the floor drain.



Figure 3.1 - Aggregate Washing Table

**3.2.2. Drying Oven.** The aggregate used in all specific gravity and absorption testing was dried in an Grieve oven, seen in Figure 3.2, capable of maintaining temperatures of  $110 \pm 5$  °C ( $230 \pm 9$  °F). For this testing, a Grieve model #333 oven was used to oven dry the aggregate for 24 hours. The aggregate remained in the same pan that it was washed in.





Figure 3.2 - Grieve Oven

**3.2.3. Aggregate Specific Gravity and Absorption.** Specific gravity of the fine aggregates, more specifically the fraction of aggregates passing the #4 sieve, were tested in accordance with ASTM C128. The test procedure was performed by using a saturated surface dry (SSD) sample and a Chapman flask that had a known volume of 500 ml. The specific gravity and absorption setup can be seen in Figure 3.3 below.



Figure 3.3 - Fine Aggregate Specific Gravity and Absorption Setup

Specific gravity of the coarse aggregates, more specifically the fraction of aggregates retained on the #4 sieve and above, was tested in accordance with ASTM C127. The test procedure was performed by using a SSD sample, a wire basket to hold the SSD sample, and water tank to suspend the wire basket in (Figure 3.4).



Figure 3.4 - Coarse Aggregate Specific Gravity and Absorption Setup

**3.2.4. Mix Specific Gravity.** The maximum theoretical specific gravity of the loose asphalt mix was tested in accordance with AASHTO T 209. The test procedure was performed by using a pan to cool and separate the loose mix, a pycnometer to hold the loose mix and water, a vacuum pump system to remove air from the specimen and pycnometer, a water bath and weigh-below scale system to weigh the pycnometer holding the loose mix sample after the vacuum has been applied (Figures 3.5 and 3.6).



Figure 3.5 - Pycnometer; Cooling Pan and Fan



Figure 3.6 - Vacuum Setup

The bulk specific gravity of the compacted asphalt pucks was tested in accordance with AASHTO T 166. The test procedure was performed by using a water bath and a weigh-below scale system to weigh the compacted asphalt pucks both under water and when the specimen was surface dried. The maximum theoretical and bulk specific gravity setup can be seen in Figure 3.7 below.



Figure 3.7 - Specific Gravity Weigh-Below Setup

For this particular study, the Corelok Method (ASTM D6752) was used as an additional method to determine the bulk specific gravity of the compacted specimens used in APA and AMPT testing. This was done using an automated Corelok vacuum chamber manufactured by Instrotek (Figure 3.8). Along with the vacuum chamber, a weigh-below and water bath setup was used in conjunction to record all dry and submerged compacted specimen weights used for the specific gravity calculation. It was found that the Corelok generated a lower Gmb value for the pucks when compared to the traditional AASHTO T 166 method of testing. This in turn increased the % Va for the pucks on average of 1-2%. After discovering the difference in actual % Va, the AASHTO T 166 method was used for the remainder of testing.



Figure 3.8 - Corelok Vacuum Chamber

With using the AASHTO T 166 method for bulk specific gravity testing, the pucks were exposed to water submersion and absorption. To speed up the drying process, a CoreDry Rapid Vacuum Drying Machine (Figure 3.9) was obtained from Instrotek. This machine uses vacuum to pull the moisture out of the pores in the vacuum chamber and condenses the moisture in the cold trap chamber to remove all moisture from the asphalt pucks.



Figure 3.9 - CoreDry Rapid Vacuum Drying Machine

**3.2.5. Gradation.** Sieve analysis of all aggregate samples was tested in accordance with ASTM C 136. The test procedure was performed using a stack of 12 in sieves and a Roto Sifter shaker to shake the sample for a minimum of 10 minutes as seen in Figure 3.10 below. After the shaking, each size from the individual sieves was weighed and placed in separate containers to hold the individual samples until further testing or use.



Figure 3.10 - Standard 12 in. Sieves

**3.2.6. Gyrotory Compaction.** The gyrotory compactor used in this study was an AFGC125X manufactured by the Pine Instrument Company. TSR and Hamburg specimens were compacted in accordance with AASHTO T 312. The specified amount of mix outlined in the mix design was heated to the appropriate compaction temperature based on the binder PG being used and placed in the 150 mm (6 in) diameter molds. The mold containing the mix was then placed into the gyrotory compactor. During compaction of the specimen, a loading ram applied a pressure of 600 +/- 18 kPa to the loose Potosi and Jefferson City In-Spec mix, or 200 +/- 18 kPa to the loose Jefferson City

Out-of-Spec mix. The difference in pressures was due to the difference in stiffness between the Potosi and Jefferson City mixes and the ability to hit the target specimen height during the final gyration of the gyratory compactor. This pressure was held constant while the mix was compacting. The gyratory compaction setup can be seen in Figure 3.11 below.



Figure 3.11 - Pine Gyratory Compactor

**3.2.7. Marshall Compaction.** Specimens during the trial mix design phase of this study were compacted in accordance with the Marshall Method. The MoDOT 401 specification allows a compactive effort via 35 gyrations using the gyratory compactor or 35 blows (each side) with a Marshall hammer. Most designers in Missouri have found that poorer quality aggregates break down excessively using the gyratory compactor, rendering low voids. Thus, designs are based on the 35 blow Marshall method. In this study, a couple of mixes were attempted using the gyratory method, but this resulted in very low voids. Thus the remainder of the mix design specimens were compacted with the Marshall hammer. The specified amount of mix was based on the mix specific bulk specific gravity and maximum specific gravity values calculated, outlined in the mix

design. Using a three piece mold consisting of the bottom plate, forming mold, and top collar, 102 mm diameter specimens were compacted by use of a 10 lb hammer with a flat tamping face and an 18 in height of drop (Figures 3.12 and 3.13). Once the specimens were compacted, they were extruded from the forming mold, seen in Figure 3.14, by use of a small jack with flat circular plate for a base. Temperature during mixing and compaction of the loose HMA was verified using a handheld Fluke Infrared Thermometer.



Figure 3.12 - Marshall Bottom Plate, Forming Mold, and Top Collar



Figure 3.13 - Marshall 10 lb Hammer and Heating Plate





Figure 3.14 - Marshall Puck Extruder

**3.2.8. Tensile Strength Ratio.** A comparison of moisture induced damage was done using the APA (Hamburg) and the Tensile Strength Ratio (TSR) test. For the TSR test, specimens were compacted using the gyratory compactor in accordance of AASHTO 312 to a specified height of 95 +/- 5 mm and 150 mm in diameter. With a set six pucks, the set was separated into two separate subsets with the average air voids between the subsets as equal to each other as possible. The first subset of pucks was labeled as the conditioned subset, which were subjected to vacuum saturation, a freezing cycle, a thaw cycle in water at an elevated temperature, and lastly tested for tensile strength (Figure 3.15). The second set was labeled as the unconditioned set and were not subjected to saturation and freeze/thawing cycles. The tensile strengths of the conditioned and unconditioned sets were averaged and the tensile strength ratio was computed in accordance with AASHTO T 283.



Figure 3.15 - Indirect Tensile Strength Apparatus

**3.2.9. Specimen Coring.** Specimens used in the AMPT were cored from 150 mm (6 in.) gyratory compacted HMA specimens. The 6 in. compacted specimen was cored using a 100 mm (4 in) core bit attached to a Heavy Duty Milwaukee Dymodrill as seen in Figure 3.16 below.



Figure 3.16 - Milwaukee Dymodrill Coring Drill

**3.2.10. Specimen Sawing.** Cored specimens were cut to the length of 150 mm (6 in.) specified by AASHTO TP 79. This was done using a custom built cored-specimen holding device and a Felker Manufacturing Co. wet saw (Figures 3.17 and 3.18).



Figure 3.17 - Specimen Wet Saw



Figure 3.18 - Custom Built Cored Specimen Holder

**3.2.11. APA.** The Asphalt Pavement Analyzer was obtained by Missouri University of Science and Technology in 2001 and was designed to perform rut testing of asphalt mixtures. In the summer of 2012, the APA was retrofitted from analog control to digital control to provide both rut testing and Hamburg Wheel testing. Along with the addition of the Hamburg Wheel test equipment, updated software was provided and the manual controls originally located on the machine are now controlled using the software. The APA is a self-contained and fully automated rut testing machine (Figure 3.19). Test specimens are built to specifications outlined by AASHTO T 340 and AASHTO T 324 for both the rut test and Hamburg Wheel test, respectively. With the test samples made, they are loaded into their respective molds and locked in place on the specimen tray located inside the APA machine. Once the specimens are brought to the proper test temperature outlined in the APA instruction manual, testing can begin using the provided software. During the rut test, the APA uses three separate wheels, controlled by Programmable Logic Controllers (PLCs), to provide pressure to the hose carriage assembly on top of the test specimens, which are located on the tray (Figure 3.20). By applying pressure and moving back and forth at a specified frequency, the wheels can

simulate long term traffic loadings of a pavement over a set number of wheel cycles. This simulated test eliminates the need to observe an actual pavement structure over the full length service life.

Unlike the rut test, specimens during the Hamburg Wheel test are submerged in water at a specified high temperature to simulate the effects of water exposure to the HMA structure of a pavement life in a period of a few hours as seen in Figure 3.21 below. This simulated test eliminates the need to observe an actual pavement structure over the full length service life. Also, unlike the rut test, the hose carriage assembly is not placed on top of the test specimens. For this test, the steel wheels run directly on top of the test specimens. Once testing is complete, data is compiled in the software for analysis and the tested specimens are removed from the APA machine.



Figure 3.19 - Asphalt Pavement Analyzer (APA)



Figure 3.20 - APA Rut Test Setup



Figure 3.21 - APA Hamburg Test Setup

**3.2.12. AMPT.** The Asphalt Mixture Performance Tester was obtained by Missouri University of Science and Technology in 2012 and was designed to perform dynamic modulus and flow number testing of asphalt mixtures. Testing is performed on

100 mm (4 in.) diameter by 150 mm (6 in.) tall test specimens prepared in accordance with AASHTO PP-60. For the dynamic modulus test, the specimen was conditioned to a set temperature governed by the upper binder PG number. Once the temperature was reached, the specimen was loaded into the AMPT test chamber and subjected to load/unload cycles for three given frequencies (Figure 3.22). This load/unload cycle on the test specimen was performed at three different temperatures. Sufficient time was allowed to make sure the specimen, in its entirety, was at the proper test temperature before testing. The proper test temperature was verified by the thermocouple located in the center of the dummy specimen that was placed in the conditioning chamber with the actual test specimen.



Figure 3.22 - AMPT Test Chamber with Verification Apparatus

For flow number testing, the 100 mm diameter by 150 mm tall specimen was conditioned to either 58°C for surface mixtures or 55°C for subsurface mixtures. For this particular study, the specimens were evaluated using the confined test procedure. The confined test procedure was used for all mix testing unless unconfined testing is

requested. The specimens were wrapped with a latex membrane and the specimen was loaded into the test chamber (Figure 3.23). Once the chamber was closed, the chamber was pressurized to 10 psi, as recommended in NCHRP 9-33, and the load/unload cycling was started.



Figure 3.23 - Latex Wrapped Specimen for Flow Number Test

Temperatures of the AMPT test specimens were achieved by a Frigidaire refrigerator at 4 degrees Celsius, a BEMCO oven at 20 degrees Celsius, a Blue M oven at 40 degrees Celsius, and a Thelco oven at 58 degrees Celsius (Figure 3.24). The refrigerator and all oven temps were verified and calibrated using a Sper Scientific 4 channel data logging thermometer and dummy specimens with a thermocouple located in the center of the specimen as seen in Figure 3.25 below. The thermocouple in the dummy specimen was installed by drilling a hole into the center of the specimen, inserting the thermocouple, and securing it by filling the hole with binder. During the AMPT testing, the AMPT machine displayed the air chamber temperature by using a thermocouple located within the testing machine.





Figure 3.24 - Conditioning Chambers for AMPT Specimens



Figure 3.25 - Sper Scientific 4 Channel Data Logging Thermometer

### 3.3. MATERIALS

**3.3.1. Aggregate.** All aggregate used in this study was sampled in the fall of 2012. Jefferson City Dolomite was sampled from Capitol Quarries (Ledges #9 – #1J) located on Highway 63 in Rolla Missouri and Potosi Dolomite was sampled from the NB West Quarry (Ledge #1) located in Sullivan Missouri. Aggregate from both quarries was sampled using the mini stockpile method and a square point shovel to scoop aggregate into the individual buckets for transportation from the quarry to the Missouri S&T laboratory. The natural sand used was Missouri River sand (purchased from Rolla Ready Mix), based upon a good service record and local availability. Table 3.1 shows the fractions sampled from each quarry and their respective absorption and specific gravity values obtained through testing in accordance with AASHTO T84 and T85. This was done to obtain all size fractions to build a custom gradation for each HMA mix design. Gradations for all aggregate fractions obtained from all quarries are provided in Tables 3.2 and 3.3 below. Los Angeles Abrasion and Micro-Deval data was obtained from MoDOT testing. Gradation plots for all mixes are provided in Figures 26-28.

Table 3.1 - Specific Gravity and Absorption Data

ASTM C 127 & C 128 - Specific Gravity & Absorption									
Aggregate Source	Aggregate Type	Aggregate Size	Coarse/Fine	BSG <sub>SSD</sub>	BSG <sub>OD</sub>	ASG	Absorption	LAA	Micro Deval
Capitol	JCD	1" Clean	Coarse	2.631	2.554	2.767	3.0	30	21.5
Capitol	JCD	1/2" Clean	Coarse	2.630	2.531	2.806	3.9	30	21.5
Capitol	JCD	3/8" Clean	Coarse	2.641	2.548	2.809	3.6	30	21.5
Capitol	JCD	3/8" Clean	Fine	2.622	2.529	2.789	3.7	30	21.5
Capitol	JCD	Man. Sand	Fine	2.610	2.492	2.826	4.7	30	21.5
Capitol	JCD	Cuba Screen.	Fine	2.601	2.499	2.783	4.1	30	21.5
Capitol	MO River	Natural Sand	Fine	2.625	2.616	2.639	0.3		
Sullivan	PD	1" Clean	Coarse	2.727	2.687	2.800	1.5	26	9.6
Sullivan	PD	9/16" Clean	Coarse	2.733	2.696	2.800	1.4	26	9.6
Sullivan	PD	3/8" Clean	Coarse	2.734	2.690	2.811	1.6	26	9.6
Sullivan	PD	9/16" Clean	Fine	2.663	2.591	2.793	2.8	26	9.6
Sullivan	PD	3/8" Clean	Fine	2.710	2.660	2.800	1.8	26	9.6
Sullivan	PD	Screenings	Fine	2.715	2.661	2.814	2.0	26	9.6

Table 3.1 - Specific Gravity and Absorption Data (cont.)

ASTM D 7370 - Specific Gravity & Absorption Using CoreLok							
Aggregate Source	Aggregate Type	Aggregate Size	Coarse/Fine	BSG <sub>SSD</sub>	ASG	Absorption	
Capitol	JCD	1/2" Clean	Coarse	2.534	2.751	3.1	
Capitol	JCD	Man. Sand	Fine	2.484	2.777	4.2	
Sullivan	PD	3/8" Clean	Coarse	2.695	2.763	0.9	
Sullivan	PD	Screenings	Fine	2.672	2.808	1.8	

Table 3.2 - Jefferson City Dolomite Gradations

Jefferson City Dolomite - Percent Passing						
Sieve Size	1" Clean	1/2" Clean	3/8" Clean	Man. Sand	Cuba Screenings	Missouri River Sand
3/4	59	100	100	100	100	100
1/2	9	100	100	100	100	100
3/8	2	76	100	100	100	100
#4	2	21	39	86	97	98
#8	2	20	7	46	71	91
#16	2	20	5	24	51	79
#30	2	20	5	16	41	51
#50	2	20	5	12	34	11
#100	2	20	5	10	27	0
#200	2	19	4	8	20	0
PAN	0	18	0	0	0	0

Table 3.3 - Potosi Dolomite Gradations

Potosi Dolomite - Percent Passing					
Sieve Size	1" Clean	9/16" Clean	3/8" Clean	Sullivan Screenings	Missouri River Sand
3/4	94	100	100	100	100
1/2	53	86	100	100	100
3/8	28	48	98	100	100
#4	7	9	49	100	98
#8	5	5	10	89	91
#16	4	5	5	74	79
#30	4	4	4	64	51
#50	3	3	3	44	11
#100	2	3	3	24	0
#200	2	2	2	14	0
PAN	0	0	0	0	0

Tables 3.4-3.6 below show the gradations and aggregate sources for the Potosi Dolomite mix (PD-5), the Jefferson City Dolomite In-Spec mix (JCD-7), and the Jefferson City Dolomite Out-of-Spec mix (JCD-12). It is noted by the shaded cells on the Jefferson City mixes for which fractions contained a combination of Jefferson City Dolomite, shale, and/or montmorillonite clay. The shale was East Rosebud Shale (ERS) collected during a previous research study (Richardson, 1984). The bulk specific gravity was 2.79. The apparent specific gravity was assumed to be the same. The small stockpile was separated into the desired sizes using 12 in. sieves. The montmorillonite clay material was collected during a previous study and was evaluated using the Atterberg Limits test to determine the Liquid Limit (LL), Plastic Limit (PL), and ultimately the Plasticity Index (PI) of the clay. Upon evaluation, it was determined that the montmorillonite clay had a LL of 370, a PL of 67.5, and a PI of 303. This verified that the previously collected sample was indeed a highly plastic clay. The specific gravity was assumed to be equal to the JCD screenings. It is important to note that all fractions, except for the #200 JCD screenings, were not washed upon building specimen gradations.

Also shown in the gradation plots is the restricted zone. Although it is no longer required in MoDOT specifications, the concept of the restricted zone is still useful for mixtures containing significant amounts of natural sand (eg., JCD mixes).

Table 3.4 - Potosi Dolomite Mix Gradation (PD-5)

PD-5 Gradation			
Sieve	Source	% Passing	%IR
1"	-	100.0	0.0
3/4"	-	100.0	0.0
1/2"	9/16" PD	97.7	2.3
3/8"	9/16" PD	90.2	7.5
#4	3/8" PD	52.8	37.4
#8	3/8" PD	30.0	22.8
#16	PD Screenings	19.4	10.6
#30	Natural Sand	15.5	3.9
#50	Natural Sand	10.0	5.5
#100	PD Screenings	7.0	3.0
#200	PD Screenings	5.0	2.0
Pan	PD Screenings	0.0	5.0

Table 3.5 - Jeff City Dolomite In-Spec Gradation (JCD-7)

JCD-7 In-Spec Gradation			
Sieve	Source	% Passing	%IR
1"	-	100.0	0.0
3/4"	-	100.0	0.0
1/2"	1" JCD/Shale	98.0	2.0
3/8"	1/2" JCD/Shale	87.0	11.0
#4	1/2" JCD/Shale	53.0	34.0
#8	JCD Manufactured Sand	31.0	22.0
#16	Natural Sand	18.0	13.0
#30	Natural Sand	13.0	5.0
#50	Natural Sand	9.0	4.0
#100	Natural Sand	8.0	1.0
#200	JCD Screenings	7.0	1.0
Pan	JCD Screenings/Clay	0.0	7.0

Table 3.6 - Jeff City Dolomite Out-of-Spec Gradation (JCD-12)

JCD-12 Out-Spec Gradation			
Sieve	Source	% Passing	%IR
1"	-	100.0	0.0
3/4"	-	100.0	0.0
1/2"	1" JCD/Shale	98	2.0
3/8"	1/2" JCD/Shale	87	11.0
#4	1/2" JCD/Shale	53	34.0
#8	JCD Manufactured Sand	38	15.0
#16	Natural Sand	28	10.0
#30	Natural Sand	23	5.0
#50	Natural Sand	19	4.0
#100	Natural Sand	17	2.0
#200	JCD Screenings	12	5.0
Pan	JCD Screenings/Clay	0.0	12.0

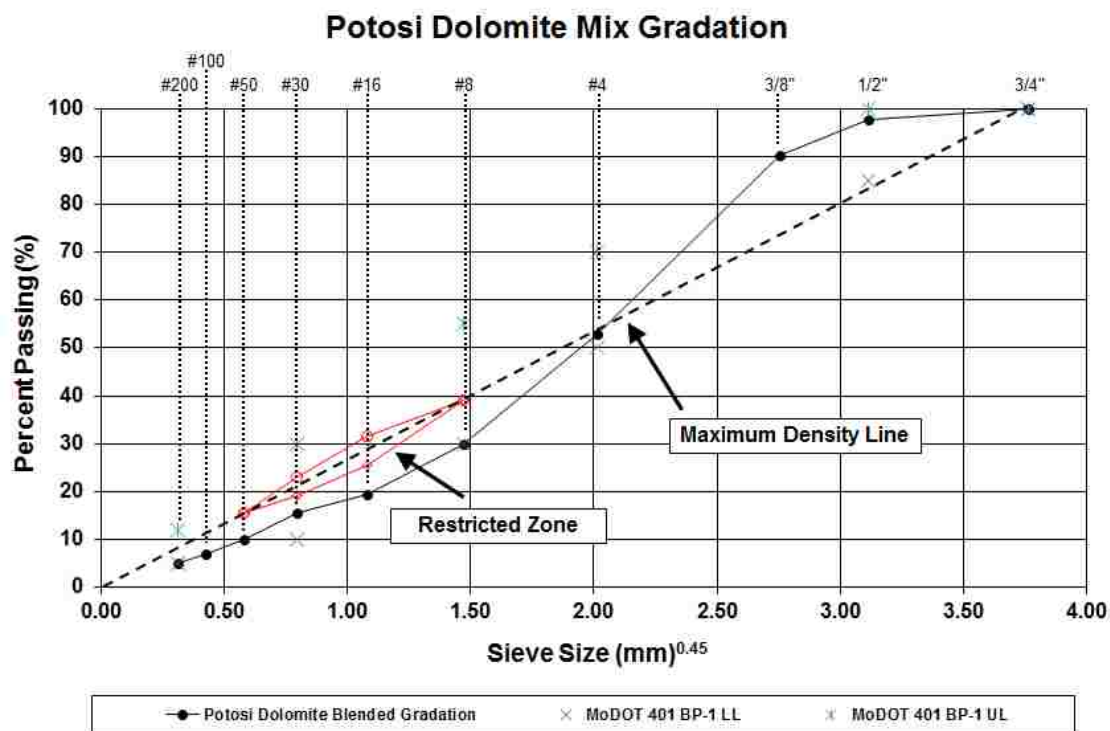


Figure 3.26 - Potosi Dolomite Mix Gradation

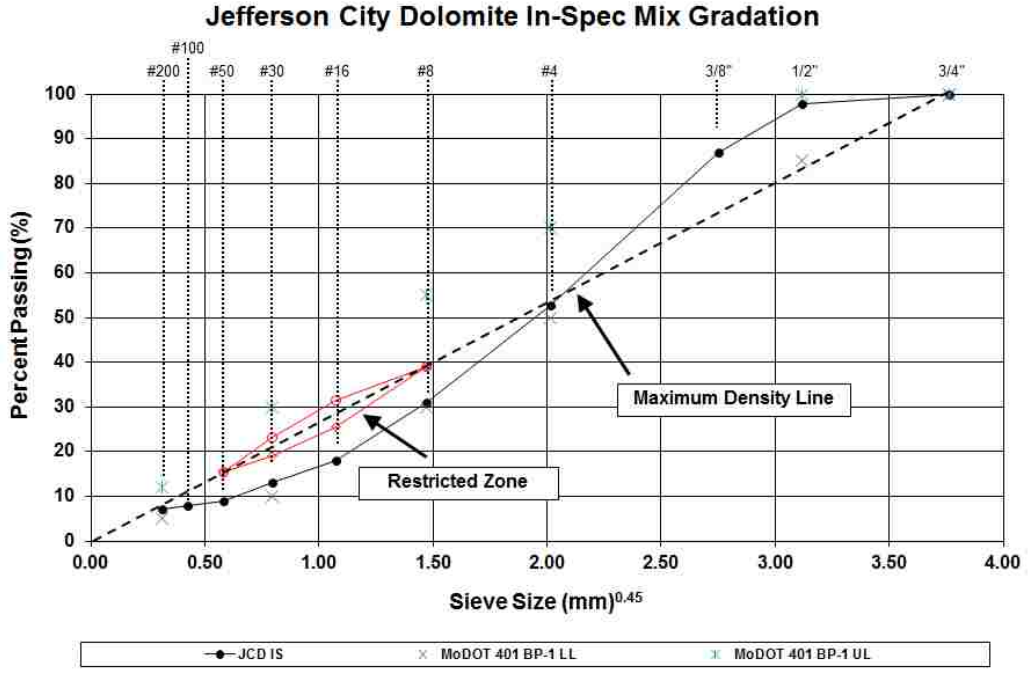


Figure 3.27 - Jefferson City Dolomite In-Spec Mix Gradation

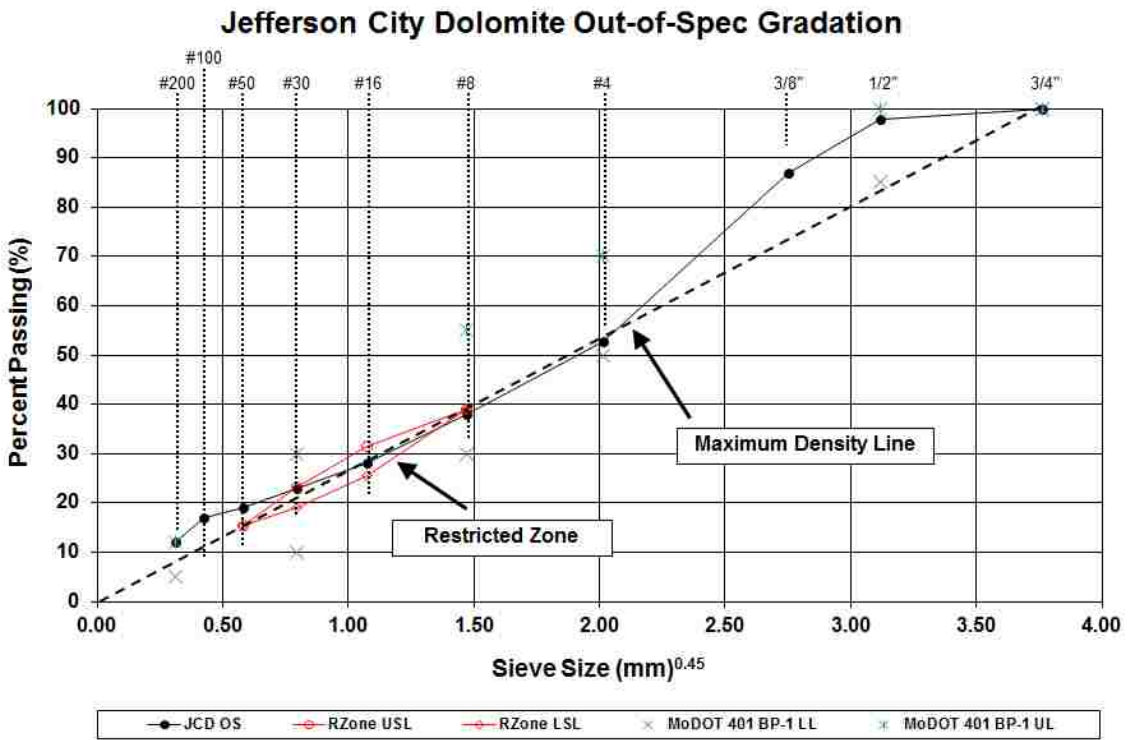


Figure 3.28 - Jefferson City Dolomite Out-of-Spec Mix Gradation

**3.3.2. Binder.** The binder used for all mixes in this study was obtained from NB West of St. Louis Missouri. The binder is a PG64-22 produced by Conoco Phillips and distributed from the St. Louis Missouri terminal. This binder is a conventional PG64-22 binder that contains no additives or modifiers. The binder was sampled from the binder tank located at the NB West hot mix facility in Sullivan Missouri. During the sampling process, hot binder was taken from the storage tank and placed into individual five gallon buckets. During the testing phase of this project, the five gallon buckets were heated up and the binder was then placed into individual one gallon cans for ease of use and to avoid multiple re-heatings of the binder. Mixing and compaction temperatures were determined by the temperature-viscosity plot (Figure 3.29) with the SP-2 manual recommended allowable range of 170 +/- 20 centipoise for mixing and 280 +/- 30 centipoise for compaction. The Brookfield Viscometer was used to determine the viscosity at two different temperatures (135°C and 165°C), in which that data was used to generate the temperature-viscosity plot.

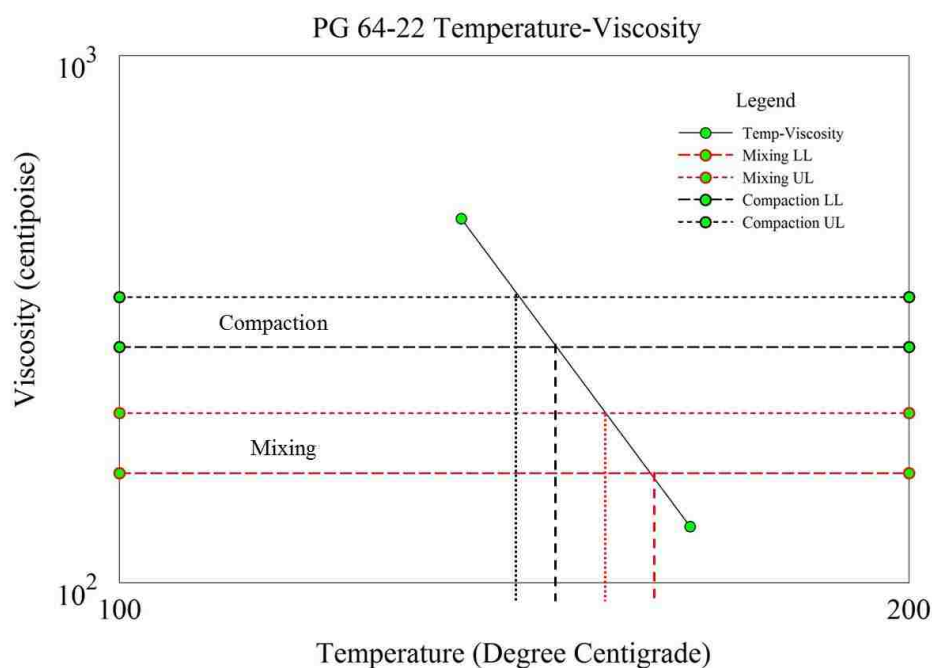


Figure 3.29 - Temperature-Viscosity Plot



### 3.4. TEST PROCEDURES

**3.4.1. Aggregate Preparation.** For the asphalt mix design phase it was determined that an optimized gradation for each type of mix would be used. This was done by oven drying the aggregate to a constant mass and fractioning each aggregate sample according to size. For each aggregate sample, it was separated into the following sizes based on the material that was retained on the sieve:  $\frac{3}{4}$  in.,  $\frac{1}{2}$  in.,  $\frac{3}{8}$  in., #4, #8, #16, #30, #50, #100, #200, and Pan. With each aggregate sample fractioned, an optimized gradation was developed by choosing a combination of certain aggregate sizes from certain aggregate samples based on the material properties.

Washing of the aggregates was not done in the mixes made during this study. The only exception was the minus #200 for the Jefferson City Dolomite Screenings.. This was completed using deep stainless steel pans and a wash table. The wash table consists of six overhead spray nozzles and a large open table with wood boards spaced out to allow water to flow to the floor drain.

**3.4.2. Aggregate Specific Gravity and Absorption.** Specific gravity and absorption of all aggregates used in this study was performed in accordance to ASTM C127 and C128 for both coarse and fine aggregates respectively.

Before the optimized gradations were built, each sample obtained from the quarries was separated using standard 12 in. sieves in accordance to ASTM C136 (Figure 3.30). A limit of 2000 grams of oven dry material was used to prevent overfilling and clogging of the individual sieves. After allowing the stack of sieves to shake for a minimum of 10 minutes in the Roto Sifter (Figure 3.31), the stack was removed from the shaker and material from each sieve was placed in its respectively marked bags for storage until further use. To accurately determine the percentage of minus #200, the steps outlined in ASTM C117 were followed.



Figure 3.30 - Standard 12 in Sieves



Figure 3.31 - Standard Roto-Sifter

**3.4.3. Mix Specific Gravity.** The maximum theoretical specific gravity was determined using AASHTO T 209. This was done by taking the loose hot mix and placing it in a large rectangular pan. While in the pan, the loose mix was gently separated until cooled to room temperature and all particles were separated. Next an empty, dry, pycnometer was weighed. Next, the scale was zeroed and the loose cooled mix was placed into the pycnometer. The initial dry weight of the mix was recorded. Then water was added to the pycnometer until the water surface was approximately 1 in. above the top surface of the loose mix. This was done to ensure air would not reach the loose mix during the next step. Then the pycnometer was placed into the vacuum apparatus and vacuum was applied for 15 minutes until air was removed from the loose mix sample (Figure 3.32). After slowly releasing the vacuum and being careful to avoid exposing the mixture to air, the pycnometer was moved to the weigh-below system where the pycnometer was placed on the hanging basket. The loose mix was submerged for 10 minutes and the submerged weight was recorded. Then the pycnometer was removed from weigh-below system and completely cleaned. The empty pycnometer was then placed back on the weigh-below system and the submerged weight of the empty pycnometer was recorded, and the maximum theoretical specific gravity ( $G_{mm}$ ) was calculated.



Figure 3.32 - Vacuum System

In this study, all test specimens were compacted using the gyratory compactor by the steps outlined in AASHTO T 312. The specimens were allowed to cool to room temperature before further testing. During this study, the bulk specific gravity was calculated using two different methods; using AASHTO T 166 and the Corelok Method (ASTM D6752 – 11). The AASHTO T 166 method consisted of a weigh-below system and a scale as shown in Figure 3.33 below. The cooled puck was first weighed in air. Then the puck was placed on the basket hanging from the scale, inside the water bath. The puck was submerged for 5 minutes and the submerged weight was recorded. Then the puck was removed, quickly surfaced dried with a damp towel, and placed back on the scale. The saturated surface dry (SSD) weight was then recorded and the bulk specific gravity ( $G_{mb}$ ) was calculated.



Figure 3.33 - Specific Gravity Weigh-Below System

If test specimens needed to be verified again, the specimens were dried before further testing using the CoreDry Rapid Vacuum Drying Apparatus (ASTM D7227 – 11). The CoreDry uses vacuum chamber in conjunction with a cold trap chamber to pull the water out of the asphalt pores and condensate said vapor inside the cold trap (Figure 3.34).



Figure 3.34 - CoreDry Vacuum Chamber

This effectively removes all water trapped inside the asphalt pucks and on the surface. First the room temperature puck was placed inside the larger vacuum chamber on top of the specimen basket and the lid was placed on top to seal the chamber. Then the cold trap was checked with a clean, lint-free towel to make sure it was completely dry before the machine was started. With CoreDry on, the appropriate program selected, and the lids in the proper place, the start button was selected. Vacuum was applied to pull water from the pores of the puck. After the maximum vacuum was achieved, the chamber was pressurized and the cold trap accumulated any water vapor from the vacuum chamber. The vacuum/pressurizing cycle was applied until the vacuum on the display read 6 mmHg. If the 6 mmHg or less of vacuum was not achieved on the first cycle, another cycle began. Once the 6 mmHg or less of vacuum was achieved, the machine automatically stopped and the chamber was pressurized to allow the lids to be

removed. The cold trap was then wiped free of any moisture and the preparation was repeated on the next damp specimen.

Unlike the traditional method of AASHTO T 166, during the CoreLok Method, the test specimens were not subjected to filling the air voids with water. With the initial dry puck weight, the specimen was placed inside a polymer bag and the bag assembly was placed inside the Corelok vacuum chamber (Figure 3.35).

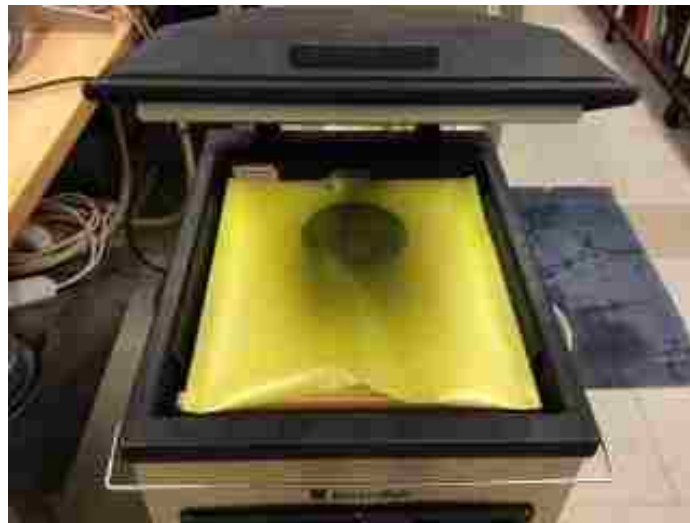


Figure 3.35 - CoreLok Vacuum Chamber

With the bag assembly roughly in place, a sliding plate was placed underneath the puck/bag. This allowed the puck/bag to move when the vacuum was applied. With the plate in place, the bag was checked to make sure no edges touched the outside perimeter of the chamber and that approximately 1 in of the bag was over the seal bar. With the bag assembly in the proper location, the chamber lid was closed and vacuum was applied. The vacuum and seal bar duration was set by a predetermined program on the Corelok machine. Once the vacuum cycle was complete, the puck/bag assembly was removed from the chamber and placed on the basket located in the water bath setup. Next the submerged weight of the bag assembly was recorded. With the submerged weight recorded, the bag assembly was removed from the water bath and the bag was cut,

allowing the puck to be removed. Next, the puck was reweighed and this was recorded as the final dry weight. If the final puck weight was 5 or less grams different than the initial puck weight, it was deemed a valid test. If the weight difference was more than 5 grams, the puck must be dried and the test must be restarted. With the final dry weight, the bulk specific gravity of the puck was calculated.

The CoreLok method was initially used to determine  $G_{mb}$  of the test specimens. However, through observation in the laboratory and further literature review, it was determined that the CoreLok method over-estimated  $G_{mb}$ , which in turn under-estimated the % air voids of the test specimens by an average of 1-2%. Due to the difference in actual % air voids, the AASHTO T 166 method was used for determining  $G_{mb}$  of the test specimens.

**3.4.4. Gyrotory Compaction.** Test specimens were compacted using the Pine Instruments Company gyrotory compactor in accordance with AASHTO T 312 (TSR and Hamburg specimens). The loose hot mix asphalt (HMA) sample was weighed and placed in a stainless steel pan. The pan containing the sample was then placed into an oven and allowed to age for two hours, with hand stirring after the first hour, at the specified compaction temperature. For this study, a compaction temperature of 135°C was specified based on the binder PG number and experience from previous research and field practice. While the HMA sample is aging, a stainless steel mold with a diameter of 150 mm (6 in), consisting of a bottom plate, mold, and top plate, was also heated to the same compaction temperature of 135°C. After the HMA had aged, the mold assembly and HMA sample were removed from their respective ovens and placed on the table located next to the Pine gyrotory compactor. A paper disk was placed in the bottom of the mold and a funnel was placed into the top of the mold. Then the HMA mix was given a quick stir in the pan and the entire sample was then poured into the mold. The sample was poured quickly into the mold to prevent the chance of segregation of the HMA within the mold assembly. After it was poured into the mold, the sample was leveled with a spatula and another paper disk was placed on top. Then the top plate was placed on the top of the HMA sample and the entire mold assembly was placed into the gyrotory

compactor (Figure 3.36). The mold was rotated until the anti-rotation cog was at the 3 o'clock position and the safety door was shut. The compaction was then started and the loading ram applied a 600 +/- 18 kPa (Potosi Mix and Jefferson City In-Spec Mix) or 200 +/- 18 kPa (Jefferson City Out-of Spec Mix) pressure to the mix until the set puck height was achieved. The difference in pressures was due to the difference in stiffness between the Potosi and Jefferson City mixes and the ability to hit the target specimen height during the final gyration of the gyratory compactor. According to AASHTO T 283 Tensile Strength Ratio (TSR), pucks are required to be 95 +/- 5 mm in height and according to Tex-242-F Hamburg pucks are required to be 62 +/- 2 mm in height. For the Potosi mix, the TSR puck height was set at 95.4 mm and the Hamburg puck height was set at 62.4 mm in the Pine Gyratory Compactor. For the Jefferson City In-Spec mix, the TSR puck height was set at 95.5 mm and the Hamburg puck height was set at 62.3 mm in the Pine Gyratory Compactor. For the Jefferson City Out-of-Spec mix, the TSR puck height was set at 96 mm and the Hamburg puck height at 62.7 mm in the Pine Gyratory Compactor. This was done for each mix to ensure the last gyration would provide the target puck height to be 95 mm on the TSR pucks and 62.1 mm on the Hamburg pucks. However, the 95 mm and 62.1 mm target height was not achieved for every test specimen, although they were all within a 0.3 mm range of the target puck height. Once the compaction was complete the HMA puck was extruded from the mold assembly and the puck was cooled by a fan.





Figure 3.36 - Pine Gyrotory Compactor

**3.4.5. Marshall Compaction.** Compaction of test specimens during the trial mix design phase of this study was done by the Marshall Method. Preliminary mixes were first compacted using the gyrotory compactor using 35 gyrations. However the minimum specification for VMA could not be achieved due to the higher compactive effort from the gyrotory compactor. Loose HMA was weighed and placed into a pan and aged for two hours at the specified compaction temperature. For this study, a compaction temperature of 135°C was specified based on the binder PG number and experience from previous research and field practice. While the HMA sample was aging, a steel mold with a diameter of 100 mm (4 in), consisting of a bottom plate, mold, and top plate, was also heated to the same compaction temperature of 135°C (Figure 3.37). It is important to note that the Marshall Method specifies heating all tools to the compaction temperature; therefore all spatulas and funnel were heated in the same oven as the molds. After the HMA had aged, the mold was secured in the compaction pedestal and a paper disk was placed in the bottom of the mold and the funnel in the top of the mold (Figure 3.38).



Figure 3.37 - Marshall Bottom Plate, Forming Mold, and Top Collar



Figure 3.38 - Marshall Compaction Pedestal with Mold Secured in Place

The HMA was removed from the oven, given a quick stir, and poured quickly into the mold to prevent the chance of segregation of the HMA within the mold. The funnel was then removed and using a pointed spatula the HMA mix was spaded around the perimeter of the mold 15 times and 10 times in the center of the mix. Then the mix was mounded on the top and a final paper disk was placed on top. Unlike the gyratory compactor, there is no top plate. Compaction using this method was done by using a 10 lb slide hammer, heated by a hotplate to compaction temp, with a flat tamping face the same diameter of the mold and a throw of 18 inches (Figure 3.39). The HMA was compacted with 35 blows, as specified by MoDOT for BP mix designs, on the first side of the mold. The mold, while holding the partially compacted puck, was then inverted and re-assembled. The final 35 blows with the hammer were applied and the mold/puck assembly was cooled until the mold could be handled by touch of the hand. For this study, it was deemed cool to the touch and ready for extrusion when the mold and puck had reached a temperature of approximately 40°C, as this temperature was not hot enough to burn bare skin but was still hot enough to allow the puck to be extruded from the mold easily without causing further compaction from the jack. The puck was then extruded by using a small jack, seen in Figure 3.40 below, with the face of the jack just slightly smaller than the puck diameter. The puck was fully extruded and placed on a cooling tray until it was at room temperature and ready for further testing.



Figure 3.39 - Marshall Compaction Hammer and Heating Plate



Figure 3.40 - Marshall Puck Extruder

**3.4.6. Tensile Strength Ratio.** A comparison of moisture induced damage was done using the APA (Hamburg) and the Tensile Strength Ratio (TSR) tests. For the TSR test, specimens were compacted in accordance of AASHTO 312 to a specified height of  $95 \pm 5$  mm and 150 mm in diameter. The set of six pucks was separated into two separate subsets with the average air voids between the subsets as equal to each other as possible. The first subset of pucks was labeled as the conditioned subset. These pucks were subjected to 10-26 in Hg of vacuum for a period of 5-10 minutes until they were between 70% and 80% saturated (Figure 3.41).



Figure 3.41 - Vacuum Saturation Setup

If a puck was saturated beyond 80%, the puck was discarded and not used for further testing. With conditioned subset vacuum saturated, the pucks were individually wrapped in plastic film and placed into a plastic bag containing 10 ml of water. The bags were then sealed and placed into a freezer at a temperature of  $-10 \pm 3^{\circ}\text{C}$  ( $0 \pm 5^{\circ}\text{F}$ ) for a minimum of 16 hours. After the freeze cycle, the pucks were removed from the plastic bag, the plastic wrapped was removed, and the pucks were placed into a  $60 \pm 1^{\circ}\text{C}$  ( $140 \pm 2^{\circ}\text{F}$ ) water bath for a duration of  $24 \pm 1$  hour (Figure 3.42).



Figure 3.42 - Water Bath for Conditioned Pucks

After the first water bath cycle, the pucks were then moved to the final water bath at a temperature of  $25 \pm 0.5^{\circ}\text{C}$  ( $77 \pm 1^{\circ}\text{F}$ ) for a duration of 2 hour  $\pm$  10 minutes. For all water baths, there was a minimum of 1 in of water above the puck surface. After the final water bath cycle, the conditioned pucks were removed and individually broken on the Geotest indirect-tensile strength testing machine where a 2 in/min loading rate was applied until the puck was split into two halves (Figure 3.43). The strength of the three conditioned individual pucks were averaged together and labeled as  $S_2$ .



Figure 3.43 - Indirect Tensile Testing Apparatus

The unconditioned subset, or dry subset, was not subjected to saturation, freeze cycling, or hot water bath thawing. The three pucks were placed into individual bags and placed into the  $25 \pm 0.5^{\circ}\text{C}$  ( $77 \pm 1^{\circ}\text{F}$ ) water bath. The specimens were in the bags to prevent exposure to moisture, and were in the water bath for the same duration of 2 hours  $\pm$  10 minutes to obtain the same testing temperature as the conditioned subset. The

pucks were then individually broken on the indirect-tensile strength testing machine where a load was applied until the puck was split into two halves. The strength of the three unconditioned individual pucks were averaged and labeled as  $S_1$ . The Tensile Strength Ratio (TSR) of the pucks was then found by dividing  $S_2$  by  $S_1$  and multiplying the number by 100 to obtain the %TSR. Diameter and thickness for all test specimens were measured using a digital caliper and recorded to the nearest 0.1 mm.

**3.4.7. Specimen Coring.** In this study, a pre-determined amount of loose HMA, based on volumes calculated using mix specific characteristics such as  $G_{mb}$  and  $G_{mm}$ , was compacted in a 150 mm diameter mold using the Pine gyratory compactor to make AMPT test specimens. After cooling to room temperature, the mold and compacted sample was transferred to the core drill. Once the mold was secured, the drill was turned on, the water was turned on, and the 100 mm (4 in.) core drill bit was lowered until the bit reached the top surface of the compacted specimen. While applying adequate pressure, the bit cut through the specimen and created a 100 mm diameter AMPT test specimen as outlined by AASHTO TP 79. Once the cut was complete, the bit was raised and the mold was removed from the drill platform. The cored sample was removed from the drill bit and transferred to the specimen wet saw for further alterations.

**3.4.8. Specimen Sawing.** A wet saw was used to cut the AMPT specimens. The cored specimen was secured in the custom made device on top of the sliding tray located on the wet saw. Both ends were cut to create a 150 mm long specimen for use in the AMPT as specified by AASHTO TP 79.

**3.4.9. APA – Hamburg.** Test specimens for the APA Hamburg test are compacted in accordance with AASHTO T 324. The 150 mm (6 in.) diameter specimens were compacted to 65 mm tall and to a target of 7.0 +/- 1.0% air voids. The specimens were then cooled to room temperature. For the Hamburg test, the specimens must be cut with a wet saw on one side so the two pucks can be placed directly against each other (Figures 3.44 and 3.45).



Figure 3.44 - APA Hamburg Test Specimens

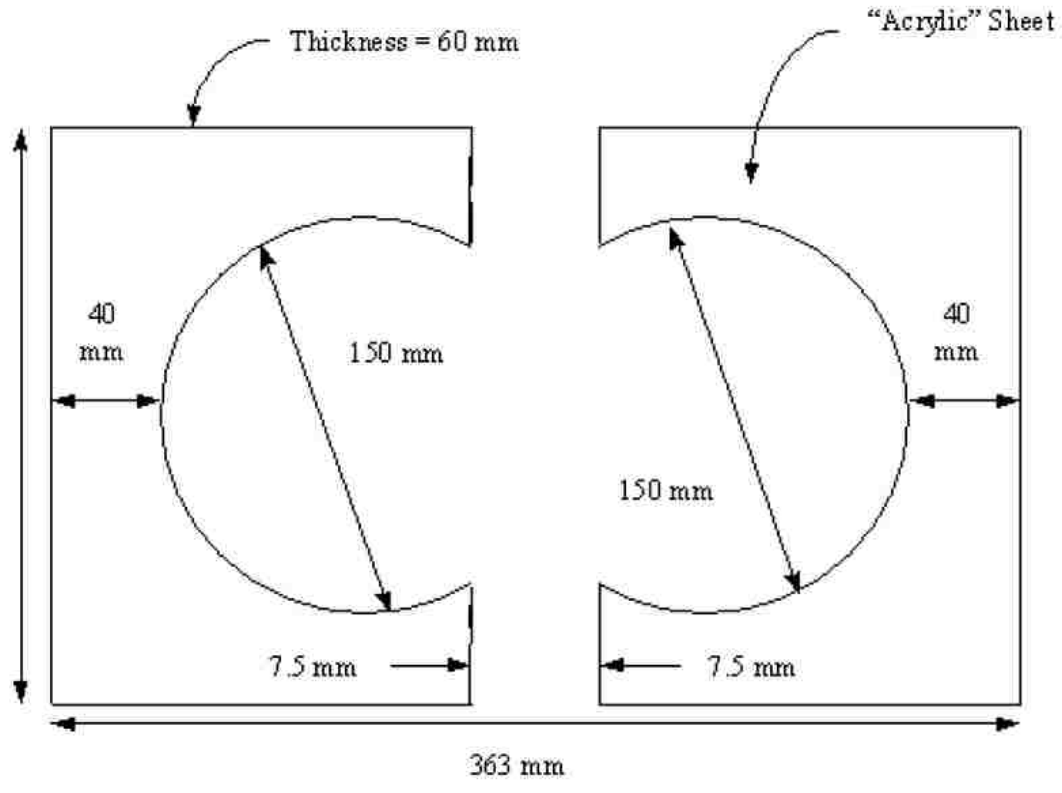


Figure 3.45 - Hamburg Mold Plan View and Dimensions

This creates one long specimen rather than two separate specimens. Based on extensive research done by the Texas Department of Transportation (TxDOT), the gap



between the mold halves should not exceed 7.5 mm. The gap allows the specimens to come together during the pre-compaction phase of the Hamburg test. In almost all cases, the gap will close by the end of the Hamburg test. With the pucks cut, they are placed into the Hamburg molds and the entire mold assembly is placed on the sliding test tray (Figure 3.46). With the molds in place, the tray was locked into place and the mold alignment bar applied to secure molds. The sliding tray was then locked into place. During the Hamburg test, the chamber doors stay open during the Hamburg test cycle. On the control bar the water tray was raised, water pump turned on, and the water heater was turned on to one performance grade below the high temperature of the PG binder number. Initially the water was heated to 58°C for testing as outlined in the APA user manual. Upon literature review of past research and following the Tex-242-F procedure developed by the TxDOT, the temperature was set to 50°C. By setting the water temperature at 50°C, the Hamburg tests did not end prematurely before a stripping slope was developed and provided more usable data. Specimens were heated while submerged for a minimum of 30 minutes (Figure 3.47). Under the Setup tab, Hamburg test was chosen. Within the window that pops up on the screen, 20000 cycles was chosen as the default test length. With the cycle length set, the rutting test was started. During the test, the wheels applied a 158 lb load directly to the test specimens. The software recorded five rut depth measurements every minute along the length (approximately 255 mm slab specimen) of the test specimens and took the average of all five. The average values recorded throughout the test was the data used to generate the number of passes vs. rut depth chart. When the test was complete, the wheels were raised. The sliding test tray was pulled out of the machine and the molds containing the test specimens were removed from the APA machine. The data was then analyzed to determine if the chart (Figure 3.48) showed a stripping inflection point (SIP), the point where HMA specimen began to show signs of stripping due to the water and wheel load action. It was also important to evaluate the number of cycles until 12.5 mm of rut depth had been achieved. According to research done by TxDOT, it is recommended that PG 64-XX mixes should achieve 5000 cycles and have less than 12.5 mm of total rut depth.



Figure 3.46 - APA Hamburg Specimens on Sliding Tray

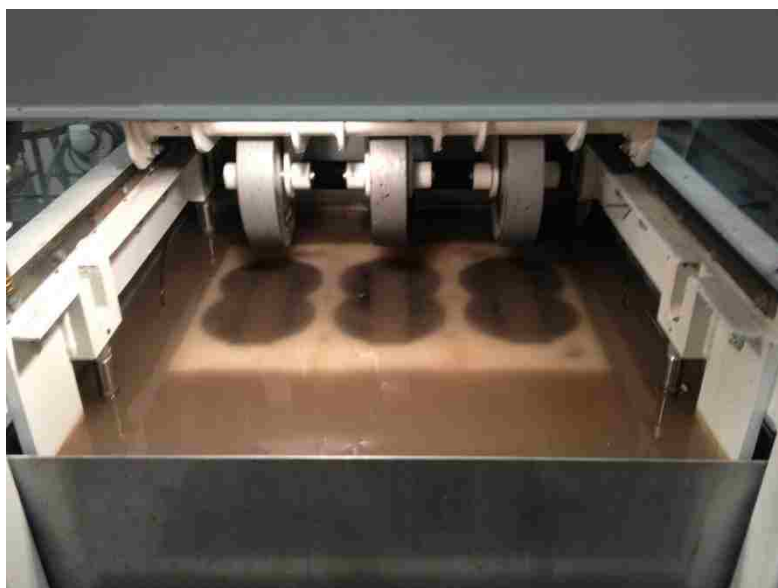


Figure 3.47 - APA Hamburg Specimens Submerged in Water

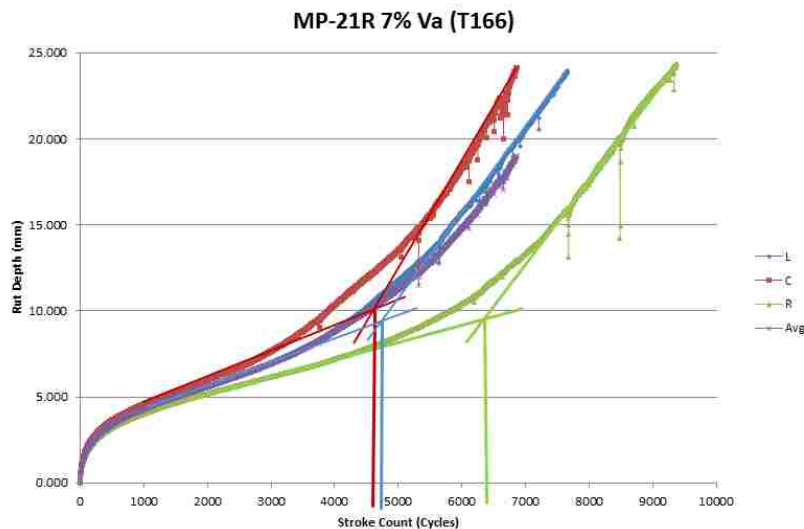


Figure 3.48 - APA Hamburg Results Chart

**3.4.10. AMPT.** The Asphalt Mixture Performance Tester (AMPT) was used for both dynamic modulus and flow number testing in this study. Testing is performed on a set of six, 100 mm (4 in.) diameter by 150 mm (6 in.) tall test specimens at 7 +/- 1.0% air prepared in accordance with AASHTO PP-60. For the dynamic modulus test, gauge points were attached to the specimen by use of a standard two part epoxy (Figure 3.49) and the specimen was conditioned to a series of temperatures governed by the upper binder PG number. Once the initial test temperature was reached, the specimen was loaded into the AMPT test chamber, the LVDTs were attached, chamber was closed (Figure 3.50), and the specimen was subjected to load/unload cycles for three given frequencies (Table 3.7). It is important to note that the lowest test temperature was completed first and the test temperature increased in order as outlined by Table 3.7 (MoDOT Physical Lab Procedure). After the sample was tested at the initial test temperature, it was placed in the next conditioning chamber for the next test temperature. This was done until the specimen was tested at all three test temperatures. Conditioning chamber specimen temps were verified during each change in temperature by using a Sper Scientific 4 channel data logging thermometer and a thermocouple located in the center of a dummy specimen. After completion of testing, the data was analyzed by use of the dynamic modulus results plot as seen in Figure 3.51 below.



Figure 3.49 – Gauge Points Attached on Specimen Side



Figure 3.50 - Specimen Loaded Into Test Chamber with LVDTs Attached

Table 3.7- AMPT Dynamic Modulus Test Temps and Frequencies

PG 58-XX & Softer		PG 64-XX & PG 70-XX Or PG 64-XX Gr. S or H		PG 76-XX or PG 64-XX Gr. V and Stiffer	
Temp °C	Loading Freq. Hz	Temp °C	Loading Freq. Hz	Temp °C	Loading Freq. Hz
4	10,1,0.1	4	10,1,0.1	4	10,1,0.1
20	10,1,0.1	20	10,1,0.1	20	10,1,0.1
35	10,1,0.1,0.01	40	10,1,0.1,0.01	45	10,1,0.1,0.01

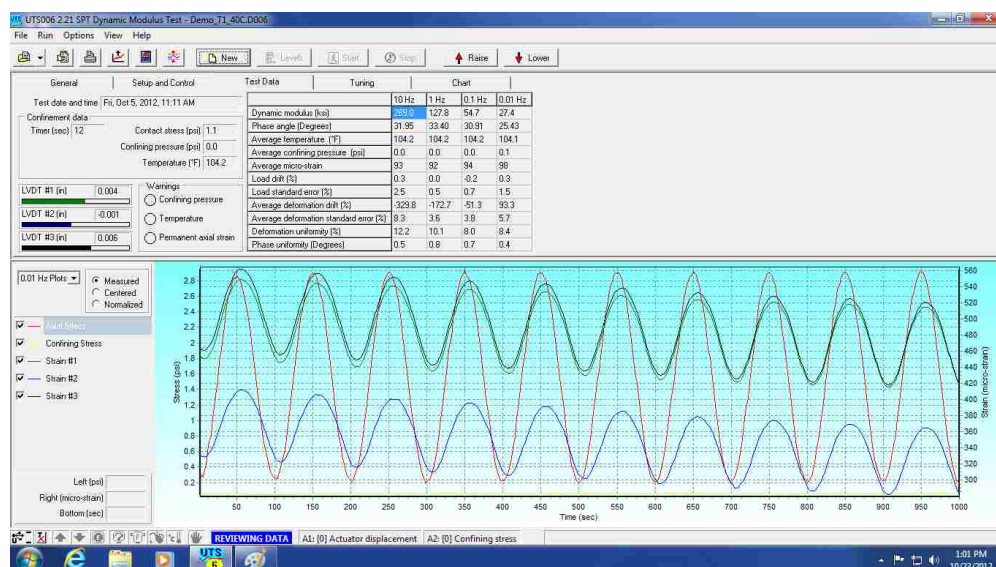


Figure 3.51 - AMPT Dynamic Modulus Results Plot

Once all dynamic modulus testing was completed, the gauge points were removed. The upper and lower platens were then installed and the latex membrane was installed. This was done using the vacuum collar and the gauge point fixing jig, as seen in Figure (3.52 and 3.53) below. Then the specimen assembly was conditioned in the oven set at the desired flow number test temperature. The set temperature is governed by the type of HMA (Table 3.8; MoDOT Physical Lab Procedure). All flow number tests are run as confined unless unconfined is requested.



Figure 3.52 - Specimen with Platens and Vacuum Collar with Latex Membrane



Figure 3.53 - Latex Membrane Installed Over Specimen and Platens

Table 3.8 - AMPT Flow Number Recommended Parameters

Test Condition	NCHRP 9-33 Recommended Values	
Temperature	58°C for Surface Mixes; 55°C for Subsurface Mixes	
Confinement	69 kPa (10 psi) all mixtures	Unconfined (0 kPa), if requested
Axial Stress	690 kPa Deviator Stress 35 kPa Contact Stress	600 kPa Deviator Stress 30 kPa Contact Stress

Once the specimen assembly reached the set test temperature, the assembly was loaded into the test chamber and the chamber was closed. The test specimen was subjected to load/unload cycles until flow of the asphalt mixture was recorded by the software. The data was then evaluated by use of a flow number plot as seen in Figure 3.54 below.

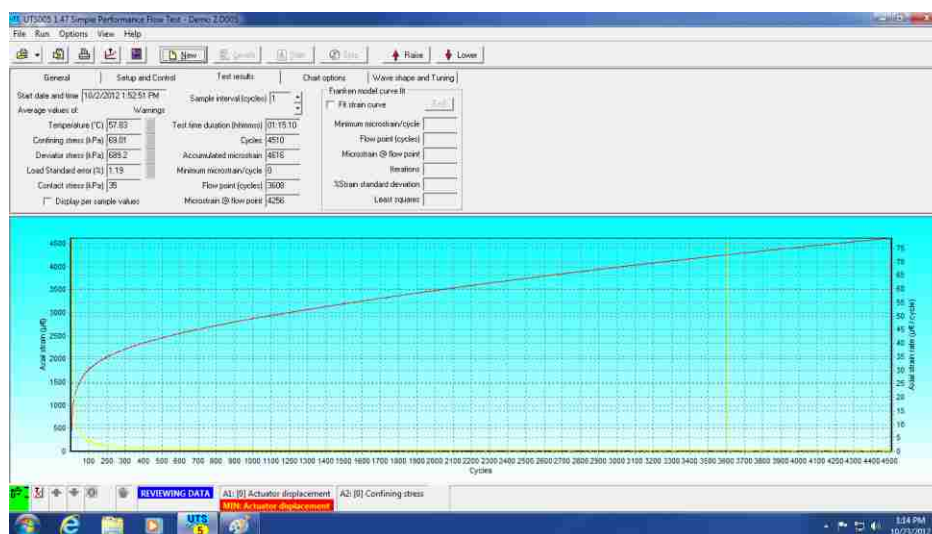


Figure 3.54 - AMPT Flow Number Results Plot

## 4. RESULTS AND DISCUSSION

### 4.1. MIX DEVELOPMENT

Using several fractions, many trial mix designs were made, tested, and evaluated. For example, in this study, 21 trials for the Potosi mix, 26 trials for the Jefferson City In-Spec mix, and 19 trials for the Jefferson City Out-of-Spec mix were evaluated during the mix development phase. Many of the trial mixes exhibited volumetric properties just outside the target volumetrics of 3.5% air, 13.5% VMA, and within the range of 60-80% VFA. The major difficulty was to achieve exactly 3.5% air voids while still maintaining acceptable VMA and VFA, while keeping to the objectives of the relative amounts of screenings, natural sand, deleterious materials, and binder content. Details of each mix are shown in Appendix A. Small changes, such as substituting natural sand for manufactured sand on the small fractions (#16-#100), reducing or adding binder, and compaction types (gyratory vs. Marshall), were made to fine tune the mixes.

The first obstacle was developing the gradation. Using several fractions, a blended gradation was constructed using the MoDOT 401 specifications as a guideline. Small batches were made and tested. Changes to the small fractions were made but the mixes never satisfied the target volumetrics. Next, past industry gradations that satisfied the MoDOT 401 specifications were evaluated. Minor tweaks were made but they also did not achieve the desired target volumetrics. Then a gradation that has been used successfully in MS&T labs was evaluated and tweaked. With the minor changes to the fine fractions of the gradation and percent binder, the target volumetrics were met. The biggest obstacle during all mix trials was the VMA. As binder would be removed or added, the VMA would fluctuate on either side of the 13.5 +/- 0.5% range. This would in turn affect the VFA. By changing the sand fractions of the gradation, the VMA was fine-tuned to lie within the acceptable range.

Compaction type was also another variable that affected the volumetrics of the mixes. Initially the gyratory compactor was used to generate pucks. Even though the machine was set at 35 gyrations, the % air of the pucks were well below the 3.5% target.



After seeing this trend, the compaction type was switched to the Marshall hammer. This provided a lower compactive effort yet still allowed the mixes to be compacted properly. One minor obstacle was encountered during while using the Marshall compaction method. During the testing phase, the original hammer had broken at the base. Several attempts were made to fix the hammer, but ultimately a new hammer was purchased. Upon evaluating the same trial mixes with the new hammer, it was found that the compactive effort of both hammers were slightly different. This meant minor tweaks to the trial mix designs had to be made in order to achieve the proper volumetrics.

Another change made during the mix development stage was the compaction and mixing temperatures. The ovens were initially set at 175°C and 145°C for mixing and compaction, respectively. In an attempt to stiffen the mix during compaction and increase the % air, the temperature of the compaction oven was lowered to 135°C. For the Hamburg testing, the target % air was set at 7%. However, the first set of test specimens (JCD Out-of-Spec) made averaged 6.8%. In order to effectively compare all three mixes, the target % air for all of the two remaining mix types (TSR and Hamburg, Potosi and Jefferson City In-Spec) was changed to 6.8%. Another reason for the change in target % air was an issue that arose during the testing of Hamburg specimens. Due to the large maximum rut depth set in the software, the machine had trouble pushing all three wheels over the mold humps present at large rut depths. This caused the machine to enter protection mode and stop the test. The test could not be restarted and the specimens had to be discarded and remade. This caused some materials to become scarce and resulted in the change of the target % air to 6.8%.

#### **4.2. MIX DESIGN**

The purpose of three mixes was to simulate three quality levels of mix. The higher-quality mix contained tough, low absorption aggregate, and percent passing the #200 at the low end of the 5-12% by mass range set by MoDOT. The mid-quality mix containing less tough, higher absorption aggregate, and the amount of percent passing the #200 in the middle of the 5-12% by mass range set by MoDOT. The low-quality mix containing less tough, higher absorption aggregate, and the amount of percent passing the

#200 at the upper end of the 5-12% by mass range set by MoDOT. The higher-quality mix contained Potosi Dolomite which has a lower absorption (1.4% coarse fraction and 2.1% fine fraction on average) than the Jefferson City Dolomite (3.4% coarse fraction and 4.2% fine fraction on average). For the Jefferson City In-Spec mix (mid-quality mix), the percent passing the #200 was set at 7%. For the Jefferson City Out-of-Spec mix, the % passing the #200 was set at 12%, which is the upper end of the limit set by MoDOT Section 401.3. This was to simulate the worst case scenario and to simulate what the effect of excessive dust may have on physical lab testing and distress predictions. For both Jefferson City mixes, shale was added to some of the gradation fractions to simulate the influence of shale in physical lab testing. Montmorillonite clay was combined with the minus #200 fraction for both Jefferson City mixes to also simulate the influence of clay dust on physical lab testing. The mix gradations can be found in Section 3.3. For the trial mix design, a target of 3.5% air voids and 13% VMA was set. For Hamburg specimens, a target of 6.8% was set. The mix design results for all test specimens can be found in Table 4.1 below (MoDOT Quarterly Report) In general, the literature indicates that among other things, rutting decreases with tougher aggregate, less deleterious shale, lower effective binder content, proper void contents, and lower rounded natural sand content. In this study, the Potosi Dolomite mix rutted the least of the three mixes. This was attributed to less break down of the aggregate (dolomite), zero shale, proper air void and VMA contents, less natural sand, and possibly less clay dust, despite having a greater effective binder content and a lower total dust content. Stripping has been shown to increase with increased break down of aggregate, increased amounts of shale and clay, greater silica-based aggregate content (natural sand), and lower effective binder contents. The Potosi Dolomite stripped the least. This could be attributed to less break down, zero shale and clay dust, less natural sand, and a greater effective binder content, despite a lower calcareous dust content.

Table 4.1 – Final Mix Properties

Parameter	BP-1	BP-1 Good	BP-1 Marginal, In-Spec	BP-1 Marginal, Out-Spec
	Specification	Design	Design	Design
Aggregate Formation		Potosi Dolomite	Jefferson City Dolomite	Jefferson City Dolomite
Aggregate:				
Absorption, %	4.5% max.	1.4-2.0	3.0-4.1	3.0-4.1
LAA	55 max.	26	30	30
Micro Deval		9.6	21.5	21.5
Gradation				
% Passing:				
¾ in.	100	100	100	100
½ in.	85-100	98	98	98
#4	50-70	53	53	53
#8	30-55	30	31	38
#30	10-30	16	13	23
#200	5-12	5.0	7.0	12.0
Mixture:				
Natural sand, %		9.4	23.0	21.0
Shale	2.0% max	0	2.0	2.0
Clay, dispersed	3.0% max.	0	3.0	3.0
Binder, %		5.9	6.1	5.8
Effective binder, %		4.6	4.5	4.1
Effective binder by volume, %		10.7	10.2	9.5
Dust/binder		1.1	1.6	3.0
Air voids, %	3.5	3.5	3.5	1.7
VMA	13.5	14.2	13.7	11.2
VFA	60-80	75.3	74.5	84.5
TSR	70 min.	86	28	23
Tolerance/Action Limit:				
Binder, %	±0.3			-0.3
Passing #8, %	±5.0/10.0			+7.0
Passing #200, %	±2.0/4.0			+5.0

### 4.3. SPECIMEN PAIRING

For both the TSR and Hamburg testing, specimen pairing was a crucial step in obtaining reproducible and applicable results. For TSR testing, the  $V_a$  average of the conditioned subset should equal to the  $V_a$  average of the unconditioned subset, or as close as possible. Careful planning and several combinations were tried until this was achieved, for not only within each individual mix, but also when comparing all three mixes. As shown in the summary data, the averages for the unconditioned specimens were extremely close to each other within all three mixes. Also, the averages for the

conditioned specimens were exactly the same for all three mixes. This provided great specimens for comparative use during TSR testing of all three mixes and eliminated the variable of differing  $V_a$  from being a cause of differing results.

For Hamburg testing, the pucks with similar  $V_a$  averages were paired within each individual mold. This allowed the simulated slab to have uniform rutting across the paired pucks. Due to the pairing, each of the three molds had a different average  $V_a$  (Table 4.2). Also, within each Hamburg test, the left mold always contained the paired specimens with the highest  $V_a$  average, with the center mold containing the next lowest, and the right mold containing the lowest. This eliminated any variability between mixes that the mold location could have on the test results.

#### **4.4. RUTTING**

In this particular study, three mixes containing different gradations and two sources of aggregates were evaluated for rutting potential. All three mixes (PD-5, JCD-7, and JCD-12) were tested for moisture susceptibility (stripping) using two methods: the Hamburg Wheel Tracking Device (HWTD) and the Tensile Strength Ratio (TSR) test. Beginning with the HWTD, three sets of specimens were compacted in accordance with AASHTO T 312 and prepared for the HWDT in accordance with AASHTO T 324-11 and Tex-242-F. All three mixes were subjected to continuous pressure of 158 lbs by the three steel wheels. The wheels moved back and forth until 20,000 cycles had been completed or a maximum rut depth of 24 mm had been reached, causing the wheel to retract up and no longer apply pressure. Even though the Hamburg test generally indicates the moisture susceptibility (stripping) of a HMA, the severity of the creep slope can also indicate the rutting potential of a HMA. For the Potosi Dolomite mix (PD-5), it was evident that severe rutting was present with the creep slope only making it to roughly 5500 cycles (average of all three specimens) on the Hamburg test. As pointed out by the Texas DOT in one of their recent studies, the acceptable minimum cycle count for their PG 64-XX based mixes is 5000 cycles at no more than 12.5 mm of rut depth. As evident in Figure 4.2 below, it can be concluded that the Potosi mix would meet, although barely, the minimum cycle count at the max rut depth of 12.5 mm. Upon examining the In-Spec

Jefferson City Dolomite mix (JCD-7), the cycle count for the average of the three specimens tested was roughly 3040 cycles (Figure 4.2), which was well below the 5000 minimum suggested by the Texas DOT. It was concluded that the poor quality of the Jefferson City Dolomite, as evident by the higher absorption when compared to the Potosi Dolomite and the general overall lower quality of the Jefferson City Dolomite/Shale combination, contributed to the earlier breakdown and deterioration of the JCD-7 mix. Quality of mixes can be determined from a number of test methods. Traditionally, MoDOT considers absorption as the most salient property that defines the quality of aggregate. Other properties that are recognized as important are LAA, MicroDeval, wet ball mill, Iowa Pore Index, vacuum saturated bulk specific gravity, point load strength, sieved slake durability, and plasticity index (Richardson, 2009a; Richardson, 2009b).

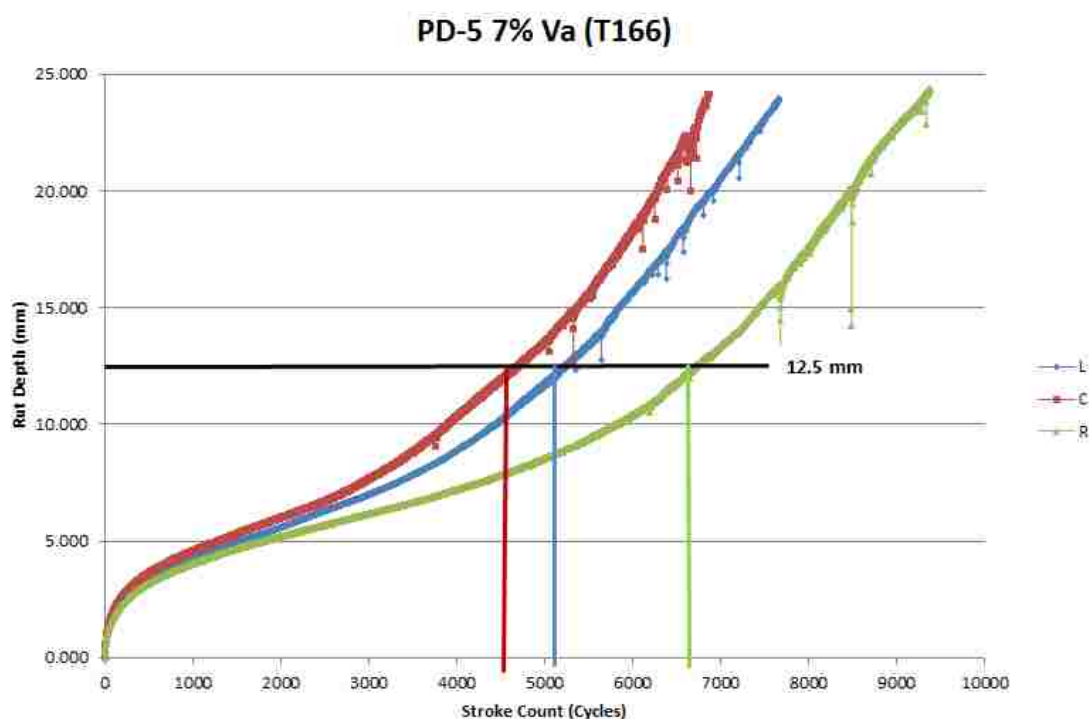


Figure 4.1 - PD-5 Hamburg Rutting Plot



Figure 4.2 – JCD-7 Hamburg Rutting Plot

Upon examining the Out-of-Spec Jefferson City Dolomite mix (JCD-12), the same results of the PD-5 mix cannot be concluded due to the lack of a stripping slope on the data plot. The cycle count for the average of the three specimens tested was roughly 2440 cycles, which was worse than the Jefferson City In-Spec mix (Figure 4.3). This was well below the 5000 minimum suggested by the Texas DOT. As before, it was concluded that the poorer quality of the Jefferson City Dolomite, when compared to the Potosi Dolomite, contributed to the earlier breakdown and deterioration of the JCD-12 mix. Despite the higher dust to binder ratio, which usually results in a stiffer mix that is more resistant to rutting, the Jefferson City mixes contained enough clay and natural sand to act as a lubricant in the matrix. The rut depth summary data for all three mixes can be found in Table 4.2 below. It was also evident among all three mixes that the average percent air between the specimens did affect the rate at which the specimens rutted. During testing, the specimens with the lowest average percent air had a lower rate of rutting.

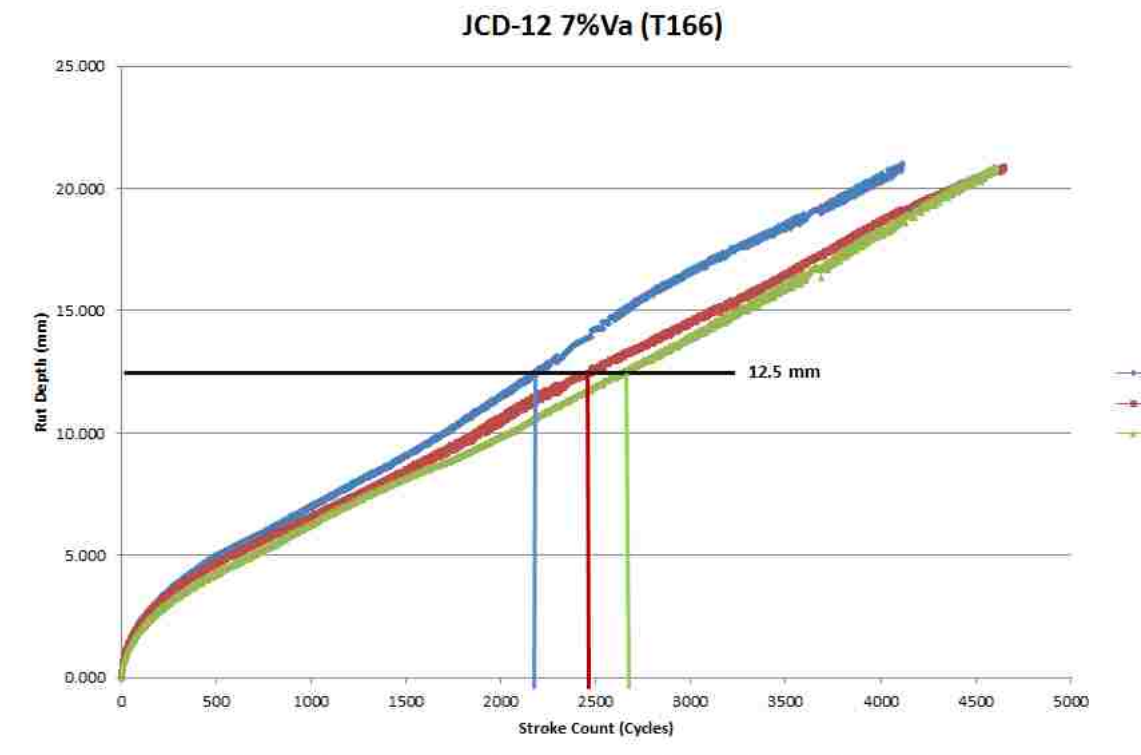


Figure 4.3 – JCD-12 Hamburg Rutting Plot

Table 4.2 - Hamburg Rutting Summary Data

<b>Hamburg Summary Data</b>					
Mix ID	Average Left % Air	Average Center % Air	Average Right % Air	Stroke Count @ 12.5 mm Rut Depth	Stroke Count @ SIP
PD-5	7.04	6.70	6.59	5553	5217
JCD-7	7.00	6.73	6.58	3043	1717
JCD-12	7.06	6.94	6.85	2438	-

#### 4.5. STRIPPING

In general, during the Hamburg test, the observer would usually notice four distinct areas of the results plot: the post-compaction consolidation, creep slope, stripping inflection point (SIP), and stripping slope (Figure 4.4). As noted by the FHWA,

Hamburg post-compaction consolidation is the densification of the HMA test specimens during the first 1000 passes of the steel wheels. The creep slope is accumulation of the deformation due to other factors besides moisture and is used to describe rutting susceptibility. The SIP and stripping slope are the key indicators of moisture damage in the test specimens. The SIP is noted as the point at which the creep slope and the stripping slope intersect and indicates the point at which moisture damage begins. Lastly, the stripping slope is the accumulation of permanent deformation due to moisture (FHWA - Hamburg). Beginning with the Potosi Dolomite mix (PD-5), the test did not reach the full 20,000 cycles before max rut depth was achieved. For all three specimens, the stroke count did not make it past 10,000 cycles and the average cycle count for 12.5 mm of rut depth was roughly 5600 cycles. Upon drawing the creep slope and stripping slope lines, it was found that the average cycle count for the SIP was roughly 5200 cycles (Figure 4.5).

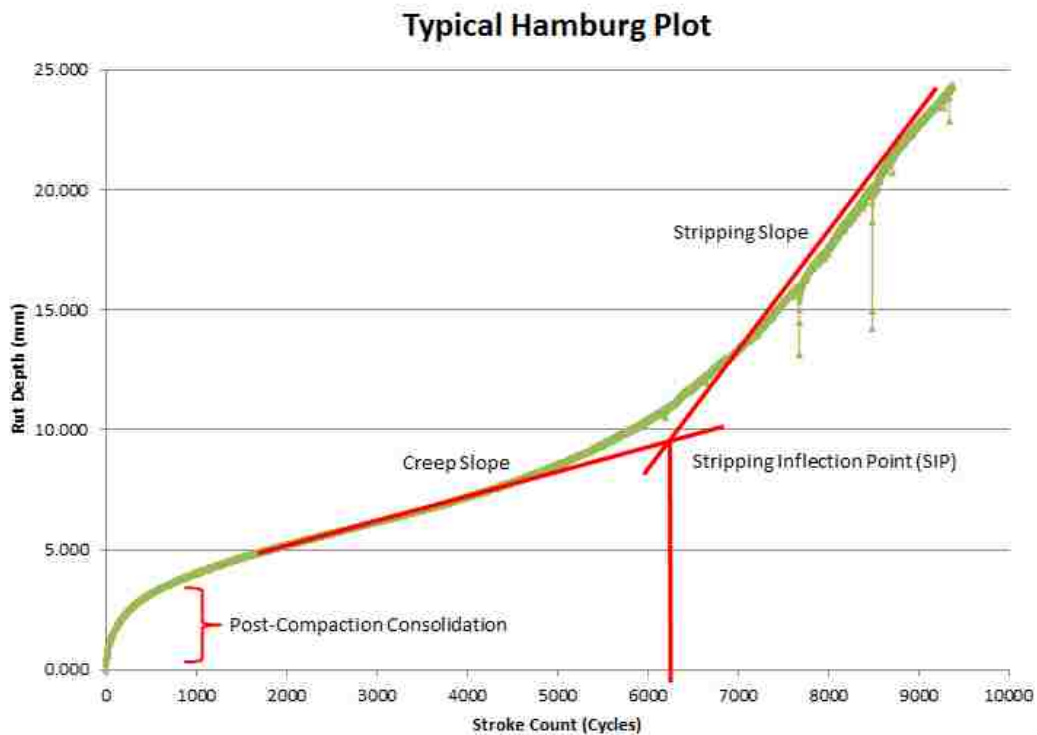


Figure 4.4 - Typical Hamburg Plot with Labels



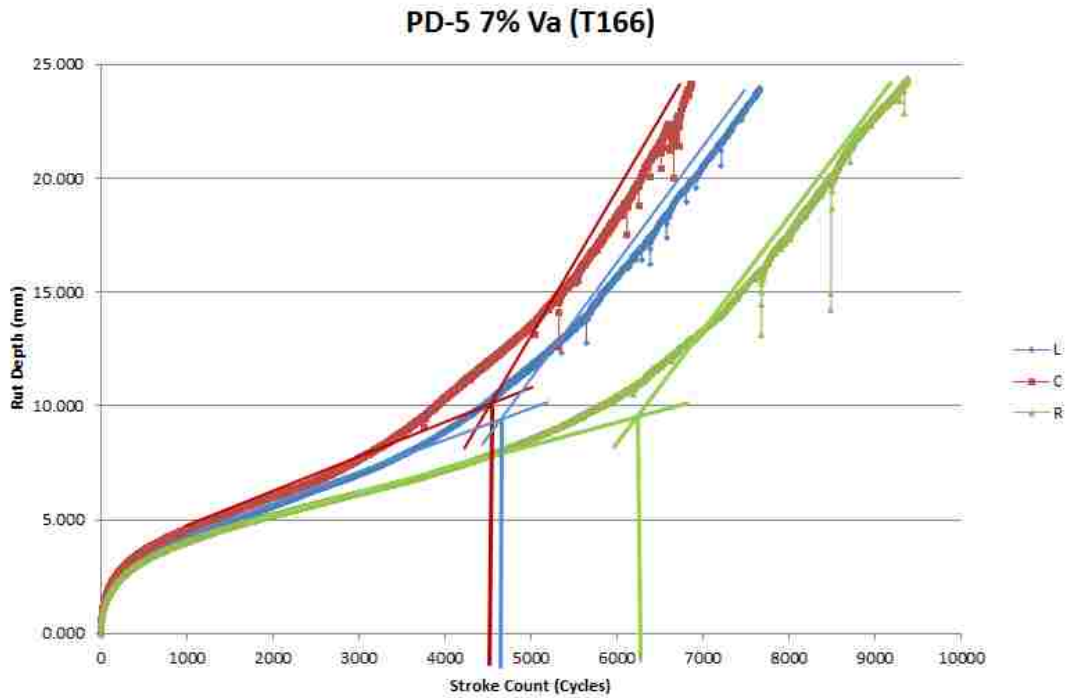


Figure 4.5 – PD-5 Hamburg SIP Plot

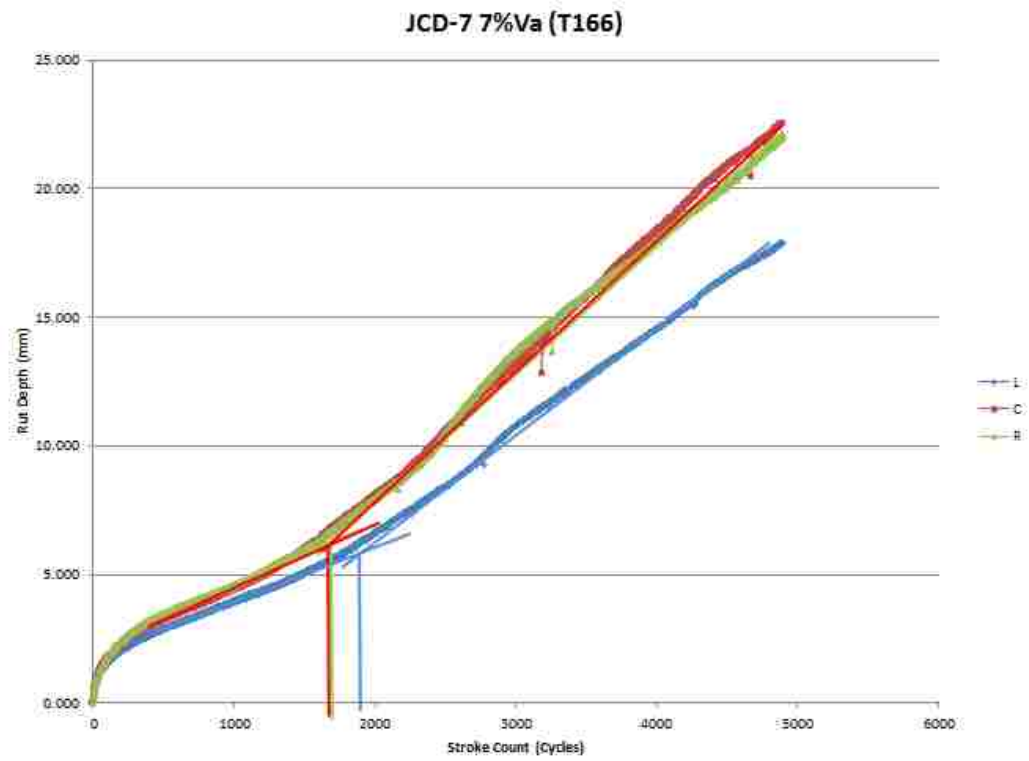


Figure 4.6 – JCD-7 Hamburg SIP Plot

This was considered early when compared to most HMA mixes with higher PG graded binders or modified binders but was expected due to the PG 64-22 binder used with this particular mix. As shown by extensive research by TxDOT, the lower PG binders, which are typically softer, exhibit less resistance to stripping. Upon evaluating the Jefferson City Dolomite In-Spec mix (JCD-7), the results were less favorable than the PD-5 mix. After drawing the creep slope and stripping slope lines, it was found that the average cycle count for the SIP was roughly 1700 cycles (Figure 4.6). This was significantly lower than the PD-5 mix but expected due to the lower quality dolomite being used as well as the addition of shale to the stone matrix and clay to the dust fraction. Upon evaluating the Jefferson City Out-of-Spec mix (JCD-12), the results were even less favorable than the JCD-7 mix. In this study, it was not possible to draw a conclusion on whether the slope was from rutting, stripping, or a combination of both, and therefore a SIP could not be identified (Figure 4.7). If the mix was subjected to more cycles from the steel wheels, a stripping slope may be identified but this was not possible due to the APA machine rut depth limits. It was concluded that the extreme rutting was due to the excessive amount of dust/clay dust in the mix which acted as a lubricant in the matrix causing severe rutting in a short amount of time. The Hamburg summary data can be found in Table 4.3 below. It was also evident that the average percent air between specimens affected the location of the SIP. It was noticed that the SIP of the samples increased as the average percent air decreased. This is expected due to the possibility of less interconnected voids within the specimens, therefore reducing the amount of moisture subjected to the internal structure of the specimens.

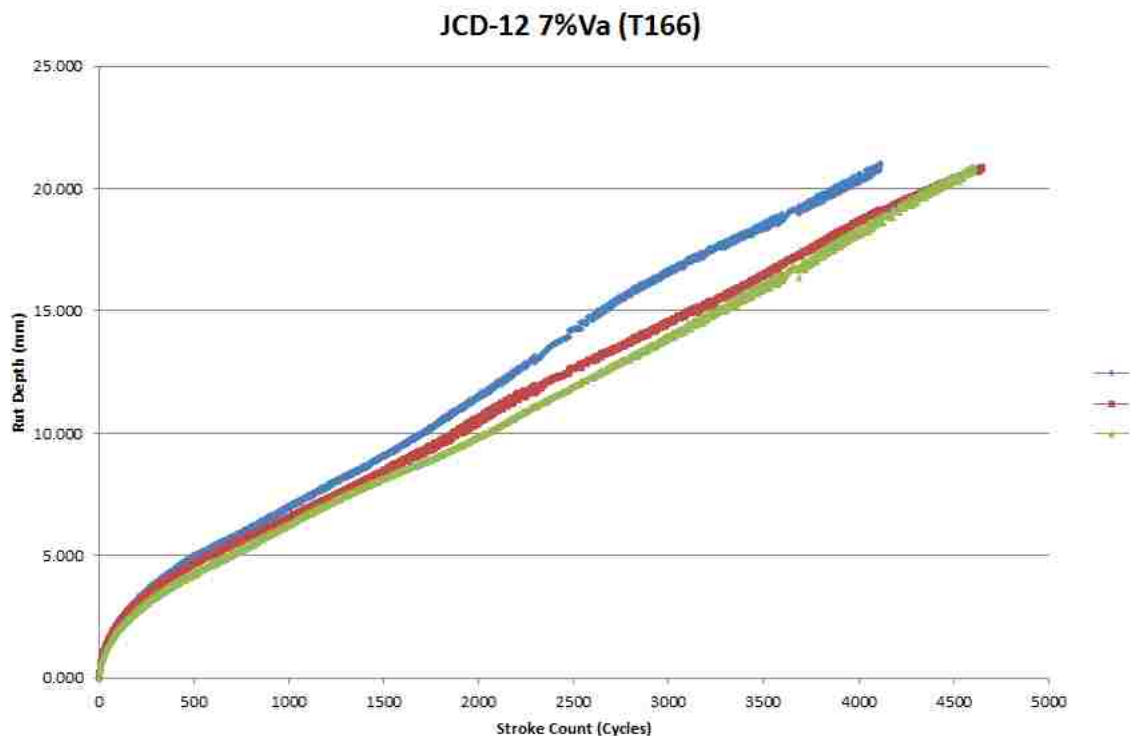


Figure 4.7 – JCD-12 Hamburg SIP Plot - No SIP Present

Table 4.3 - Hamburg SIP Summary Data

<b>Hamburg Summary Data</b>					
Mix ID	Average Left % Air	Average Center % Air	Average Right % Air	Stroke Count @ 12.5 mm Rut Depth	Stroke Count @ SIP
MP-21R	7.04	6.70	6.59	5553	5217
M-26R	7.00	6.73	6.58	3043	1717
M-19R	7.06	6.94	6.85	2438	-

The next phase of testing for moisture susceptibility of the three mixes included the Tensile Strength Ratio (TSR) test. Starting with the Potosi Dolomite mix (PD-5), the TSR measured to be 86%. For MoDOT BP mixes, it is required that the mix must meet or exceed 70% for TSR values to be considered a passing result. The measured TSR was expected for the PD-5 mix due to the mix using the higher quality aggregate of the two types used in this study. Upon evaluating the failure plane of both the conditioned and unconditioned specimens, it was noticeable that the conditioned pucks showed signs of

moisture induced damage by stripping of the binder from aggregate faces (Figure 4.8). This presented the concern that even though the mix passed the 70% TSR minimum, the mix is still susceptible to stripping.



Figure 4.8 – PD-5 Unconditioned Top/Conditioned Bottom

In comparison, the Jefferson City In-Spec mix (JCD-7) did not fare as well. The TSR for this mix measured to be 28%, which was much lower than the PD-5 mix and failed the MoDOT minimum. This was expected due to the lower quality aggregate along with the addition of shale and clay to the mix. These specimens appeared to absorb more water into the matrix. This was physically evident due to the spongy nature of the conditioned specimens as well as the increase in size. On average, the conditioned pucks diameter and height swelled by 3 mm. Upon evaluating the failure plane of both the conditioned and unconditioned specimens, it was noticeable that the conditioned pucks

showed signs of moisture induced damage by stripping of the binder from aggregate faces (Figure 4.9).



Figure 4.9 – JCD-7 Unconditioned Top/Conditioned Bottom

Upon evaluating the Jefferson City Out-of-Spec mix (JCD-12), the results were very similar to the JCD-7 mix. The TSR measured to be 23%, which was the lowest of the three mixes tested in this study. This was expected due to the additional amount of dust/montmorillonite clay, from 7% (JCD In-Spec) to 12% (JCD Out-of-Spec), in the mix gradation. Much like the JCD-7 mix, the lower quality of aggregate, shale, and clay dust contributed to the increased absorption of water during the conditioning phase. This was evident in the spongy nature of the conditioned specimens as well as the physical increase in size. Again, much like the JCD-7 mix, the conditioned pucks swelled in diameter and height by 3 mm. Upon evaluating the failure plane of both the conditioned and unconditioned specimens, it was not noticeable that the conditioned pucks showed severe signs of moisture induced damage by stripping of the binder from aggregate faces (Figure

4.10), although weakening of bonds could still be present. The extreme loss in strength could also be attributed to the spongy nature of the matrix with the excessive dust/clay dust and shale mixture that absorbed large amounts of water and the fracture of the lower quality aggregate. With the large amounts of absorbed water, the freeze/thaw cycle severely weakened the bonds in the matrix.



Figure 4.10 – JCD-12 Unconditioned Top/Conditioned Bottom

As pointed out in research done by Hunter and Ksaibati, the use of different aggregates provided varying TSR results. Generally, it was shown in their research, as well as the research done in this study, that higher quality and more durable aggregate provided higher TSR values. The TSR summary data can be found in Table 4.4 below. As shown, the average wet ITS decreases along with the TSR. This was a good indicator that the lower quality mixes performed poorly after the conditioning cycle, and further

reinforced the detrimental effects of shale, high dust contents, and the addition of clay to the mix.

Table 4.4 - TSR Summary Data

TSR Summary Data					
Mix ID	Average Dry % Air	Average Wet % Air	Average Dry ITS	Average Wet ITS	TSR (%)
PD-5	6.8	6.8	89	77	86
JCD-7	6.9	6.8	95	26	28
JCD-12	6.7	6.8	94	21	23

Another objective of this study was to compare results from the Hamburg test with results from the TSR test to see if there is any correlation between the two (Figure 4.11). The literature indicates that as a mix is more prone to stripping, both TSR values and the number of Hamburg cycles to failure will decrease, thus supporting the hypothesis that there should be a correlation between these two parameters.

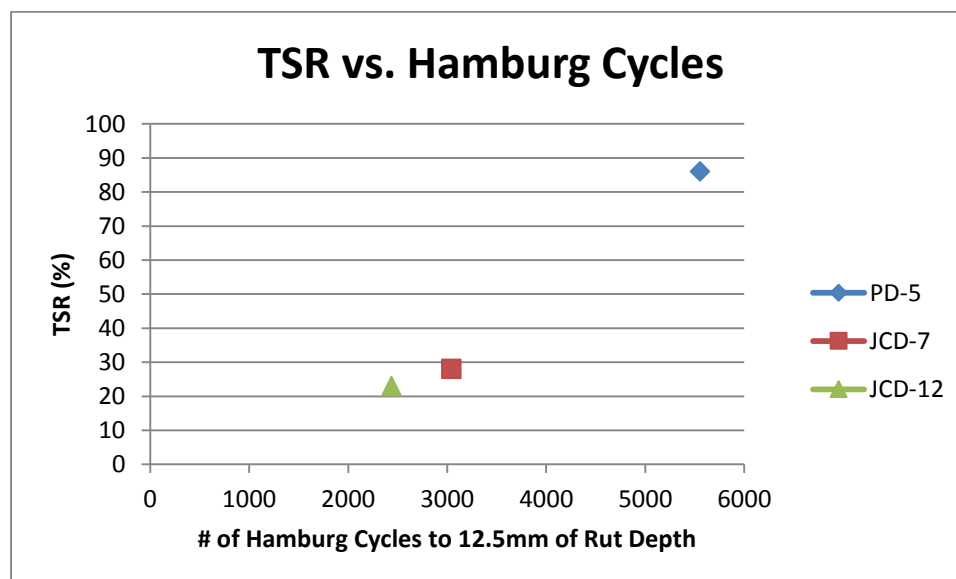


Figure 4.11 - TSR/Hamburg Data Correlation

Hamburg testing data showed that the Potosi Dolomite mix (PD-5) and Jefferson City Dolomite In-Spec mix (JCD-7) did exhibit signs of stripping. However the Jefferson City Dolomite Out-of Spec mix (JCD-12) did not exhibit significant signs of stripping. It is important to note that the number of cycles until the Stripping Inflection Point (SIP) achieved was larger for the PD-5 mix when compared to the JCD-7 mix. This was expected due to the higher quality of aggregate in the PD-5 mix. It was also noticeable that the aggregate in the Jefferson City mixes was severely damaged in the Hamburg testing. Generally the aggregate was broken and fractured through the entire specimen. However, the aggregate in the Potosi mix was not broken or fractured. This was likely due to the Potosi aggregate being more durable. When comparing those observations with the TSR data, the TSR data was generally in agreement. The PD-5 mix did pass the TSR recommended minimum of 70% and upon visual inspection of the failure plane, stripping was present. Moving to the JCD-7 mix, it did not pass the 70% minimum. It was considerably lower and upon visual inspection, stripping was present. However, with the JCD-12 mix, the TSR value was the lowest of the three mixes. Visually there were signs of stripping but the severity could not be determined.

#### **4.6. MEPDG**

For this particular study, all three mixes were evaluated for long term pavement performance using the Mechanistic-Empirical Pavement Design Guide (MEPDG) software. For all three mixes, a 4 in crushed stone base was selected, as well as a semi-infinite thick A-6 subgrade with a resilient modulus of 2515 ksi. The climate of Rolla Missouri was chosen to simulate local weather conditions throughout the calendar year. Along with local weather, an ADTT of 400 was selected to simulate local traffic levels. All three mixes were evaluated to predict fatigue cracking, rutting, and smoothness (IRI) over a design life of 35 years and for both 3 inch and 5 inch asphalt layer thicknesses. Besides the variable of asphalt layer thickness, two levels of air voids were selected; the ideal mix design air void as well as the actual Hamburg air void. Starting with fatigue cracking, several trends appeared. Within the years vs. VFA plot (Figure 4.12), it was apparent that the mixes with the design air voids did not reach the failure set limit of 2000 ft/mi as quickly as the Hamburg air void mixes. This was due to the estimation



equations used to develop the fatigue cracking results over the life cycle of the pavement. As shown in Equation 12 (Section 2.3.3), “M” is a function of effective asphalt content by volume and percent air voids in the HMA mixture, i.e. VFA. As the VFA increased, M increased, thus increasing C (Equation 11, Section 2.3.3). Due to the increase in C, the allowable number of axle-load applications increases, or  $N_{FHMA}$  (Equation 10, Section 2.3.3), thus allowing more axle load applications before fatigue cracking occurs. Among the two design thickness tested, the 5 inch pavement exhibited the same trend as the 3 inch pavement but with slightly longer life expectancies for fatigue cracking (Figure 4.12).

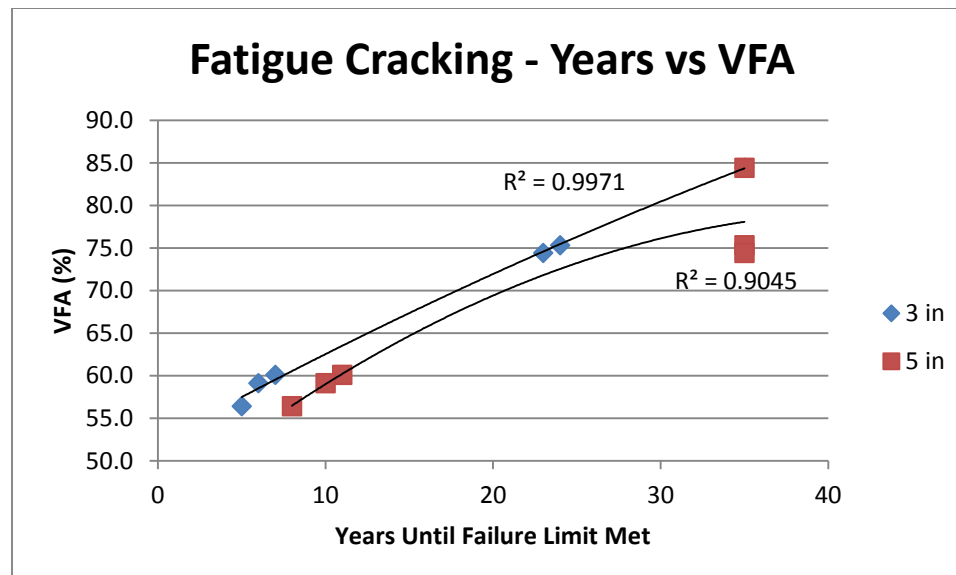


Figure 4.12 - Fatigue Cracking - Years vs. VFA

The next trend that was evident was the years vs. %Va until the fatigue cracking failure limit was exceeded. As seen in Figure 4.13, the mix design air void specimens performed longer than the Hamburg air void specimens. Again, this leads back to the fatigue cracking estimation equations where the VFA plays a role in allowable axle load applications until fatigue cracking occurs. This also agrees with the common knowledge of as air voids decrease, VFA increases, thus improving the cracking resistance of the HMA. Much like the VFA plot, the 5 in pavement exhibited the same trend as the 3 inch

pavement but with slightly longer life expectancies for fatigue cracking. In the study performed by Tarefder and Sumea, they also reported that the fatigue cracking estimations were sensitive to air voids and binder content much like the results found in this study.

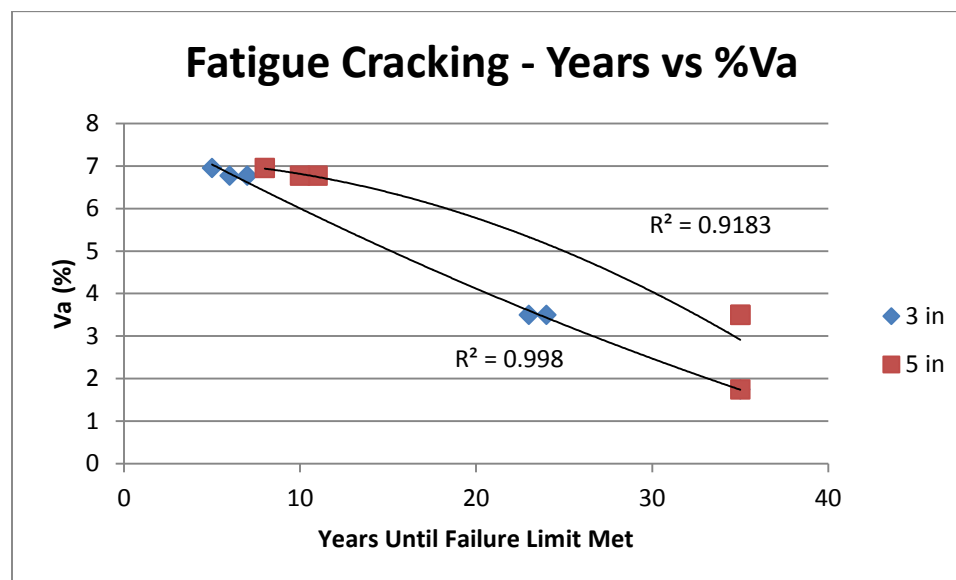


Figure 4.13 - Fatigue Cracking - Years vs. % Va

Moving to the rutting analysis, several trends were noticed but further evaluation was needed. When looking at the rutting years vs. VFA plot (Figure 4.14), as VFA decreased, the number of years until the rutting failure limit was met was decreased. This was opposite of the results expected. In theory, as VFA increases, the amount of rutting, more specifically plastic rutting, should increase due to the larger volume of binder between the aggregate particles. This excess binder often acts like a lubricant between the particles allowing the mix to rut, especially when the pavement is exposed to high temperatures. Due to this trend, further examination of the rutting estimation equations was needed. Looking at Equation 1 (Section 2.3.2), all variables are held constant for the analysis except for the elastic strain calculated by the structural response model, or  $\epsilon_{r(HMA)}$ . This was found by looking at how the MEPDG software estimates the dynamic

modulus,  $E^*$ , of each mix and how the dynamic modulus affects the rutting prediction. For this particular study, dynamic modulus was estimated using the Witczak estimation equation (Bari and Witczak). This equation is a function of VFA, % passing the #200, binder viscosity ( $\eta$ ), the % accumulated on the #4, 3/8 in., and 3/4 in. sieves, as seen below. It is important to note that the MEPDG Level 3 does not use Dynamic Shear Rehometer (DSR) binder data or AMPT data. By using the Witczak equation, it was found that the dynamic modulus for all three mixes were close to each other. It was also evident that as the VFA increased, the dynamic modulus increased (Figure 4.15). The values for the four sieves listed above were similar for all three mixes except for the % passing the #200. For this sieve, the values increase in the order of 5%, 7%, and 12% for the Potosi Dolomite, Jefferson City In-Spec, and the Jefferson City Out-of-Spec, respectively. This showed that the % passing the #200, along with the VFA, has an impact on the estimation of  $E$ . Knowing this, it was shown that an increase in dust creates a stiffer mix, resulting in a mix that was more resistant to rutting over time. Tying this back into rutting prediction equation where strain is the only variable changing, it was evident how the stiffer mixes with greater  $E^*$  results in lower strains for a given load, thus predicting accumulated rutting at a slower rate over time (Figures 4.14 and 4.15). These trends agree with the findings by Tarefder and Sumeer. They also reported a trend of lower rut depths with higher dynamic modulus values. They also found that binder content and air voids affect the rutting prediction.

$$\log E^* = -1.25 + 0.29\rho_{200} - 0.0018(\rho_{200})^2 - 0.0028\rho_4 - 0.058V_a - 0.822 \frac{V_{beff}}{V_{beff} + V_a} + \frac{3.872 - 0.0021\rho_4 + 0.004\rho_{38} - 0.000017(\rho_{38})^2 + 0.0055\rho_{34}}{1 + e^{(-0.603313 - 0.313351 \log(f) - 0.393532 \log(\eta))}}$$

where:

- $E^*$  = dynamic modulus of mix,  $10^5$  psi
- $\eta$  = viscosity of binder,  $10^6$  Poise
- $f$  = loading frequency, Hz
- $\rho_{200}$  = % passing #200 (0.075 mm) sieve
- $\rho_4$  = cumulative % retained on #4 (4.76 mm) sieve

- $\rho_{38}$  = cumulative % retained on 3/8 in (9.5 mm) sieve
- $\rho_{34}$  = cumulative % retained on 3/4 in (19 mm) sieve
- $V_a$  = air void, % by volume
- $V_{beff}$  = effective binder content, % by volume

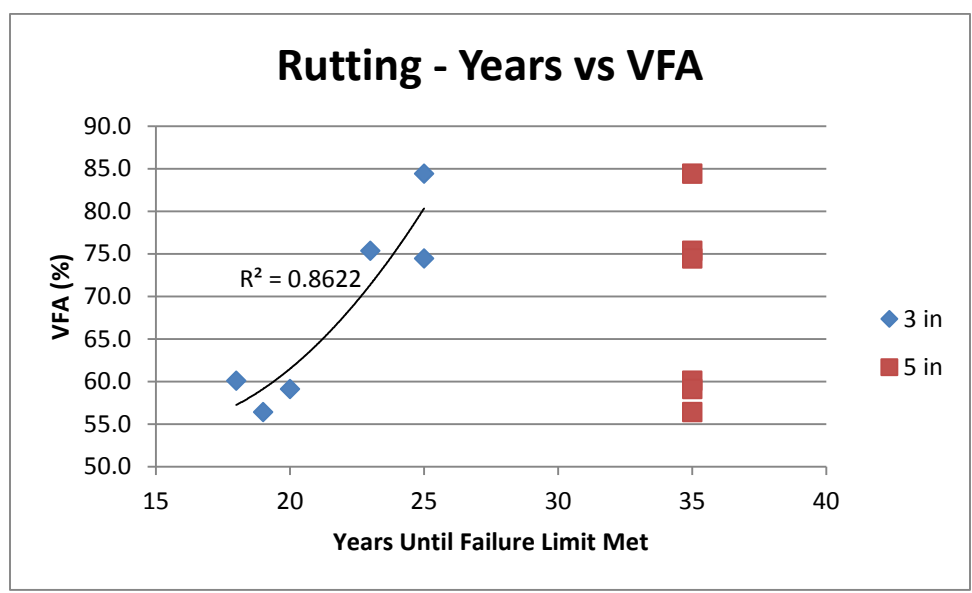


Figure 4.14 - Rutting - Years vs. VFA

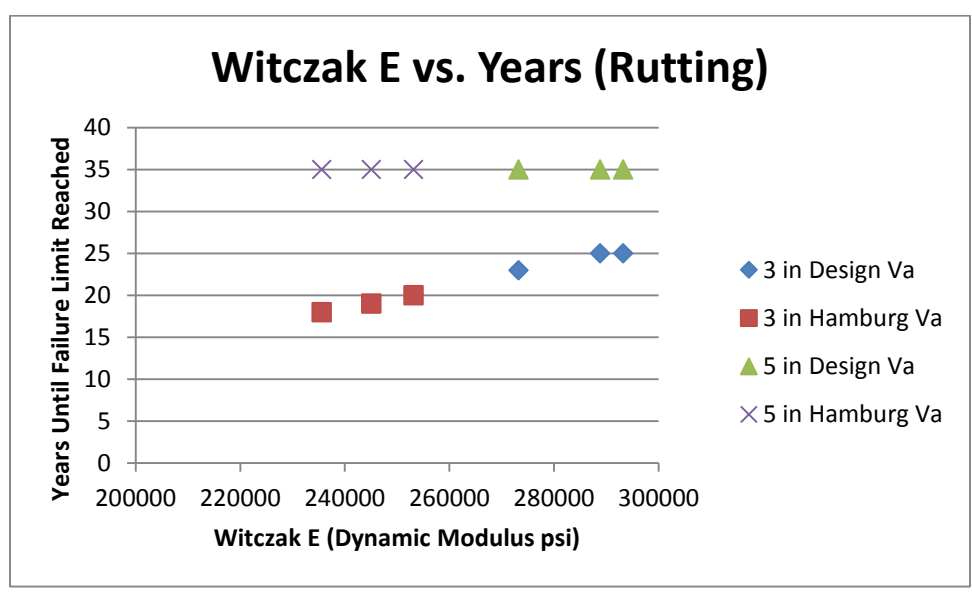


Figure 4.15 - Rutting - Witczak E vs. Years

Lastly, the smoothness (IRI) prediction data was analyzed. To understand the results, it was important to understand the estimation equation used by the MEPDG software. Equation 17 (Section 2.3.4) is a function of the rut depth estimated by the software as well as the total area of fatigue cracking. As shown in Figure 4.16, as VFA increases, the number of years until the IRI failure limit was reached increases. This is expected as the fatigue cracking was reduced as the VFA increases (Figure 4.12). Also, as VFA increased, the rutting rate decreased (Figure 4.12). When looking at the %Va vs. years plot (Figure 4.17), it was also shown that as the %Va decreases, the number of years until the IRI failure limit was reached also increased.

Overall the mix design parameters greatly affected the fatigue cracking, rutting, and IRI predictions generated by the MEPDG software. As show in Table 4.5 below (MEPDG Sensitivity Summary), the change in design air voids vs. Hamburg air voids caused a large change in pavement distress predictions, and in most cases (Fatigue cracking and IRI) cut the number of years by more than half. In the experimental data, the only large change in in VFA was with the JCD Out-of-Spec design air voids, which seemed to impact the fatigue cracking prediction, although this conclusion is clouded by the drop in air voids (3.5% to 1.8%). However, within the design air void and Hamburg air void data, it was indicated that the software was not sensitive to mix design changes.

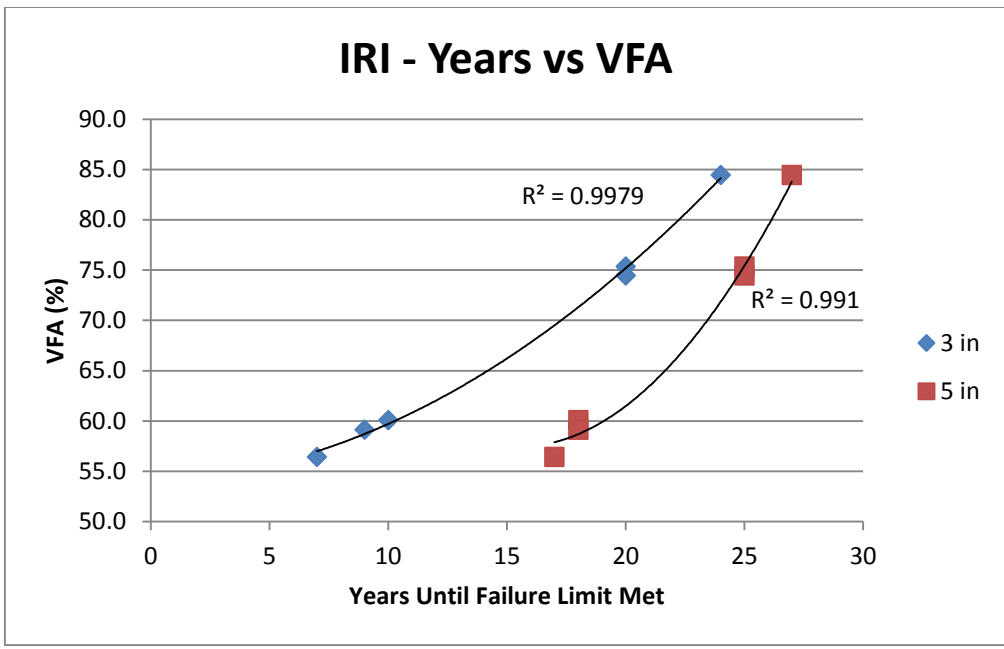


Figure 4.16 - IRI - Years vs. VFA

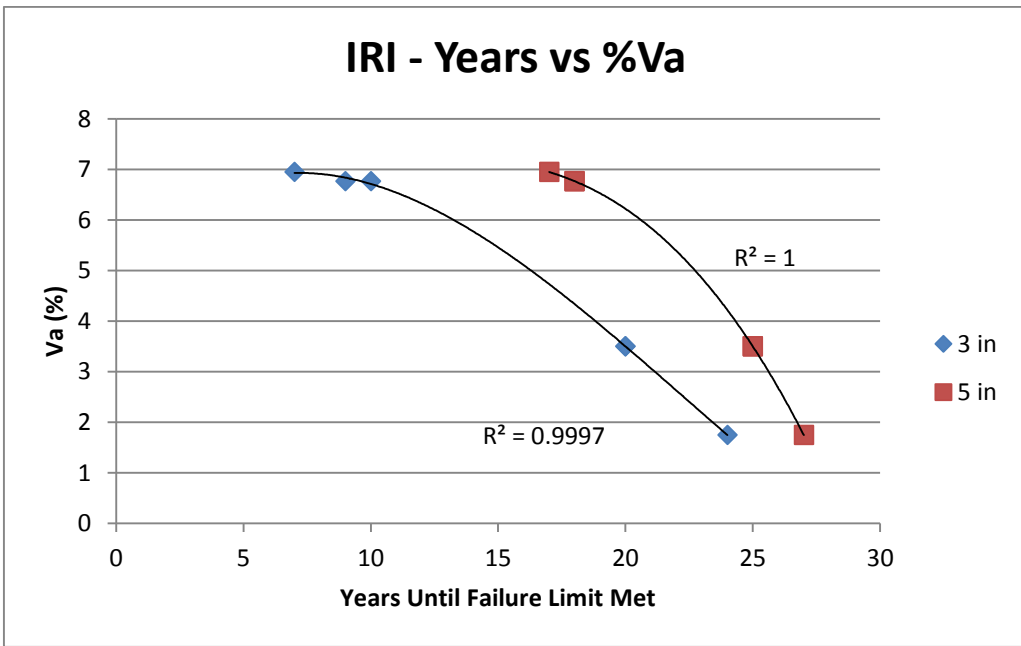


Figure 4.17 - IRI - Years vs. %Va

Table 4.5 - MEPDG Sensitivity Summary

Sensitivity of MEPDG to Mix Design								
Design Air Voids					Hamburg Air Voids			
Mix ID	VFA	Fatigue Life (yrs)	Rutting Life (yrs)	IRI Life (yrs)	VFA	Fatigue Life (yrs)	Rutting Life (yrs)	IRI Life (yrs)
PD-5	75.4	24	23	20	60.1	7	18	10
JCD-7	74.5	23	25	20	59.1	6	20	9
JCD-12	84.4*	35	25	24	56.4	5	19	7

\*Air Voids = 1.8%

#### 4.7. AMPT

For this study, only one mix was tested using the Asphalt Mixture Performance Tester (AMPT). This was due to technical difficulties with the cooling system on the AMPT. Despite the technical difficulties, one trial run of the Potosi Dolomite mix was tested, however, the specimen air voids for the cored specimen was 5.34% which was below the 7 +/- 0.5% tolerance outlined in AASHTO TP 79-11. This specimen was tested at all three standard test temperatures, in order, set by TP 79-11; 4°C, 20°C, and 35°C, respectively. Upon reviewing the results for this specimen, it was observed that the computed dynamic modulus  $E^*$ , decreased as the temperature of the specimen increased (Table 4.6). This was expected as the mix should be less stiff and less resistant to deformation as the temperature increases. This change in  $E^*$  is shown in Figures 4.18-21 below.  $E^*$  values were computed using the Witczak equation for comparison to the values found during AMPT testing. The computed values were higher than the AMPT values (273 ksi computed vs. 189 ksi AMPT).

Table 4.6 - AMPT Summary Data

AMPT Summary Data		
Mix ID	Dynamic Modulus (ksi)	Temperature (Celsius)
PD-5	868.8	4
	189.3	20
	12.2	40

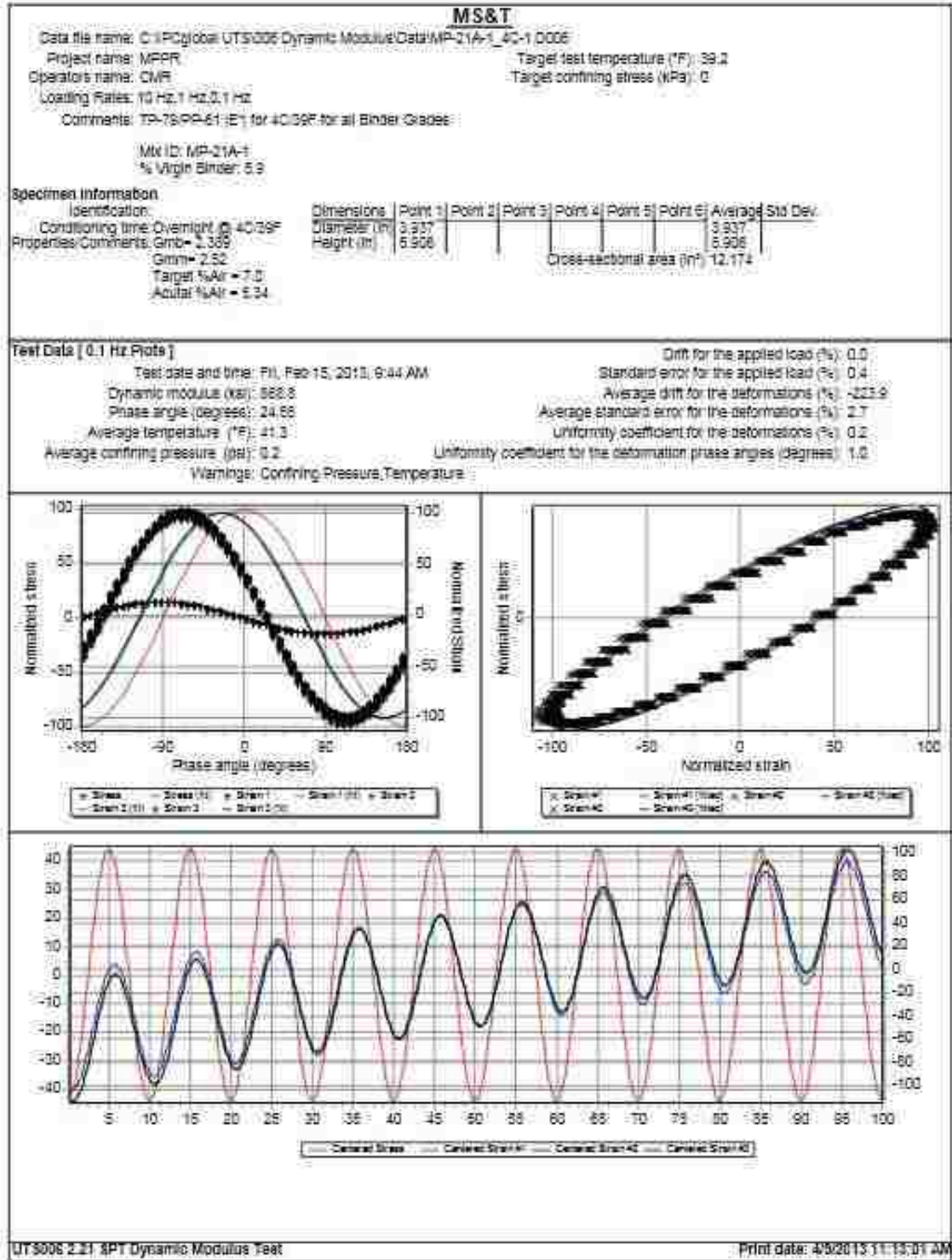


Figure 4.18 – PD-5 - 4°C



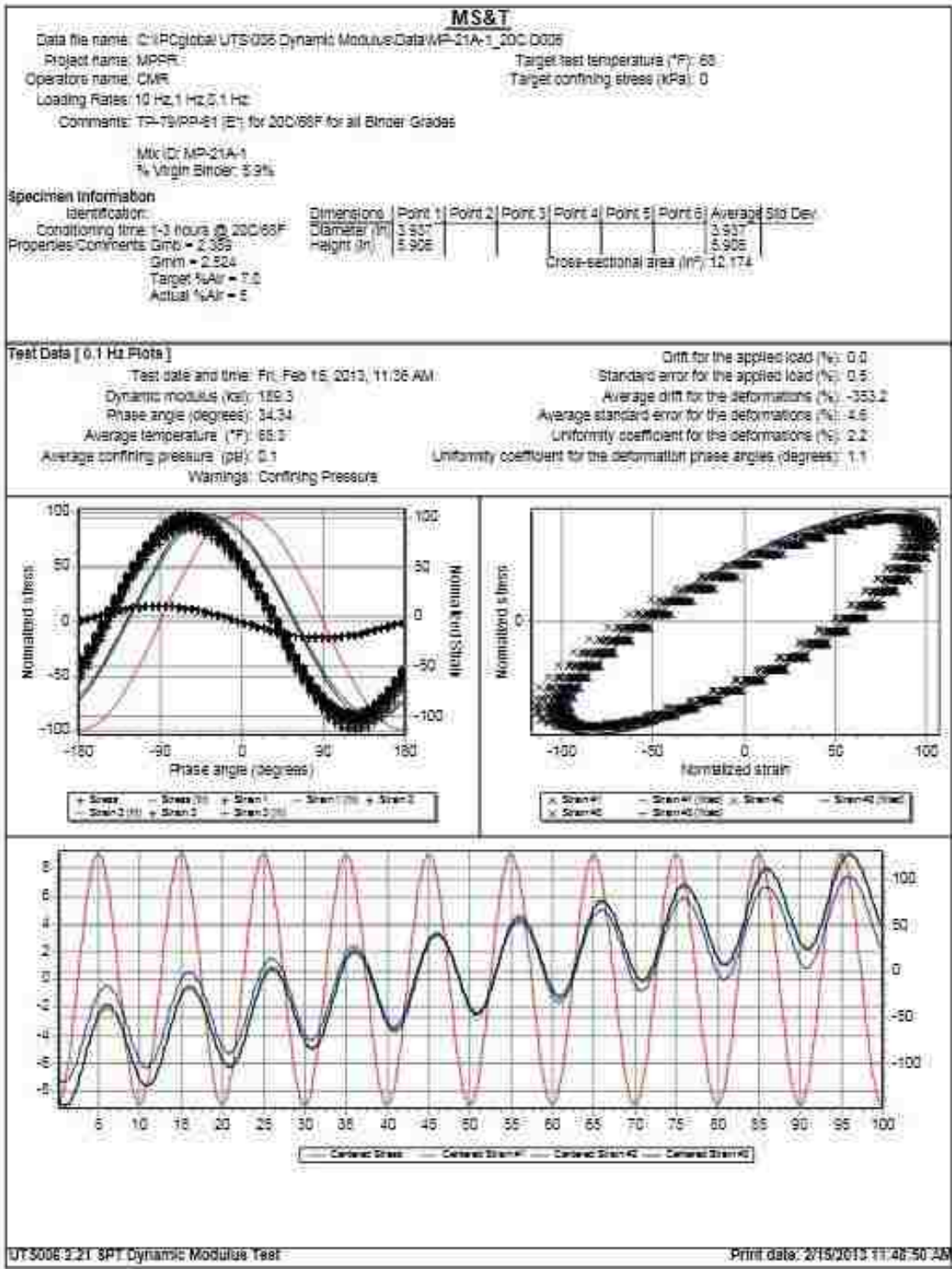


Figure 4.19 – PD-5 - 20°C

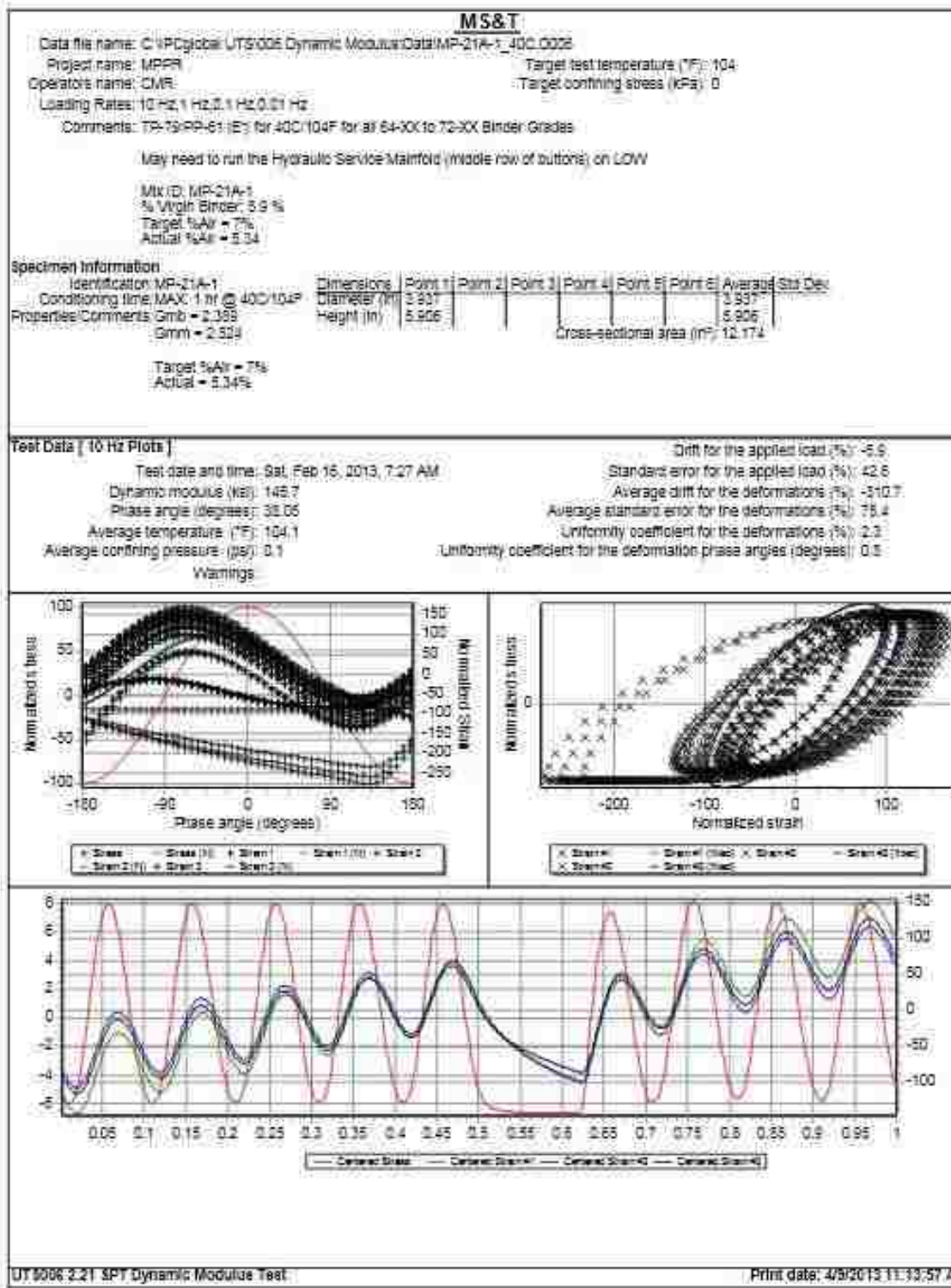


Figure 4.20 – PD-5 - 40°C

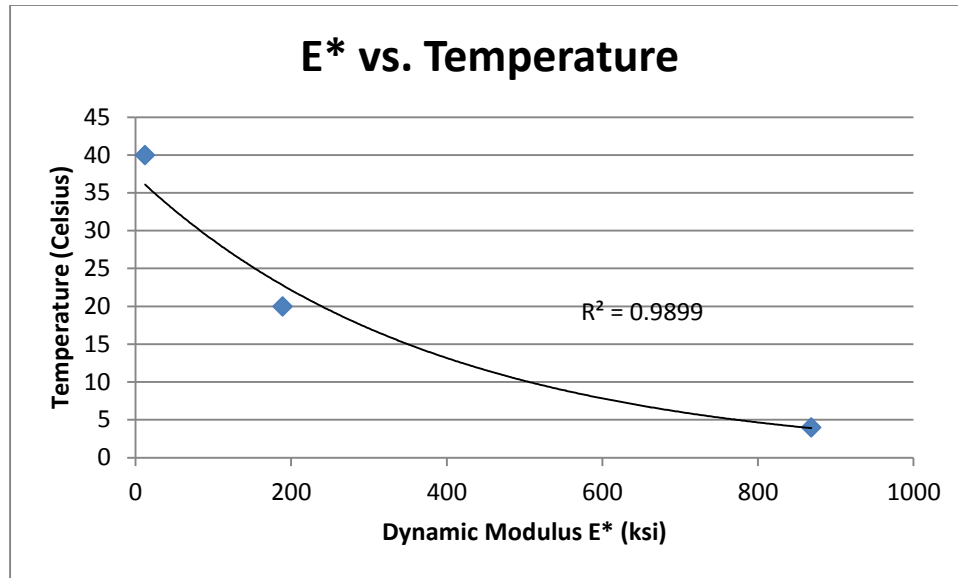


Figure 4.21 – PD-5 AMPT Summary Plot

## 5. SUMMARY AND CONCLUSIONS

### 5.1. SUMMARY

In this study, two sources of aggregates were tested within the requirements outlined by MoDOT specifications for BP-1 mixes. The BP-1 mixes, using Potosi Dolomite and Jefferson City Dolomite, were each used to develop a mix design and then tested them for stripping using the Hamburg Wheel Tracking Device and compared those values with Tensile Strength Ratio results to see if there was a correlation. Also, within the Jefferson City Dolomite mix, two subset mixes were made: an In-Spec mix with an acceptable amount of dust/clay (7%) and shale, and an Out-of-Spec mix with the same amount of shale and clay but at the upper limit of total dust (12%) and a lower binder content. After the Hamburg testing and TSR testing, the test specimens were visually evaluated for signs of binder being stripped from the aggregate surfaces. All test specimens were made in accordance with AASHTO and/or ASTM standards and all test procedures were performed following AASHTO and/or ASTM standards. The initial mix designs and volumetrics were designed using the Marshall Method.

### 5.2. CONCLUSIONS

From this study, it is clear that the use of lower quality aggregate, greater dust and shale contents, and lower effective binder contents can accelerate the stripping susceptibility of the HMA. Also, with excessive dust and shale, the strength within the matrix can be severely decreased when compared to a HMA using a higher quality aggregate. It was also clear that the results from Hamburg testing have a good correlation to results obtained from TSR testing when it comes to ranking several different asphalt mixtures.

**5.2.1. Hamburg.** Upon evaluating the Hamburg specimens, the SIP of the Potosi mix was indicated at a larger cycle count than both Jefferson City mixes, with the In-Spec and Out-of-Spec mix in decreasing cycle count, respectively. It was physically noticeable that the Jefferson City Dolomite was not as durable when subjected to the constant load from the steel Hamburg wheels by evidence of aggregate fractures and

degradation. Looking at the aggregate surface, stripping of the binder was present in all cases even though a SIP was not developed by the data for the JCD Out-of-Spec mix. This was likely due to the extreme rut depth developed during the Hamburg testing and low cycle count where the stripping slope could not develop before the maximum rut depth limit was achieved. The maximum rut depth limit was set at 24 mm for this particular study. It is important to note that at this extreme of a setting, the APA machine could not always complete testing. When the angle of the wheel arms were too extreme from high rut depths, this allowed the wheel to slam into the edges of the mold, causing the carriage motor amps to spike and force the machine into safety mode. By going into safety mode, the machine stopped movement of the carriage and ceased data collection. Fortunately only one mix design, Jefferson City In-Spec, experienced this issue. Data was recorded until the rut depth of 21 mm was achieved and was deemed acceptable for evaluating due to the evidence of a creep slope and stripping slope, which was required to generate a SIP.

**5.2.2. TSR.** For this study all three mixes were tested for their tensile strength ratio. For the Potosi Dolomite mix, the average dry indirect tensile strength (ITS) was 89 whereas the average wet (conditioned) ITS was 77, giving the Potosi mix a TSR value of 86%. This particular mix passed the MoDOT TSR minimum of 70% outlined in the BP-1 specification. This was likely due to the higher quality aggregate, zero levels of shale and clay, lower amount of natural sand, and less overall dust. This allowed less loss of internal strength of the matrix during the freeze/thaw cycle. Although the Potosi mix passed the 70% minimum, the failure plane surface did show signs of stripping of the binder from the aggregate surface. The Jefferson City In-Spec mix, however, did not pass the 70% minimum set by MoDOT. The average dry ITS was 95 whereas the average wet ITS was 26, resulting in a TSR value of 26%. This was likely due to the poorer quality of the Jefferson City Dolomite, Presence of shale and montmorillonite Clay dust, and lower effective binder content. The greater shale/clay dust content was the likely cause of the swelling of the conditioned pucks, which was the result of water absorption into the matrix. The absorption of the water led to damage of the bond between the aggregate and the binder resulting in a severe loss of internal strength. The

Jefferson City Out-of-Spec results were similar, but even less favorable, than the In-Spec mix. The average dry ITS was 94 whereas the average wet ITS was 21, resulting in a TSR value of 23%. Much like the In-Spec mix, this was likely due to the poorer quality and higher absorptive nature of the Jefferson City Dolomite. The gradation also included shale and Montmorillonite Clay, but much more dust overall (12% vs. 7%) than the In-Spec mix. The clay dust along with the shale accounted for the swelling of the pucks during the conditioning process and ultimately leading to the loss of internal strength in the matrix. The decrease of the TSR value from the In-Spec mix was expected due to the lower binder content and possibly the higher amount of dust.

**5.2.3. MEPDG.** Evaluation of all three mixes for distress predictions was done using the Mechanistic-Empirical Pavement Design Guide (MEPDG). For this study, all three mixes were evaluated at the design percent air, both 3 and 5 in pavement thicknesses, Rolla climatic conditions, a subgrade resilient modulus ( $M_r$ ) of 2515 psi, an ADTT of 400, and a design life of 35 years. With these parameters, fatigue cracking, total rutting, and smoothness (IRI) was predicted over the 35 year design life. Looking at the data, it was apparent that the mixes with the design air voids did not reach the failure set limit of 2000 ft/mi as quickly as the Hamburg air void mixes. This was due to the estimation equations used to estimate the fatigue cracking results over the life cycle of the pavement. The main governing factor of the estimation equations was the VFA of the mix. As the VFA of the mix increases, the allowable number of axle-load application increases ( $N_{fHMA}$ ), thus increasing the resistance to fatigue cracking (Equation 10, Section 2.3.3). This was expected as mixes with higher VFA tend to exhibit stronger bonds between the aggregate and binder within the matrix, thus increasing the fatigue cracking resistance. Rutting prediction was also evaluated using the MEPDG software. However, the trend observed by the predictions did not meet expectations. It was expected that as VFA increases, the rutting potential and amount would increase. The trend predicted by software was actually the opposite. In the rutting estimation equation, strain of the pavement layer was the only variable not held constant. Since strain was changing, it made sense that the dynamic modulus ( $E^*$ ) of the mix was influencing the rutting estimation of each mix. This required further exploration and the understanding of how

the software estimated rutting. It was discovered that the software relied on the dynamic modulus estimated by the Witczak estimation equation. This equation relied on the gradation parameters rather than mix specific mechanistic properties to estimate  $E^*$ . Knowing this, as the amount of dust increased, the dynamic modulus increased, thus improving the resistance to rutting over time. This supported the findings of the mixes with higher dust having more resistance to rutting over time. Last, but not least, the smoothness (IR) prediction of the software was evaluated. IRI was a function of the rut depth estimated by the software as well as the total area of fatigue cracking. The results showed as VFA increases, the number of years until the IRI failure limit was reached increases. This was expected as the fatigue cracking and total rutting was reduced as the VFA increases. It was also shown that as the %Va decreases, the number of years until the IRI failure limit was reached also increased. Again, as %Va decreases, the VFA increases, resulting in an increase in the number of years until the IRI failure limit was reached. Overall, the MEPDG predictions did not seem sensitive to the mix variations used in this study.

**5.2.4. AMPT.** For this particular study, only one trial of AMPT testing was completed on the Potosi Dolomite mix due to technical difficulties with the AMPT machine. However, this particular cored specimen had an %Va of 5.34% which was outside the specified %Va range of 7 +/- 0.5%. Despite the low %Va, testing was completed. The specimen was tested at the specified temperatures of 4°C, 20°C, and 35°C respectively as outlined by AASHTO TP-79 for a PG 64-22 mix. Upon evaluating the data, it was shown that as temperature of the specimen increased, the dynamic modulus ( $E^*$ ) decreased. This was expected as the stiffness of the mix decreases as the temperature increases.

**5.2.5. Correlations.** Correlations between the TSR and Hamburg testing were evaluated for this particular study. It was shown that a good correlation between the two existed. Both the TSR and Hamburg Test ranked the mixes in the order of increasing resistance to stripping in the same order of Jefferson City Dolomite Out-of-Spec, Jefferson City Dolomite In-Spec, and Potosi Dolomite, respectively. This was expected

as the Jefferson City mixes both contained shale and Montmorillonite Clay dust in the gradation fractions. With the addition of these two materials, the stripping susceptibility was expected to increase at a faster rate, along with the loss of internal strength of the matrix.



## 6. RECOMMENDATIONS

Due to the presence of shale and montmorillonite clay dust, lower effective binder contents, and lower aggregate quality, the susceptibility of HMA mixes to stripping was increased. Although the Jefferson City mixes failed to meet the recommendations set by TxDOT, the Potosi mix did follow trends experienced by TxDOT with their non-modified binder mixes (PG 64-XX). As shown in other research studies, the addition of RAP and/or stripping agents can further improve the stripping susceptibility of the mixes, especially for low PG numbered binder mixes and plant mixes. Evaluation of the mixes using the MEPDG prediction software further reinforced the Hamburg and TSR testing results showing that the mixes were susceptible to rutting even at the mix design percent air required by MoDOT, with the Hamburg and TSR percent air performing less favorably. If BP mixes or any other low volume, low ADTT mixes are to be used for pavement surfaces, it is recommended that a good quality aggregate that has low absorption, minimal dust, minimal (if any) shale and clay, and sufficient effective binder content be used. This would help reduce weakening of the internal strength of the matrix. It is also recommended that the tests described by Richardson (2009a and 2009b) be considered as aggregate quality indicators for the aggregate being used in future plant mixes. This could provide an early outlook on the behavior of the mix before it is put to use.

## 7. FUTURE RESEARCH

Recommended future research would include the full spectrum of AMPT testing of all mixes to further evaluate the rutting prediction models generated by the MEPDG software. With actual mix specific  $E^*$  data, the rutting prediction would no longer rely on gradation inputs which do not necessarily provide mix specific  $E^*$  values. It is also recommended to perform APA-Rutting testing to estimate rutting resistance of the three mixes in a manner different from Hamburg testing and to see if there is a rutting correlation between the Hamburg and Rutting results. It is also recommended that sustainable materials, such as RAP, be added to the mixes to determine the influence of the materials on Hamburg, TSR, MEPDG, and AMPT results.

APPENDIX A.  
MIX DEVELOPMENT TABLES

Potosi Dolomite Mix Trials													
Trial #	Gradation	Compaction Temperature	Hammer	Pb	minus #200	% Natural Sand	Va	VMA	VFA	d/b	Peffv	Gse	Comments
1	Realistic	140	Old	5.00	4.3	0.0	6.70	14.8	54.5	1.3		2.792	
2	Realistic	140	Old	6.40	5.2	0.0	4.40	15.5	71.9	1.1		2.802	Glossy
3	Realistic	140	Old	6.40	7.0	0.0	3.30	14.6	77.3	1.5		2.799	Glossy
4a	Realistic	140	Old	6.30	7.0	0.0	3.30	14.2	77.2	1.5		2.800	Glossy
4b	NB West	140	Old	5.80	6.5	0.0	5.60	15.2	63.3	1.6		2.803	
5	CE 312	140	Old	6.10	7.0	0.0	3.50	14.2	75.6	1.6		2.794	Glossy
6	CE 312	140	Old	5.90	7.0	18.2	3.30	14.1	76.6	1.6	10.5	2.778	
7	CE 312	140	Old	5.80	7.0	18.2	3.25	13.8	76.7	1.6	10.5	2.765	
8	CE 312	140	Old	5.70	7.0	18.2	2.90	13.3	77.8	1.6	10.6	2.759	
9	CE 312	140	Old	5.55	7.0	18.2	3.25	13.2	75.5	1.6	10.0	2.765	
10	CE 312	135	Old	5.45	7.0	7.6	3.36	12.9	74.0	1.7	9.5	2.779	
11	CE 312	135	New	6.00	7.0	18.2	2.35	13.6	82.7	1.5	11.0	2.770	
12	CE 312	135	New	5.65	7.0	18.2	2.60	13.0	80.1	1.6	10.5	2.760	
13	CE 312	135	New	5.50	6.0	19.2	3.09	13.2	76.6	1.4	10.1	2.757	
14	CE 312	135	New	5.90	7.0	18.2	2.60	13.6	80.9	1.6	11.1	2.757	
15	CE 312	135	New	5.35	5.0	20.0	3.95	13.6	70.9	1.2	9.7	2.758	
16	CE 312	135	New	5.45	5.0	20.0	3.60	13.4	73.2	1.2	9.8	2.762	
17	CE 312	135	New	5.50	5.0	9.4	4.10	13.8	70.4	1.2	9.7	2.774	
18	CE 312	135	New	5.75	5.0	9.4	3.70	14.0	72.9	1.2	10.3	2.779	
19	CE 312	135	New	5.85	5.0	9.4	3.66	14.2	74.0	1.1	10.5	2.780	
20	CE 312	135	New	6.00	5.0	9.4	3.31	14.2	76.6	1.1	10.9	2.771	
21	CE 312	135	New	5.90	5.0	9.4	3.50	14.2	75.3	1.1	10.7	2.782	

\* 35 Blow Marshall for All

Jefferson City Dolomite In-Spec Mix Trials													
Trial #	Gradation	Compaction Temperature	Hammer	Pb	minus #200	% Natural Sand	Va	VMA	VFA	d/b	Peffv	Gse	Comments
1*	Industry #1	Old	Old	7.16	8.2+	0.0	0.00	11.4					Un-washed Screening
2*	Gapped	Old	Old	5.70	8.0+	0.0	0.70	8.9					"
3	Close	Old	Old	5.70	8.0+	0.0	2.30	10.5					"
4	Industry #1	Old	Old	5.70	8.2+	0.0	2.10	10.3					"
5	Industry #2	Old	Old	5.30	5.7+	0.0	2.60	10.1					"
6	Industry #3	Old	Old	5.30	5.0+	0.0	2.90	10.6					"
7	Gapped	Old	Old	6.00	6.0+	0.0	1.70	10.6					"
8	Opt. Industry #1	Old	Old	5.30	5.0	0.0	4.20	11.7					
9	CE 312	Old	Old	5.70	5.0	0.0	5.90	13.5	56.6				
10	CE 312	Old	Old	6.50	5.0	0.0	5.00	14.4	65.2		9.4		
11	CE 312	Old	Old	6.50	6.0	6.0	3.90	13.8	71.9	1.4	9.9	2.656	Added Shale and Clay
12	CE 312	Old	Old	6.20	10.0	6.0	2.50	11.7	79.0	3.9	9.2	2.674	"
13	CE 312	Old	Old	6.10	10.0	6.0	3.30	12.4	73.5	3.9	9.1	2.670	"
14	CE 312	Old	Old	6.00	11.0	6.0	2.70	11.4	76.7	3.9	8.7	2.690	"
15	CE 312	Old	New	6.20	6.0	24.0	4.40	14.3	69.4	1.4	9.9	2.626	"

Jefferson City Dolomite In-Spec Mix Trials (cont.)													
16	CE 312	Old	New	6.20	7.0	24.0	5.50	15.3	63.7	1.6	9.9		Spreadsheet Error
16R	CE 312	Old	New	6.20	7.0	23.0	4.40	14.3	69.0	1.6	9.9	2.676	Spreadsheet Error
17	CE 312	Old	New	6.20	8.0	23.0	3.40	13.4	74.4	1.8	10.0	2.669	Added Shale and Clay
18	CE 312	Old	New	6.15	8.0	23.0	3.10	13.1	76.7	1.8	10.0	2.614	"
20	CE 312	New	New	6.00	8.0	23.0	2.70	12.6	78.3	1.9	9.9	2.658	"
21	CE 312	New	New	5.70	8.0	23.0	3.84	13.2	70.8	2.0	9.3	2.651	"
22	CE 312	New	New	5.70	8.0	18.0	4.27	13.4	68.0	2.0	9.1	2.651	"
23	CE 312	New	New	6.00	8.0	5.0	5.25	13.9	62.1	2.0	8.6	2.670	"
24	CE 312	New	New	6.20	7.0	23.0	3.10	13.6	76.7	1.6	10.4	2.654	"
25	CE 312	New	New	6.05	7.0	23.0	3.70	13.7	73.4	1.6	10.1	2.650	"
26	CE 312	New	New	6.10	7.0	23.0	3.50	13.7	74.5	1.6	10.2	2.654	"

\* 35 Gyration; All others = 35 Blow Marshall

Jefferson City Dolomite Out-of-Spec Mix Trials												
Trial #	Gradation	Compaction Temperature	Hammer	Pb	minus #200	% Natural Sand	Va	VMA	VFA	d/b	Peffv	Comments
12	CE 312	140	Old	6.2	10.0	6.0	2.5	11.7	79.0		9.23	Cloudy Rice
13	CE 313	140	Old	6.1	10.0	6.0	3.3	12.4	73.5		9.14	Cloudy Rice
14	CE 314	140	Old	6.0	11.0	6.0	2.7	11.4	76.7		8.75	Cloudy Rice
19	CE 315	135	New	5.8	12.0	21.0	1.8	11.2	84.5	3.0	9.50	Cloudy Rice

APPENDIX B.  
TEST PROCEDURES

### Determining the Amount of Loose Mix Needed to Make a Specimen at a Desired Height and % Air Voids

The procedure below outlines the steps to calculate the weight of loose mix needed to make a test specimen (puck) at a desired height (95 +/- 5 mm for TSR and 62 +/- 2 mm for Hamburg) and % air void:

1. From previous test data of volumetric TSR or Hamburg pucks, average (preferably at least 3)  $G_{mb}$  values to determine  $G_{mb,meas}$ . The previous test data must be from a mix similar to the mix of interest.
2. Average the mass ( $M_{meas}$ ) of the volumetric pucks
3. Average the puck height (from the gyratory compactor) ( $h$ ) of the volumetric pucks
4. Compute  $G_{mb}$  as if there are no side voids (dimples). Label as  $G_{mb,est}$

$$G_{mb,est} = \left( \frac{M_{meas}}{\left(\frac{\pi d^2}{4}\right) (h)} \right)$$

$h$  = height of puck that  $M_{meas}$  is from

5. Calculate “C”. Use the average of  $G_{mb,meas}$  from step 1 and  $G_{mb,est}$ :

$$C = \left( \frac{G_{mb,meas}}{G_{mb,est}} \right)$$

6. Calculate required mass (g) for desired % air for the puck of interest. Note that the height may be different than that used in Step 3:

$$Mass = \left( \frac{0.93 * \pi * \left(\frac{d^2}{4}\right) * h_x * G_{mm}}{C} \right)$$

$h_x$  = height of puck for test-of interest (cm)

$d$  = diameter of specimen (cm)



$G_{mm}$  = maximum theoretical specific gravity

When placing the loose mix in the pans before aging, it is helpful to place approximately 5 grams extra of loose mix in the pans. This accounts for the small amount of binder that will stick to the pan after aging. Drier mixes may require less than 5 grams. Trial and error is recommended to find the right amount of extra mix added, for the individual mix being tested.

## **Compaction of Bituminous Mixtures Using Marshall Method**

### **MS-2**

#### **Procedure**

This section provides a brief description of the Marshall mix design method, including the preparatory steps before performing the method, and an outline of steps to create the Marshall specimens for testing. Unlike other methods, such as the SuperPave method, the Marshall method only applies to asphalt pavement mixtures containing aggregates with maximum sizes of 25 mm (1 in.) or less (MS-2). For pavement mixtures containing aggregate sizes greater than 25 mm (1 in.) and up to 38 mm (1.5 in.), a modified Marshall Method has been developed. Due to the maximum size used for this research project, only the original Marshall Method will be outlined.

Following the MS-2 manual provided by the Asphalt Institute, a typical starting point is to determine the design asphalt content for a particular gradation by creating a series of test specimens for a range of asphalt contents. It is recommended that the series of test specimens be separated by ½ percent increments to provide data curves that show well defined relationships. Upon choosing the appropriate asphalt content, a minimum of three test specimens of the same gradation and asphalt content shall be made. For example, a test setup with one gradation and three different asphalt contents will require, at a minimum, a total of nine test specimens.

The list below outlines the minimum equipment needed to successfully create test specimens (MS-2):

- Scoop for batching aggregates, mixing spoons or trowel, and balances sensitive to 0.1 grams and with a minimum capacity of 5 kilograms
- Gloves for handling hot equipment, asphalt mixtures, and compacted specimens
- Thermostatically controlled oven for heating aggregate, binder, and equipment
- Flat bottom pans for heating aggregates
- Appropriate size metal bucket and paddle for mixing hot aggregate and binder
- Flat bottom pans for heating loose mix after mixing

- Compaction pedestal consisting of a 200 x 200 x 460 mm (8 x 8 x 18 in.) wooden post capped with a 305 x 305 x 25 mm (12 x 12 x 1 in.) steel plate. The wooden post should consist of a wood species having a dry weight 42 to 48 pcf and be secured by four angle brackets to a concrete slab (Figure 3)
- Compaction mold assembly consisting of a base plate, forming mold, and top extension collar. The forming mold shall have an inside diameter of 101.6 mm (4 in.) and a height of approximately 75 mm (3 in.); the base plate and top collar extension shall be designed to be interchangeable on both ends (Figure 1)



Figure 1 – Base Plate, Forming Mold, & Top Extension Collar

- Compaction hammer with a flat circular tamping face, 98.4 mm (3-7/8 in.) in diameter, 4.5 kg (10lb.) in weight, and made to allow 457 mm (18 in.) height of drop. Hot plate with sand on top surface (Figure 2)



Figure 2 – Compaction Hammer on Hot Plate

- Paper disks that are 100 mm (4 in.) in diameter for compaction
- A specimen extractor with a metal disk that is a minimum of 100 mm (4 in.) in diameter and 13 mm (0.5 in.) thick for extruding compacted specimens from the forming mold.
- Marking pens and/or white-out for labeling compacted specimens after extrusion

Preparing the equipment and materials before compaction is necessary to provide repeatable results and correctly compacted specimens. The list below outlines the steps needed to create successfully compacted specimens (MS-2):

- Dry aggregates to a constant oven-dry weight at 105°C to 110°C
- Separate the aggregate, by sieving, to the appropriate sizes needed for the gradation desired

- Determine appropriate mixing and compaction temperatures for the materials being used for the test specimens. The required temperature for the asphalt to be heated to must be adequate to produce viscosities of 170 +/- 20 centistokes kinematic and 280 +/- 30 centistokes kinematic mixing and compaction temperatures, respectively. These temperatures can be estimated from a plot (loglog y-axis scale for viscosity and log x-axis scale for temperature) of the viscosity versus temperature relationship for the asphalt to be used.
- The compaction mold assembly (bottom plate, forming mold, and collar extension) and compaction hammer face shall be clean and heated to a temperature between 95°C and 150°C (200°F and 300°F). The compaction mold assembly shall be heated in a thermostatically controlled oven to a temperature approximately 15°C above compaction temperature to account for some temperature loss during the time required for compaction. The compaction hammer shall be heated using a hot plate with a layer of fine sand between the plate surface and the hammer surface to ensure even heating and prevent the formation of localized hot spots on the hammer surface.
- Loose mix shall be aged in a thermostatically controlled oven for 2.0 hours before compaction of the loose mix at the designated compaction temperature to simulate short term aging and allow some absorption of the asphalt into the aggregate.

Once the appropriate steps have been taken to prepare the materials, prepare the equipment, and produce the loose mix, the loose mix shall now be compacted following the steps outlined below:

1. Remove compaction mold assembly from oven and secure the assembly in place on the compaction pedestal (Figure 3)



Figure 3 – Mold Secured in Compaction Pedestal

2. Remove funnel, trowel, and spatula from oven and place near the compaction assembly
3. Place one paper disk at bottom of forming mold
4. Place funnel into the top extension collar (Figure 4)



Figure 4 – Funnel in Top Collar

5. Remove loose mix from oven and stir
6. Dump mix quickly into the compaction mold assembly to prevent segregation of mix and then remove the funnel
7. Spade the mix around the edge of the mold assembly 15 times and 10 times in the center of the mix with a spatula
8. Pull mix away from sides of the mold assembly and form a rounded top of loose mix
9. Place second paper disk on top of the rounded mix
10. Place the heated compaction hammer on top of the loose mix and apply the initial 35 blows to the loose mix. Take care to ensure the compaction hammer stays perpendicular to the puck face and produces a level face on the asphalt puck being compacted
11. Remove compaction hammer and top extension collar
12. Invert forming mold, rotate 180 degrees, and place forming mold back onto the bottom plate of the compaction mold assembly
13. Place top extension collar back onto the forming mold
14. Place compaction hammer back onto the top of the partially compacted specimen
15. Apply the final 35 blows from the compaction hammer to the partial compacted specimen
16. Remove top extension collar and place the forming mold containing the freshly compacted specimen on a cooling rack
17. Remove the paper disk from each side of the freshly compacted specimen and label the test specimen
18. Allow the forming mold and specimen to cool until it can be held by bare hands comfortably
19. Once cooled to an acceptable temperature, place forming mold and specimen into extruder and slowly extrude specimen out of the forming mold. Take care to ensure the specimen is not damaged by the extruder in the form of scraping the sides of the specimen or additional compaction from the extrusion plate (Figure 5)



Figure 5 – Marshall Puck Extruder

20. Once fully extruded from the forming mold, place specimen back onto the cooling rack and allow specimen to cool to room temperature before further testing is resumed
21. Repeat steps 1-20 to fulfill the minimum number of test specimens required for the mix design created



**Determining the Density of Hot Mix Asphalt (HMA) Specimens  
By Means of the Superpave Gyratory Compactor  
AASHTO T 312-09**

**Equipment**

To prepare a compacted specimen using the gyratory compactor, the following equipment is needed:

1. Pine Gyratory Compactor or equivalent (Figure 1)
2. 150 mm (6 in) diameter mold with bottom and beveled top plate (Figure 2)
3. Funnel
4. Oven to heat and age HMA
5. Cooling Fan
6. Paper Disks
7. Tools (spatula, trowel, etc; Figure 2)
8. Puck cooling rack



Figure 1 – Pine Gyratory Compactor



Figure 2 – Mold, Bottom Plate, Top Plate, Funnel, Scale, Assorted Tools

### Procedure

1. Mix HMA and weigh out desired weight of mix into appropriate pans for aging. For mix with higher binder content, it is recommended that approximately 5 grams extra be added to each pan. This accounts for the small amounts of binder sticking to the pan in the next step, and allows the loose sample weight to be more accurate.
2. Place pans with HMA into oven for aging; use 2.0 hours unless special aging is requested.
3. While HMA is aging, place the stainless mold, bottom plate, top plate, funnel, and tools (spatula, trowel, etc.) into oven to heat to compaction temperature, which is obtained from binder specific Brookfield temperature-viscosity plot.
4. Once aging time has completed, remove HMA from oven along with the mold with the bottom plate installed.
5. Place first paper disc in bottom of the mold
6. Place funnel into the mold and then remove the pan containing the HMA from the oven

7. Give the HMA mix a quick stir to break up any clumps and loosen mix from the pan
8. Quickly dump the entire pan of HMA into the mold in one fluid motion to prevent any segregation of the HMA mix and then remove the funnel.
9. Using a spatula, level the top of the HMA inside the mold and place the second paper disc on top of the HMA
10. Remove the beveled top plate from the oven and place the plate on the top edge of the mold, beveled side up. Slide the plate across the mold until it drops into the mold on its own.
11. Move the mold assemble to the gyratory compactor. Orient the mold to where the anti-rotational cog is facing the operator, or at the 6 o'clock position (Figure 3).
12. Open the front door of the gyratory compactor and push the mold assembly until it is all the way back into the machine. Then rotate the mold assembly until the anti-rotational cog is between the 12 and 3 o'clock position (Figure 4). Close the front door of the gyratory compactor.



Figure 3 – Mold at 6 o'clock Position



Figure 4 – Mold at 3 o'clock Position

13. Verify that the green ready light is on and all settings are entered into the screen properly. Entered settings include selecting the proper ram pressure, the desired puck height in mm or number of gyrations, and specimen size of 150 mm or 100 mm. (Typically 600 kPa for stiff mixes and less for lower quality mixes. Some trial and error will be necessary to find what pressure works best for the individual mix. The height entered into the gyratory compactor should be slightly above the desired height for the compacted specimen. Much like the ram pressure, some trial and error will be necessary to find what entered height works best for the individual mix. This accounts for the drop in height on the last gyration.)
14. Press the “Start” button and allow machine to complete the full test.
15. Once the test is complete and green light is lit again, open door and remove mold assembly from the machine.
16. Slide the mold assembly over to the puck extruder and extrude puck until top plate is shown above the top edge of the mold. Remove top plate and paper disc.
17. Extrude puck halfway and allow fan to cool specimen for a minimum of 10 minutes.

18. Extrude puck fully and allow another cooling period of 10 minutes minimum (Figure 5).



Figure 5 – Puck Fully Extruded

19. To remove puck, grab the side and pull the puck towards the operator. **DO NOT LIFT PUCK DIRECTLY UP**
20. To carry puck to cooling rack, hold puck on its side and place the puck upside down on the cooling rack. Remove the bottom paper disc and mark puck with proper identification.
21. Allow bottom plate to fall into the mold and place mold in a proper storage area
22. Allow puck to cool to room temperature (Typically overnight) before performing any further testing.
23. Repeat steps above for replicate pucks.

**Standard Practice for Rapid Drying of Compacted Asphalt  
Specimens Using Vacuum Drying Apparatus  
ASTM D7227 / D7227M – 11**

**Equipment**

To rapidly dry a compacted asphalt specimen using vacuum, the following equipment is needed:

1. Coredry Automatic Vacuum Drying Chamber
2. Lint Free Cloth

**Procedure**

1. Turn on CoreDry machine
2. Remove vacuum chamber lid and place asphalt specimen on its side on top of the basket (Figure 1). Then place lid back on top of chamber



Figure 1 – Vacuum Chamber with Specimen

3. Remove cold trap lid and wipe the chamber with a lint free cloth to remove any moisture (Figure 2). The place lid back on top of cold trap



Figure 2 – Cold Trap Chamber with Divider

4. Select appropriate program from menu. Custom programs with different drying time and number of drying cycles can be programmed into the CoreDry, along with the cold trap cycle length.
5. Check to make sure both lids are in their proper place. Then press “start”
6. Machine will cycle between vacuum and pressure until 6 mmHg or less is achieved. Once 6 mmHg or less is achieved, the machine will automatically stop and the sample will be free of moisture.

**Bulk Specific Gravity and Density of Compacted Bituminous  
Mixtures Using Automatic Vacuum Sealing Method  
ASTM D 6752 – 11**

**Equipment**

To measure the bulk specific gravity of a compacted HMA specimen, the following equipment is needed:

1. Corelok Automatic Vacuum Chamber
2. Polymer bags
3. Weigh-below and water bath setup

**Procedure**

The Corelok vacuum chamber, manufactured by InstroTek, has the capability to measure the bulk specific gravity of both 100 mm (4 in) and 150 mm (6 in) diameter compacted or cored cylindrical specimens.

1. Compact and cool specimen to room temperature.
2. Place cooled puck on scale and record the initial dry weight
3. Remove puck from scale and place the polymer bag to be used in the vacuum process on scale. Record bag weight.
4. Open the Corelok chamber and adjust filler plates to appropriate height.  
Appropriate height should be where the polymer bag will be level with the seal bar.
5. Place the specimen sliding plate on top of filler plate(s) (Figure 1).
6. Place polymer bag inside the chamber with the open edge of the bag over the seal bar.
7. Place puck inside polymer bag and center the sliding plate under the puck and bag assembly (Figure 2).
8. Ensure that the bag edges are not touching the chamber sides and that the end of the bag is approximately 1” over the seal bar
9. Turn on Corelok machine and enter “Program 1”





Figure 1 – Filler Plate & Sliding Plate in Corelok Chamber

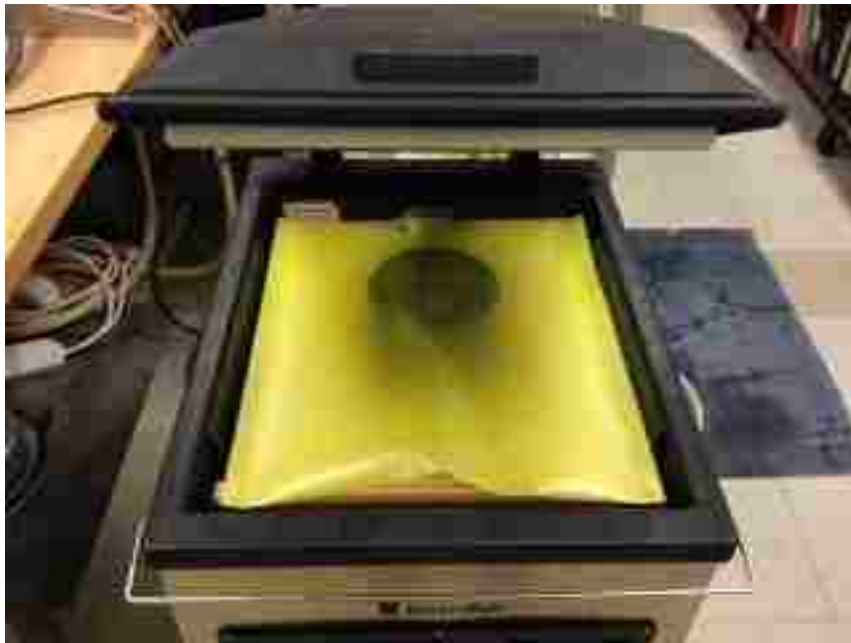


Figure 2 – Bag and Puck Placed in Chamber

10. Once the program choice has been selected, close the chamber door and allow the vacuum process to begin.

11. After the vacuum process is complete, the chamber door will open automatically. Remove the bag assembly and check for possible tears, punctures, or an inadequate seal. If any of the previous problems are identified immediately remove the puck, place in a new bag, and repeat the previous steps 1-11 of the procedure.
12. If the bag assembly is acceptable, place the bag assembly in the water bath on top of the weigh below basket. Record the specimen weight under water (Figure 3).



Figure 3 – Weigh-below and Water Bath Setup

13. Next, remove the bag assembly from the water bath, cut the bag open, and remove the puck.
14. Re-weigh the puck and record the final dry weight. If the weight is greater than the initial dry weight by more than 5 grams, dry and retest the puck.
15. With all the final weights recorded, calculate the bulk specific gravity of the specimen.

#### Calculation

The Bulk Specific Gravity is calculated by using the equation below:

$$\text{Bulk Specific Gravity} = \frac{A}{[C + (B - A)] - E - \left(\frac{B - A}{F_T}\right)}$$

- A* = initial mass of dry specimen in air, g  
*B* = mass of dry, sealed specimen, g (A + mass of plastic bag)  
*C* = final mass of specimen after removal from sealed bag, g  
*E* = mass of sealed specimen underwater, g  
*F<sub>T</sub>* = apparent specific gravity of plastic sealing material at 25°C

### Precision

Single operator 1s = 0.0124

Multi-laboratory 1s = 0.0135

**Resistance of Compacted Hot Mix Asphalt (HMA)  
To Moisture-Induced Damage (TSR)  
AASHTO T 283-07**

**Equipment**

To measure the Tensile Strength Ratio (TSR) of an asphalt specimen, the following equipment is needed:

1. Vacuum saturation system complete with vacuum pump, timer, scale, and vacuum chamber
2. Plastic wrap for conditioned specimens and plastic bags for both conditioned/unconditioned specimens
3. Freezer capable of  $-18 \pm 3^{\circ}\text{C}$  for a minimum of 16 hours
4. Two separate water baths capable of holding at  $60 \pm 0.5^{\circ}\text{C}$  and  $25 \pm 0.5^{\circ}\text{C}$
5. Indirect tensile strength loading apparatus
6. Graduated cylinder with at least 10 ml capacity
7. Plastic bags to hold compacted TSR test specimens

**Procedure**

Loose mix sample prep:

1. It is recommended that loose mix samples are obtained from the roadway or plant discharge. However, samples can also be obtained from the truck
2. Approximately 175 lbs of loose mix is required for splitting and creating the 6 test specimens required for the TSR test
3. Using a quartermaster (Figure 1), split the bulk loose mix sample into four equal samples. Remove opposing two quarters and combine as retained split. If the quartermaster step is not required, approximately 75 lbs of loose mix is needed



Figure 1 – Quartermaster

4. Combine remaining two quarters and quarter sample again
5. Combine opposite two quarters, producing two piles
6. Place each pile in its own separate square pan
7. Quarter each pile using the, metal quartering sheets. Now there are 8 separate splits (Figure 2)

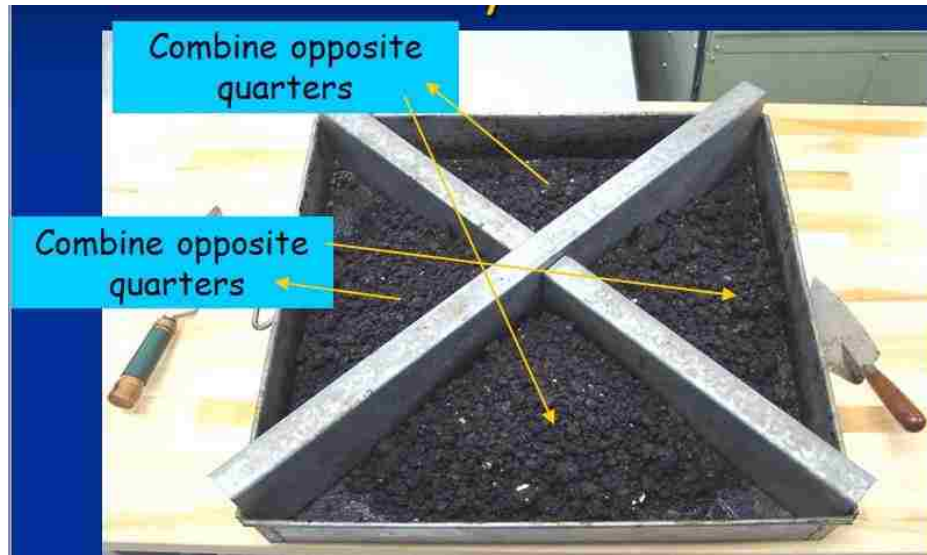


Figure 2 – Quartering Sheets

8. Pull samples from 6 splits to create all 6 pucks needed for the remainder of the TSR test (3 conditioned and 3 unconditioned)
9. Pull Rice sample from remaining two splits if necessary

**TSR test procedure:**

1. Determine TSR initial puck weights through mix design. This involves weighing out the amount of loose mix (Appendix B) to achieve the compacted air voids of 7 +/- 0.5% at a specified height of 95 +/- 5 mm for 150 mm diameter cylindrical specimens. Based on the quality and stiffness of the mix, the compaction pressure may need to be adjusted on the gyratory compactor. Stiff mixes can be subjected to the standard 600 kPa pressure whereas lower quality mixes need less pressure to compact. The pressure should be set to where the desired puck height is achieved in less than 20 gyrations to prevent excessive heat loss during compaction. The height entered into the gyratory compactor should be slightly above the desired height for the compacted specimen. Much like the ram pressure, some trial and error will be necessary to find what entered height works best for the individual mix. This accounts for the drop in height on the last gyration.
2. Compact pucks using the gyratory compaction method outlined in AASHTO T 312 (Figure 3).



Figure 3 – Gyratory Compactor

3. Allow pucks to cool to room temperature for 24 +/- 3 hours before testing resumes.
4. Perform the bulk specific gravity test of all 6 pucks in accordance with AASHTO T 166.
5. Perform the theoretical maximum specific gravity test (Rice test) of loose mix in accordance with AASHTO T 209.



Figure 4 – All 6 Pucks and RICE Sample

6. Calculate air voids (Target % air voids is 7 +/- 0.5% in a 95 mm tall puck; adjust loose mix weight before compaction until 7 +/- 0.5% is achieved in bulk specific gravity testing).
7. Group pucks into 2 groups (unconditioned and conditioned) such that the average air voids of each group is approximately equal to each other.
8. Allow unconditioned pucks to dry for 24 +/- 3 hours before testing resumes
9. For the conditioned pucks, pre-calculate partially saturated puck weights at 70 and 80% saturation. Progressively vacuum and weigh conditioned pucks under 10-26 in. of mercury vacuum for 5-10 minutes and let puck sit in water for 5-10 minutes. Repeat this step until the partially saturated puck weights are between what is necessary for 70-80% saturation (Figure 5). Lower quality mixes that contain absorptive aggregates may need to be subjected to lower levels of vacuum for shorter periods of time to obtain the correct saturated weight without exceeding the maximum of 80% saturation.
10. Determine saturated surface dry weight in accordance with AASHTO T 166
11. Calculate the degree of saturation. If under 70%, apply vacuum for an additional 1 minute, slowly release vacuum, let puck sit in water for 5-10 minutes, and



recalculate % saturation. If greater than 80%, puck is considered over-saturated and cannot be further tested.



Figure 5 – Vacuum Saturation of Puck

12. Once 70-80% saturation is achieved, wrap the conditioned pucks in plastic wrap and seal the pucks in a plastic bag with 10 ml, measured with a graduated cylinder, of additional water. Place the bags containing the conditioned samples in a freezer at  $-18 \pm 3^{\circ}\text{C}$  for a minimum of 16 hours.
13. Take the 3 unconditioned pucks and place in a water tight bag. Then move the bags containing the unconditioned pucks and place in water bath at  $25 \pm 0.5^{\circ}\text{C}$  for 2 hours  $\pm$  10 minutes (Figure 6). Ensure that the water level of the water bath is at least 1 in. above the top of the puck.



Figure 6 – Water Bath

14. Remove unconditioned pucks from water bath and test for indirect tensile strength using the indirect tensile breaking head, applying a load at the rate of 2 in. of travel per minute (Figure 7 and 8). Ensure that the bags containing the unconditioned pucks has no tears or punctures that would allow water to come into contact with the pucks. Quickly remove the puck from the bag and test after removing it from the water bath.
15. Record maximum load
16. Calculate dry indirect tensile strength, using the maximum load displayed on the machine and the specimen thickness and diameter measured with a caliper before testing of the puck (see equations in Calculation section below).



Figure 7 – Indirect Tensile Breaking Machine



Figure 8 – Indirect Tensile Breaking Head

17. Remove conditioned pucks from freezer and remove pucks from bags and place the conditioned pucks in a water bath at  $60 \pm 1^\circ\text{C}$  for  $24 \pm 1$  hour. Do not remove plastic wrap until the film thaws.

18. Remove conditioned pucks from 60°C water bath and place them in another water bath at 25 +/- 0.5°C for 2 hours +/- 10 minutes.
19. Remove conditioned pucks from water bath, immediately measure diameter and thickness, and test for indirect tensile strength using the indirect tensile breaking head, applying a load at the rate of 2 inches of travel per minute.
20. Record maximum load
21. Calculate wet indirect tensile strength
22. Calculate TSR by dividing the average of conditioned pucks tensile strength by the average of unconditioned pucks tensile strength.
23. Multiply by 100 to achieve TSR in a % (Report to nearest whole %)

### Calculations

#### SI Units:

$$S_t = \frac{2000P}{\pi tD}$$

where:

- $S_t$  = tensile strength, kPa  
 $P$  = maximum load, N  
 $t$  = specimen thickness, mm  
 $D$  = specimen diameter, mm

#### U.S. Customary Units:

$$S_t = \frac{2P}{\pi tD}$$

where:

- $S_t$  = tensile strength, psi  
 $P$  = maximum load, lbf  
 $t$  = specimen thickness, in  
 $D$  = specimen diameter, in

$$\textit{Tensile Strength Ratio (TSR)} = \frac{S_2}{S_1}$$

where:

$S_1$  = average tensile strength of the dry subset, kPa (psi)

$S_2$  = average tensile strength of the conditioned subset, kPa (psi)

## Determining Rutting Susceptibility of Hot Mix Asphalt Using the Asphalt Pavement Analyzer AASHTO T 340-10

### Calibration

It is recommended by the manufacturer of the APA equipment that the vertical displacement, applied wheel load, and test temperature calibration be performed no less than once per year. However, due to the small amount of time needed to perform the vertical displacement and applied wheel load calibration, it was suggested that both calibrations be performed before each full test.

The first step of the calibration process is the vertical calibration of each wheel arm. The steps below outline this procedure (APA manual):

1. Open APA software and APA control bar (Figure 1)
2. Bring testing chamber up to required test air temperature (Upper PG number for APA Rutting only; not required for Hamburg test)



Figure 1 – APA Control Bar

3. Ensure all molds and hose racks are removed from the APA machine
4. Start vertical calibration by clicking on the “Calibration” tab at top of APA control bar

5. Ensure wheels are oriented in such a manner that the wheels are in the middle of the test rack. Click on “Jog” button to move when assembly manually if wheels are not located in middle of the test rack
6. Once the calibration window is open, click on the “Vertical” button (Figure 2)
7. Verify that the correct amount of supply air pressure is reaching the machine by reading the pressure regulator located in the top service panel. If so, click “Yes” to “Do the wheels have adequate pressure for calibration?”
8. Click on red “Vertical Cal Off” button
9. Wheels will then automatically lower completely, scale will self-zero, and wheels will then automatically rise to highest position. The values show under each wheel column should read 103.050 +/- .050. If any of the three values are not within the tolerance range, repeat vertical calibration

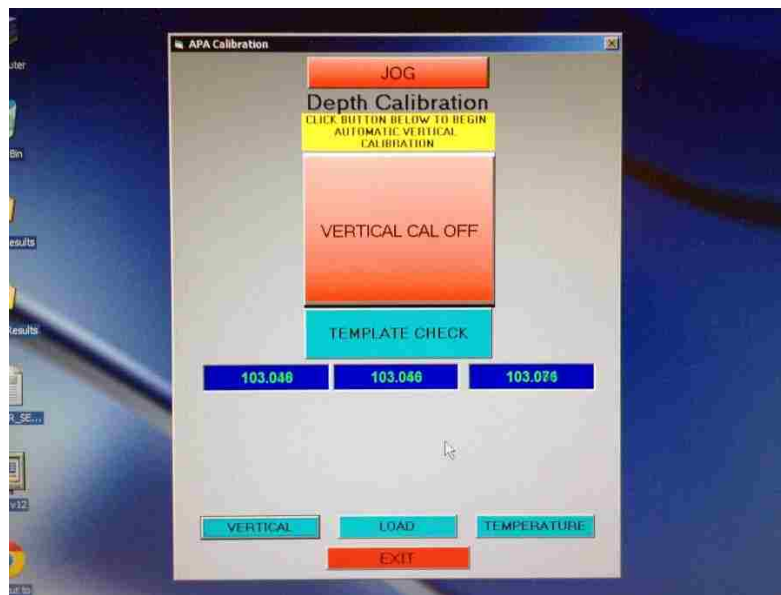


Figure 2 – Vertical Calibration

10. Continue to “wheel load calibration”

The next step of the calibration process is “wheel load calibration” for each wheel arm using the load cell and load cell meter. The steps below outline this procedure (APA manual):

1. Open APA software and APA control bar
2. Ensure all molds and hose racks are removed from the APA machine
3. Start wheel load calibration by clicking on the “Calibration” tab at top of APA control bar
4. Ensure wheels are oriented in such a manner that the wheels are in the middle of the test rack. Click on “Jog” button to move when assembly manually if wheels are not located in middle of the test tray
5. Once the calibration window is open, click on the “Load” button (Figure 3)

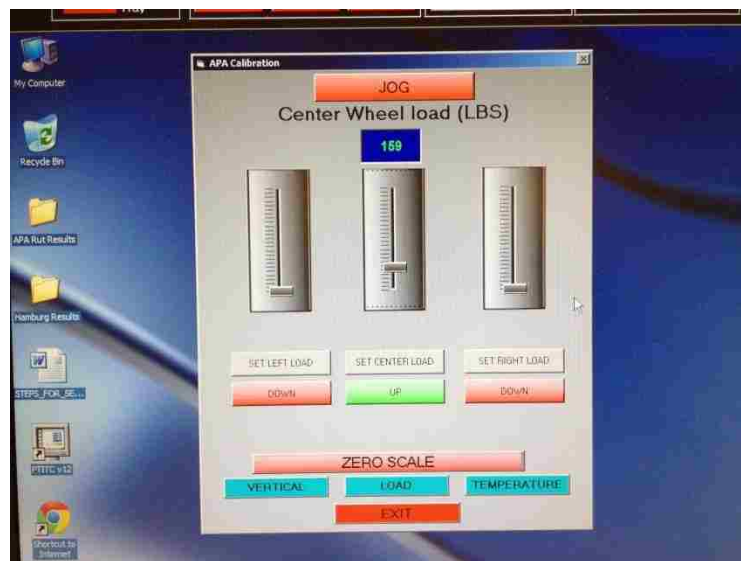


Figure 3 – Load Calibration

6. Click on the “Set Left Load” button
7. Place the load cell on the test tray, under the left wheel (Figure 4)





Figure 4 – Load Cell Under Wheel

8. Raise the left wheel load regulator bar by clicking on the bar and pulling up with the mouse cursor for initial wheel load starting point
9. Click on the “Zero Scale” button for the left wheel
10. Click on the “Down” button for the left wheel
11. Left wheel will then lower onto load cell and the initial load will be displayed in box above wheel load regulator bar and expressed in lbs
12. Contact pressure for rut testing shall be 100 lbs and 158 lbs for Hamburg testing. If the initial values are not acceptable, raise left wheel and move wheel load regulator bar up/down to adjust contact pressure. Repeat steps 10-12 until required contact pressure is displayed. The load should be within +/- 2 pounds of the desired contact pressure
13. Click on the “Up” button after desired contact pressure is achieved
14. Click on “Set Center Load” button
15. Repeat steps 7-13 for center wheel
16. Click on “Set Right Load” button
17. Repeat steps 7-13 for right wheel

### Procedure

At this point, all calibration steps have been completed and the APA is ready for the Rutting test procedure, which is outlined below:

1. Create test specimens in accordance with AASHTO T 340-10. This involves weighing out the amount of loose mix (Appendix B) to achieve the compacted air voids of 7 +/- 0.5% at a specified height of 75 +/- 2 mm for 150 mm diameter cylindrical specimens. Based on the quality and stiffness of the mix, the compaction pressure may need to be adjusted on the gyratory compactor. Stiff mixes can be subjected to the standard 600 kPa pressure whereas lower quality mixes need less pressure to compact. The pressure should be set to where the desired puck height is achieved in less than 20 gyrations to prevent excessive heat loss during compaction. The height entered into the gyratory compactor should be slightly above the desired height for the compacted specimen. Much like the ram pressure, some trial and error will be necessary to find what entered height works best for the individual mix. This accounts for the drop in height on the last gyration.
2. Compacted specimens are cooled to room temperature and then tested for bulk specific gravity and % air void content.
3. With each rutting test, three molds are used, which equates to six rutting pucks needed. The six pucks are paired so that the two pucks in each mold have as close to equal % air voids as possible. This reduces the chance of differential rutting of the two pucks which can skew the rut depth measured along the test surface.
4. Locate the temperature control section on the APA control bar. Enter the upper PG binder number being tested as the appropriate set point (SP) for the required chamber heat temperature. (It is important to note that the enter key must be hit after any changes to set points or any other value in the APA control bar. This stores the value in the box. Also, it is suggested that the “water heat” temperature be set at the same set point. This aids in heating the chamber). Click on both the “Cabin Heating” and “Water Heating” buttons to activate the heating. Allow 20-30 minutes for the water temperature to stabilize after it reaches the desired set point (Figure 1)

5. Adjust correction factors as needed for the water heat. If needed, click the “Calibration” tab at the top of the APA control bar and then “Temperature”. Enter the water temperature adjustments as needed in the respective boxes (Figure 5)



Figure 5 – Temperature Calibration

6. Slide in hose carriage assembly and connect the air supply hose at the front left corner of the hose carriage. On the right front of the carriage, verify that the air pressure in the hoses is between 90-120 psi (100 psi is the default)
7. Unlatch the test tray and slide tray through the door openings
8. Place mold and specimens in their designated areas and check the mold alignment bar on the end of the test tray (Figure 6)
9. Once all molds are in place, slide the test tray back and in place and secure both latches to the locked position



Figure 6 – Hose Carriage and Rutting Specimens

10. At this point, the front doors should be manually closed which allows the test specimens to condition in the heated chamber until they are at same temperature as the chamber. Chamber doors shall not be open for more than 6 minutes. Once doors are closed, a minimum of 10 minutes is needed for chamber temperature to stabilize
11. Locate the “Test Setup” tab at the top of the APA control bar and click. This will open the test setup window. Click on the “Rut Test” button (Figure 7)

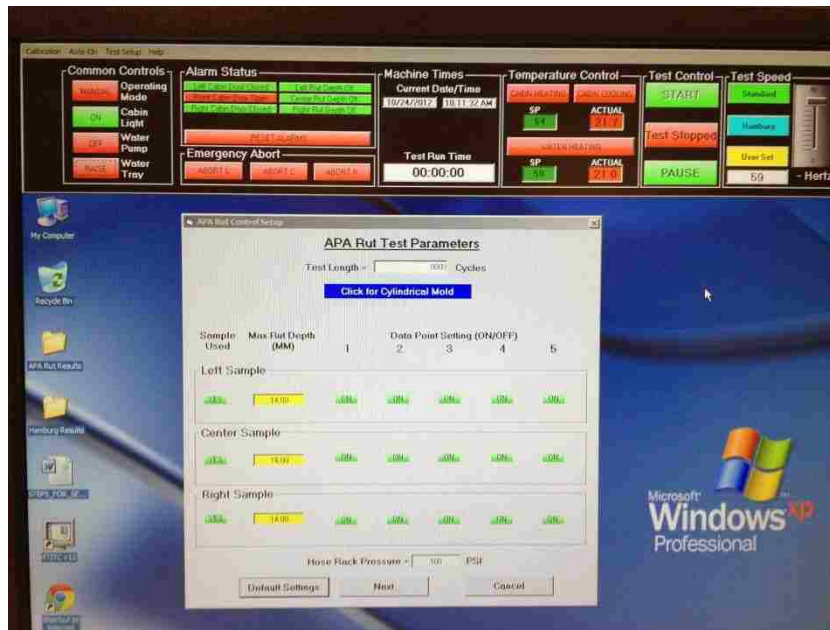


Figure 7 – Rut Test Setup

12. In the next window, enter 8000 passes as the correct pass count for the test. Enter the maximum rut depth in the appropriate window (14 is the most common default value)
13. Turn off/on the appropriate LVDT sensors measuring rut depth during the test (default is “all 5 on”)
14. If center parameter is green, proceed by clicking on the “Next” button. Select “Yes” if the test is ready to begin
15. The test data sheet Excel file will then open. It is recommended that this file be maximized on the screen
16. Under the “Common Controls” section of the APA control bar, locate the “Manual” button. Click on this button and change to “Auto” (Figure 1)
17. Locate the “Start” button on the APA control bar and click “Start” to begin test. The button will now read “Test Running”. If the test does not begin, locate the “Alarm Status” section of the APA control bar. If alarms are present, click “Reset Alarms”. For the Rut Test, no alarms should be activated.

18. If it is necessary, the test can be paused by clicking on the “Pause” button at any time during the test and resumed at a later time. However, opening the side cabin doors will result in a “Left Cabin Door” and/or “Right Cabin Door” alarm to be activated and ultimately cancelling the test
19. If it is necessary, the test can be stopped by clicking on the “Stop” button located on the APA control bar. However, the test cannot be resumed. A new test setup will be required to resume testing of the sample(s). To end testing on selected wheels without stopping the entire test, the “Abort L” (left wheel retracts), “Abort C” (center wheel retracts), and/or “Abort R” (right wheel retracts) and testing continues on the wheels not selected
20. During the test, and/or upon completion of the 8,000 cycles, mix data can be entered into the summary data sheet generated in the Excel file
21. Do not save in the default location the Excel program chooses. Create a test folder in “My Documents” that can be easily located and save all test files generated from testing there

## Hamburg Wheel-Track Testing of Compacted Hot Mix Asphalt (HMA) AASHTO T 324-11

### Calibration

It is recommended by the manufacturer of the APA equipment that the vertical displacement, applied wheel load, and test temperature calibration be performed no less than once per year. However, due to the small amount of time needed to perform the vertical displacement and applied wheel load calibration, it is suggested that both be performed before each full test.

The first step of the calibration process is the vertical calibration of each wheel arm. The steps below outline this procedure (APA manual):

1. Open APA software and APA control bar (Figure 1)
2. Set water test temperature to 50°C. For Hamburg testing, the air chamber temperature does not need to be set.

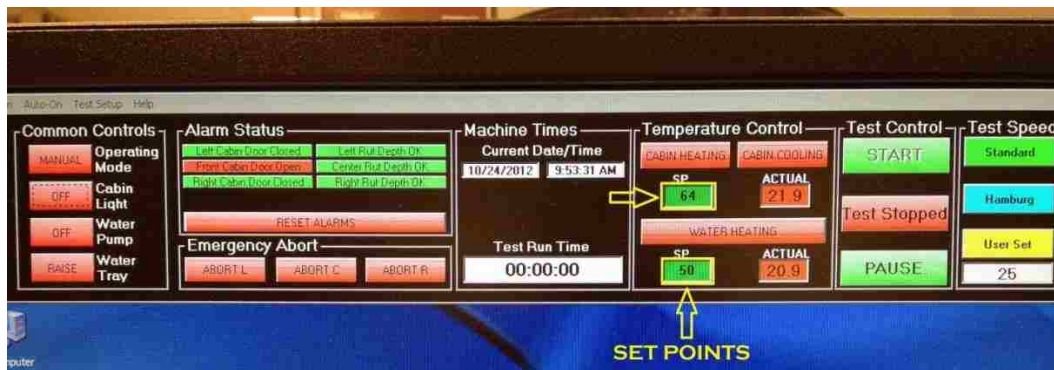


Figure 1 – APA Control Bar

3. Ensure all molds and hose racks are removed from the APA machine
4. Start vertical calibration by clicking on the “Calibration” tab at top of APA control bar

5. Ensure wheels are oriented in such a manner that the wheels are in the middle of the test rack. Click on “Jog” button to move when assembly manually if wheels are not located in middle of the test rack
6. Once the calibration window is open, click on the “Vertical” button (Figure 2)
7. Verify that the correct amount of supply air pressure is reaching the machine by reading the pressure regulator located in the top service panel. If so, click “Yes” to “Do the wheels have adequate pressure for calibration?”
8. Click on red “Vertical Cal Off” button
9. Wheels will then automatically lower completely, scale will self-zero, and wheels will then automatically rise to highest position. The values show under each wheel columns should read 103.050 +/- .050. If any of the three values are not within the tolerance range, repeat vertical calibration

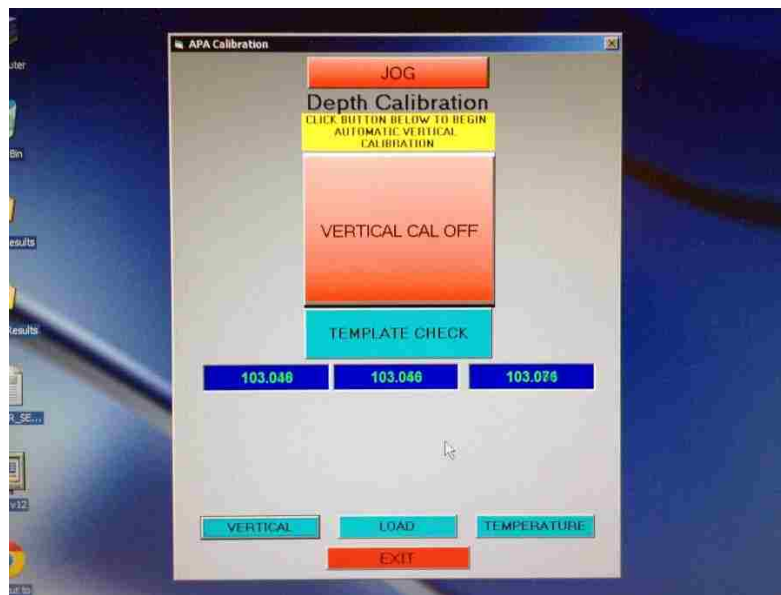


Figure 2 – Vertical Calibration

10. Continue to “wheel load calibration”

The next step of the calibration process is “wheel load calibration” for each wheel arm using the load cell and load cell meter. The steps below outline this procedure (APA manual):



18. Open APA software and APA control bar
19. Ensure all molds and hose racks are removed from the APA machine
20. Start wheel load calibration by clicking on the “Calibration” tab at top of APA control bar
21. Ensure wheels are oriented in such a manner that the wheels are in the middle of the test rack. Click on “Jog” button to move when assembly manually if wheels are not located in middle of the test tray
22. Once the calibration window is open, click on the “Load” button (Figure 3)

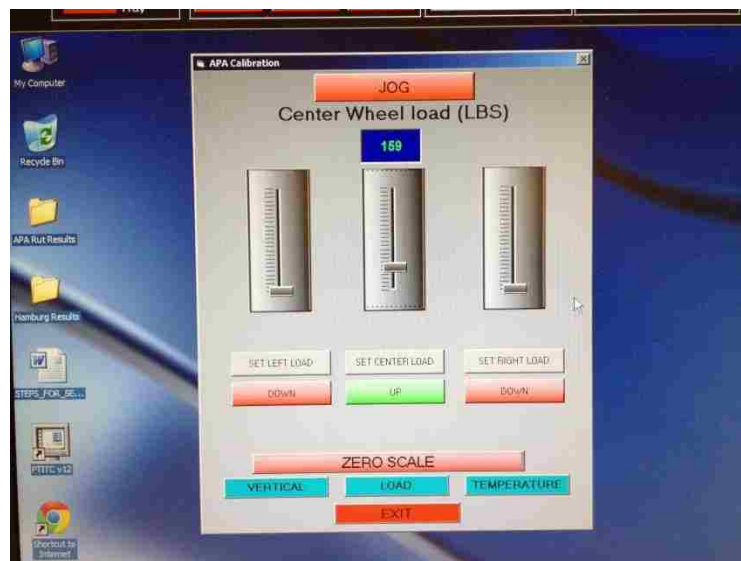


Figure 3 – Load Calibration

23. Click on the “Set Left Load” button
24. Place the load cell on the test tray, under the left wheel (Figure 4)

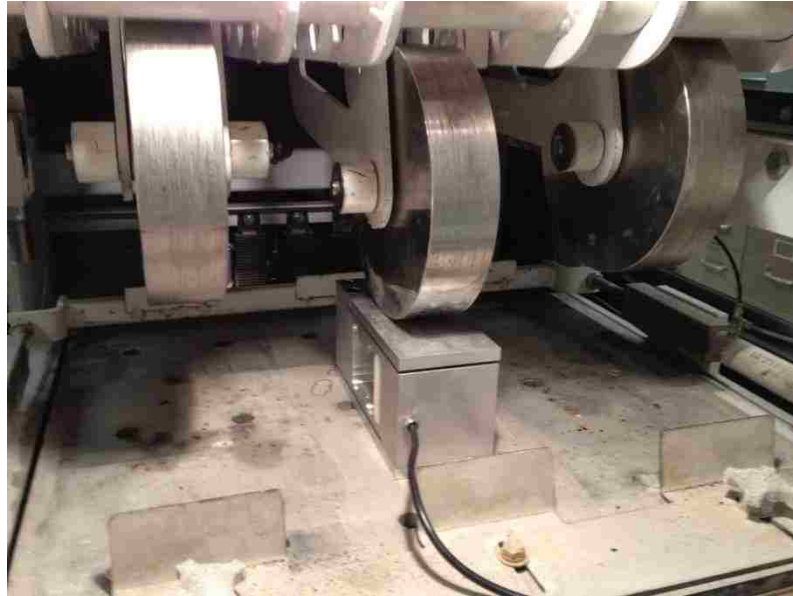


Figure 4 – Load Cell Under Wheel

25. Raise the left wheel load regulator bar by clicking on the bar and pulling up with the mouse cursor for initial wheel load starting point
26. Click on the “Zero Scale” button for the left wheel
27. Click on the “Down” button for the left wheel
28. Left wheel will then lower onto load cell and the initial load will be displayed in box above wheel load regulator bar and expressed in lbs
29. Contact pressure for rut testing shall be 100 lbs and 158 lbs for Hamburg testing. If the initial values are not acceptable, raise left wheel and move wheel load regulator bar up/down to adjust contact pressure. Repeat steps 10-12 until required contact pressure is displayed. The load should be within +/- 2 pounds of the desired contact pressure
30. Click on the “Up” button after desired contact pressure is achieved
31. Click on “Set Center Load” button
32. Repeat steps 7-13 for center wheel
33. Click on “Set Right Load” button
34. Repeat steps 7-13 for right wheel

### Procedure

At this point, all calibration steps have been completed and the APA is ready for the Hamburg testing procedure, which is outlined below:

1. Create test specimens in accordance with AASHTO T 324-11. This involves weighing out the amount of loose mix (Appendix B) to achieve the compacted air voids of  $7 \pm 1.0\%$  at a specified height of  $62 \pm 2$  mm for 150 mm diameter cylindrical specimens. Based on the quality and stiffness of the mix, the compaction pressure may need to be adjusted on the gyratory compactor. Stiff mixes can be subjected to the standard 600 kPa pressure whereas lower quality mixes need less pressure to compact. The pressure should be set to where the desired puck height is achieved in less than 20 gyrations to prevent excessive heat loss during compaction. The height entered into the gyratory compactor should be slightly above the desired height for the compacted specimen. Much like the ram pressure, some trial and error will be necessary to find what entered height works best for the individual mix. This accounts for the drop in height on the last gyration.
2. Compacted specimens are cooled to room temperature and then tested for bulk specific gravity and % air void content.
3. With each Hamburg test, 3 molds are used, which equates to 6 Hamburg pucks needed. The 6 pucks are paired so that the 2 pucks in each mold have as close to equal % air voids as possible. This reduces the chance of differential rutting of the two pucks which can skew the rut depth measured along the test surface. Once paired together, pucks are cut on one side so that the 2 pucks can simulate a “compacted slab” specimen (Figure 5). Figure 6 below shows the orientation and gap requirements of the 2 mold halves. The pucks should be touching each other.



Figure 7 - Cut Side on Hamburg Specimens

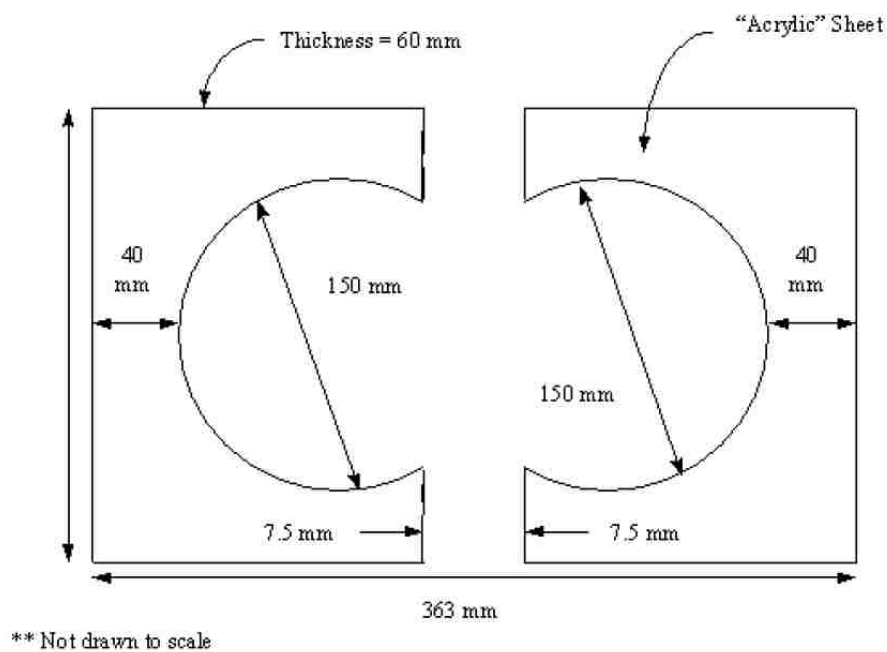


Figure 6 - Hamburg Mold Specifications

4. The water tank at the bottom of the APA carriage shall be filled with water (It is important to note that the water level should be checked before each test to ensure it is at the proper level)
5. Locate the temperature control section on the APA control bar. Enter 50°C as the appropriate set point (SP) for the required water temperature. (It is important to note that the enter key must be hit after any changes to set points or any other

value in the APA control bar. This stores the value in the box. Click on the “Water Heating” button to activate the heating. Allow 20-30 minutes for the water temperature to stabilize after it reaches the desired set point (Figure 1).

6. Adjust correction factors as needed for the water heat. If needed, click the “Calibration” tab at the top of the APA control bar and then “Temperature”. Enter the water temperature adjustments as needed in the respective boxes (Figure 7)



Figure 7 – Temperature Calibration

7. Unlatch the test tray and slide tray through the door openings
8. Place mold and specimens in their designated areas and check the mold alignment bar on the end of the test tray (Figure 8)
9. Once all molds are in place, slide the test tray back and in place and secure both latches to the locked position
10. At this point, the water tray shall be raised into place by clicking on the “Raise” button on the APA control bar (Figure 9)

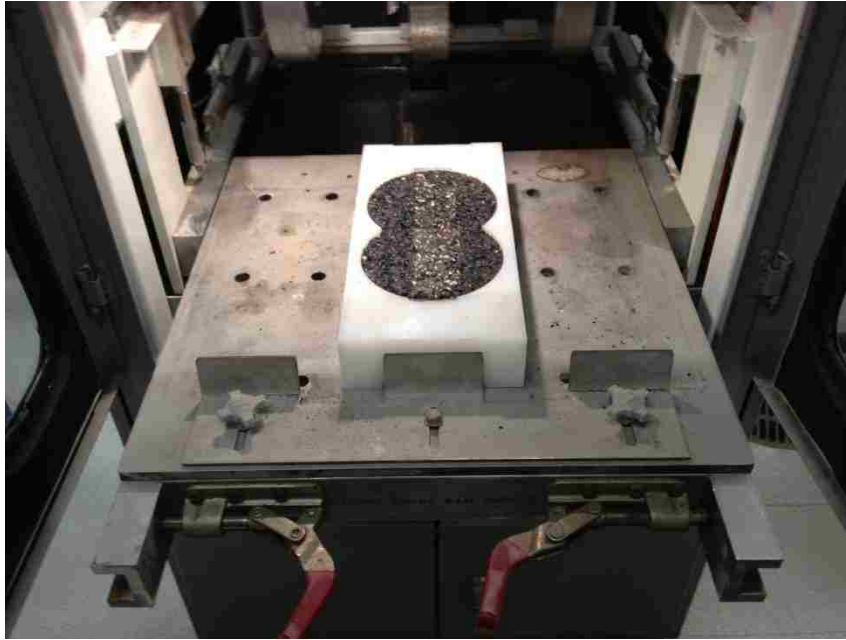


Figure 8 – Hamburg Sample in Place on Tray

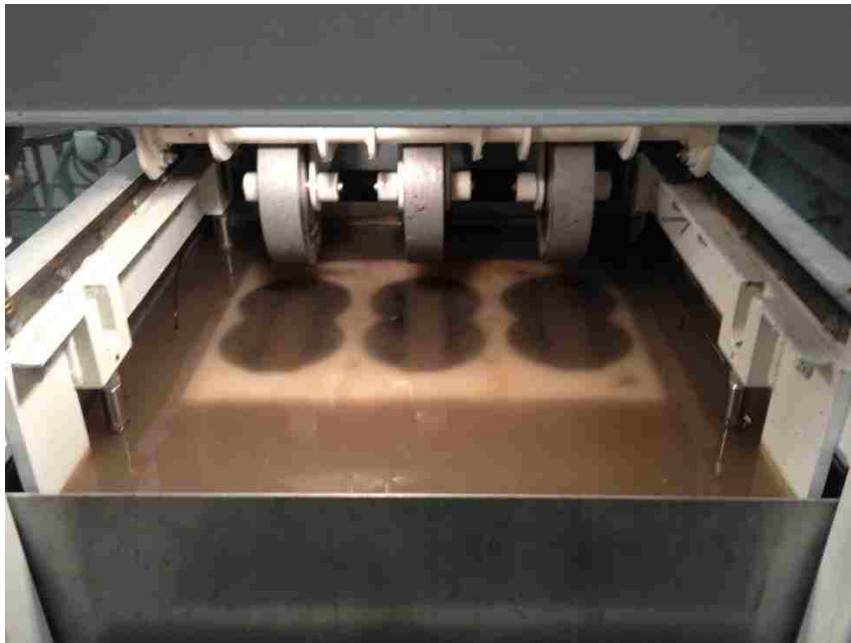


Figure 9 – Water Tray Raised

11. Once the tray is fully raised, locate the “Water Pump” button on the APA control bar. Click this button to turn on water pump and initiate the filling process

12. Allow samples to be completely submerged in the water, at appropriate temperature, for a minimum of 30 minutes before starting the Hamburg test
13. Locate the “Test Setup” tab at the top of the APA control bar and click (Figure 10). This will open the test setup window. Click on the “Moisture Test (Hamburg Type)” button. Check to ensure water level is correct and click “Yes”

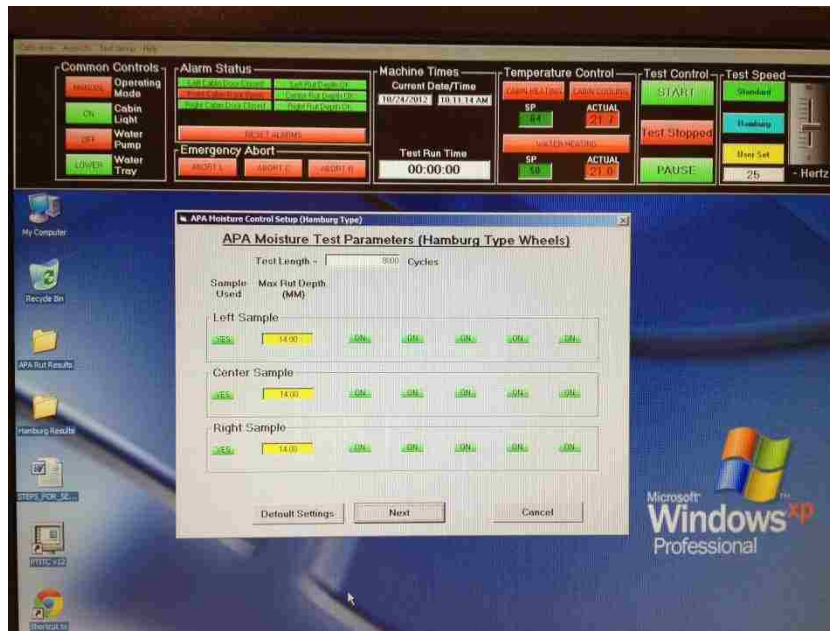


Figure 10 – Hamburg Test Setup

14. In the next window, enter 20000 passes as the correct pass count for the test. Enter the maximum rut depth in the appropriate window (14 mm is the default maximum rut depth value; enter specified maximum rut depth value here, such as 24 mm)
15. Turn off/on the appropriate LVDT sensors measuring rut depth during the test (default is “all 5 on”)
16. If center parameter is green, proceed by clicking on the “Next” button. Select “Yes” if the test is ready to begin
17. The test data sheet Excel file will then open. It is recommended that this file be maximized on the screen
18. Under the “Common Controls” section of the APA control bar, locate the “Manual” button. Click on this button and change to “Auto” (Figure 1)

19. Locate the “Start” button on the APA control bar and click “Start” to begin test. The button will now read “Test Running”. If the test does not begin, locate the “Alarm Status” section of the APA control bar. If alarms are present, click “Reset Alarms”. For the Hamburg test, the “Front Cabin Door” alarm will be activated. This alarm shall be ignored and will not stop the test
20. If it is necessary, the test can be paused by clicking on the “Pause” button at any time during the test and resumed at a later time. However, opening the side cabin doors will result in a “Left Cabin Door” and/or “Right Cabin Door” alarm to be activated and ultimately cancelling the test
21. If it is necessary, the test can be stopped by clicking on the “Stop” button located on the APA control bar. However, the test cannot be resumed. A new test setup will be required to resume testing of the sample(s). To end testing on selected wheels without stopping the entire test, the “Abort L” (left wheel retracts), “Abort C” (center wheel retracts), and/or “Abort R” (right wheel retracts) and testing continues on the wheels not selected
22. During the test, and/or upon completion of the 20,000 cycles, mix data can be entered into the summary data sheet generated in the Excel file
23. Do not save in the default location the Excel program chooses. Create a test folder in “My Documents” that can be easily located and save all test files generated from testing there
24. Figure 11 below shows a typical results plot from a complete Hamburg test. It is important to note the location of the post-compaction consolidation, the creep slope, the stripping slope, and the stripping inflection point (SIP)



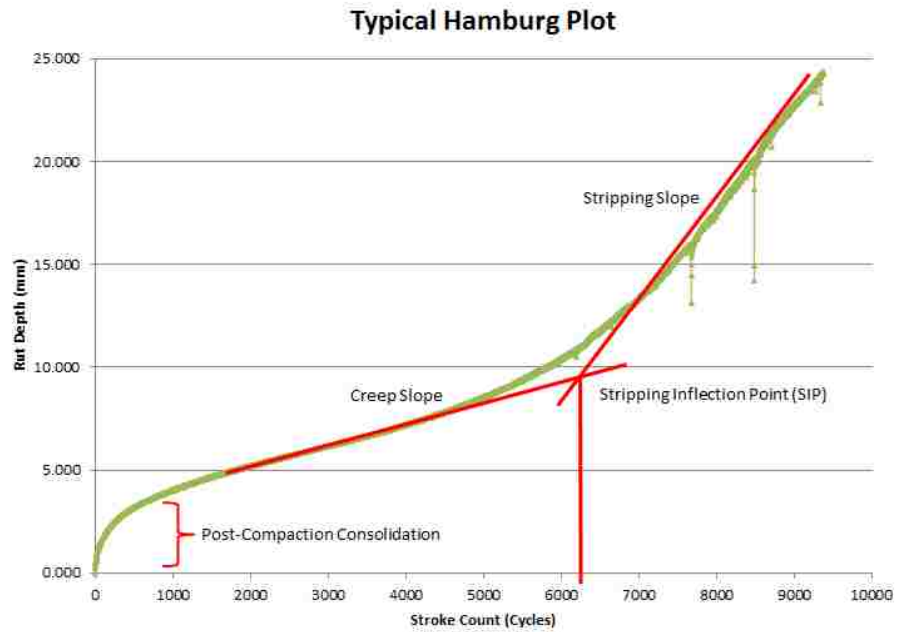


Figure 11 - Hamburg Plot with All Labels Shown

**Coring of Compacted Hot Mix Asphalt (HMA) Specimens  
Using Core Drill  
MS&T Method**

**Equipment**

1. Milwaukee Dynodrill (Figure 1)
2. 100 mm diamond core bit
3. Bottom jig to hold specimen in place

**Procedure**

1. Compact specimen in accordance with AASHTO T 312 to a specified height of 170 mm.
2. Allow specimen to cool to room temperature before coring.
3. Place 170mm compacted specimen into bottom jig (which is bolted to the floor) and tighten clamps to hold the specimen in place securely. Lower core bit, WITH DRILL OFF, until the bit touches the top of the specimen. Verify that the same thickness is present from the bit to the outside edge of the specimen for all sides. Tighten bottom jig bolts tightly to secure jig (Figure 2).
4. Raise the core bit and attached the water hose to the core drill with the valve closed. Turn the drill water supply on.
5. Turn on the drill at the slowest speed and open the water valve.
6. Lower drill bit until initial contact is made between the specimen and bit edge. Raise bit, turn off water, and turn off the drill. Check the initial cut ring to outer edge distance. It should be even on all sides. If not, loosen bottom jig bolts and move accordingly.
7. With jig in place, turn drill on, water on, and lower the bit. Core the specimen slowly with the motor amperage staying between 10-15 amps. Core specimen until bottom is reached and the core is free from the outer shell.
8. Raise bit, turn off water, and turn off core drill.
9. Loosen the clamps holding the specimen and remove the outer shell/core
10. Loosen the bottom jig bolts, remove the jig, and clean the surrounding area

11. Repeat steps 1-10 for next specimen
12. Check the diameter of the core. The average diameter should be 100 to 104 mm in accordance with AASHTO PP 60-09
13. Move cored specimen to wet saw for final AMPT specimen prep



Figure 1 - Core Drill with Diamond Bit



Figure 2 - Specimen Secured in Bottom Jig

**Sawing of Compacted Hot Mix Asphalt (HMA)  
Specimens Using Wet Saw  
MS&T Method**

**Equipment**

1. Felker Manufacturing Co. wet saw with sliding tray and diamond cutting blade designed to cut asphalt specimens (Figure 1)
2. Cored specimen locating jig with 10 mm spacer
3. Appropriate safety equipment, such as ANSI approved safety glasses, apron to protect operators clothing, and ear plugs, to operate wet saw



Figure 1 - Wet Saw with Diamond Cutting Blade

**Procedure**

1. Bolt specimen jig securely to the wet saw sliding tray (Figure 2).
2. Place the cored sample into the jig firmly against the stop plate. Close/lower the specimen latch completely until the specimen is locked into place
3. Attach the water supply hose to back of wet saw and turn on hose at the wall
4. Turn on the saw and water valve on the saw assembly
5. Make the first cut on the face of the core

6. Turn off water valve and saw motor. Allow blade to stop rotating before adjusting the specimen
7. Release specimen latch and place the 10 mm spacer against the specimen stop plate on the jig
8. Rotate core and place the core back into the jig with the freshly sawed face against the 10 mm spacer
9. Close/lower the specimen latch completely until specimen is locked into place
10. Turn on the saw and water valve on the saw assembly
11. Make final cut on the face of the core
12. Turn off water valve and saw motor. Allow blade to stop rotating before removing the specimen from the jig
13. Remove specimen from jig and verify with calipers that the average specimen height is between 147.5 and 152.5 mm in accordance with AASHTO PP 60-09
14. Verify end flatness with straightedge (carpenters square). Using feeler gauge, any gaps shown are measured. The gaps should be equal to or less than 0.5 mm in accordance with AASHTO PP 60-09
15. Verify end perpendicularity with straightedge (carpenters square). Using feeler gauge, any gaps shown are measured. The gaps should be equal to or less than 1.0 mm in accordance with AASHTO PP 60-09
16. Place specimen in oven at 52°C to dry overnight or place in CoreDry to dry immediately
17. Repeat steps 1-16 for remaining compacted specimens



Figure 2 - Specimen Jig Bolted to Wet Saw Sliding Tray

**Determining the Dynamic Modulus for Hot Mix Asphalt (HMA)  
Using the Asphalt Mixture Performance Tester (AMPT)  
AASHTO TP 79-11**

The Asphalt Mixture Performance Tester (AMPT) can be used to determine the dynamic modulus of a particular asphalt mixture as well as the flow number. The following steps outline procedures to obtain the Dynamic Modulus.

**Specimen Preparation**

1. The specimen shall be cored and sawed in accordance with the MS&T Method coring and sawing procedures previously outlined
2. The specimen shall be then prepared for the dynamic modulus test
3. Secure gauge points in fixing jig arms (Figure 1)
4. Place test specimen on the Gauge Point Fixing Jig
5. Lock jig arms in place and mark outline of gauge points with a magic marker (color based on personal preference) on the test specimen where gauge points come into contact (Figure 2)



Figure 1 - Fixing Jig Arm with Gauge Points Secured



Figure 2 - Fixing Jig Arm Secured Against Specimen Side

6. Unlock jig arms and prepare the standard two-part epoxy for securing gauge points to specimen
7. Place a small amount of epoxy to the face of the gauge point and to where the gauge point comes into contact with the specimen (previously marked on specimen in step 5 of “Specimen Preparation” outline)
8. Lock jig arms in place and allow epoxy to set (set time varies based on type of epoxy used; verify with instructions for epoxy)
9. Once epoxy has set, release the gauge points hold down and unlock the jig arms
10. Allow epoxy to cure overnight (min of 12-15 hours) before testing of specimen can resume (Figure 3)
11. Place test specimen in the first environmental chamber to reach the first test temperature. For example, if first test temperature is 4°C, then sample shall be placed in that chamber until the specimen reaches 4°C (Figure 4). Sample prep can then resume
12. With the sample at the appropriate temperature, the gauge point clips can be attached to all gauge points (Note: There are two sides to the clips; a black and silver side. For this instance, all black sides should be facing each other; Figure 5 and 6)



Figure 3 - Specimen with Gauge Points Attached





Figure 4 - Specimen in Conditioning Chamber

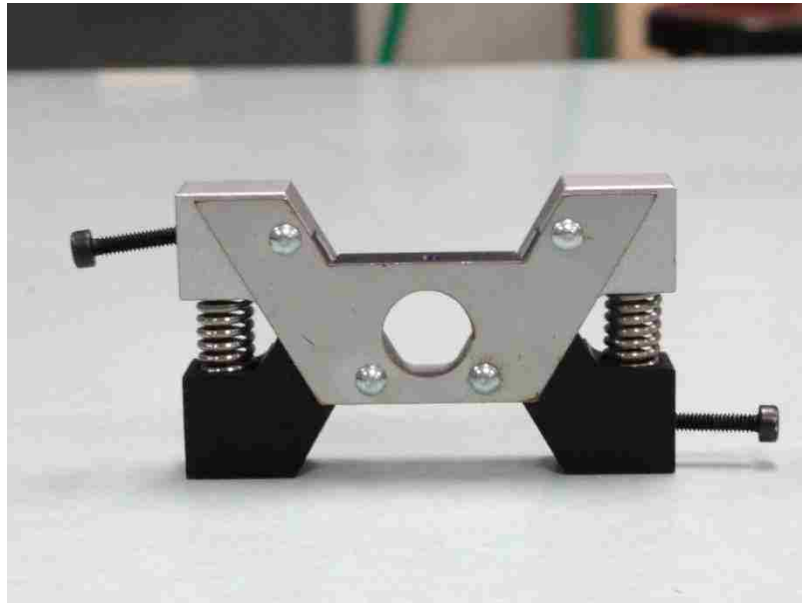


Figure 5 – Gauge Point Clip



Figure 6 - Clips attached to Gauge Points

13. With all clips installed with the black sides facing each other, the end friction modifiers can be placed between the specimen and the bottom/top platens. Either a greased double latex modifier or latex modifier can be used. Then place the specimen into the test chamber and attach the LVDTs in the proper location. The LVDTs are color coded based on which port they should be plugged in (Figure 7). If the colors do not match, the readings taken during the test will be inaccurate



Figure 7 - Specimen in Test Chamber with LVDT Attached

14. With all LVDTs secured in the proper location, lower the outer shell of the test chamber by clicking on the “Lower” button on the main tool bar and pressing both external green buttons on the front of the machine (Figure 8)



Figure 8 – External Lowering Safety Buttons

15. The LVDTs can be checked for proper function by clicking on the “Levels” button (Figure 9)
16. Allow the test specimen and chamber temperature to stabilize before beginning the test
17. Open the “Virtual Pendant” menu before beginning test. Click the “Low” button on the “Hydraulic Power Supply” row first, then click on the “High” button; allow several seconds to pass before switching from “Low” to “High”
18. Next click on the “Low” button on the “Hydraulic Service Manifold” row and allow the hydraulic oil to heat up for a minimum of 10 minutes before clicking on the “High” button (Figures 10 and 11)

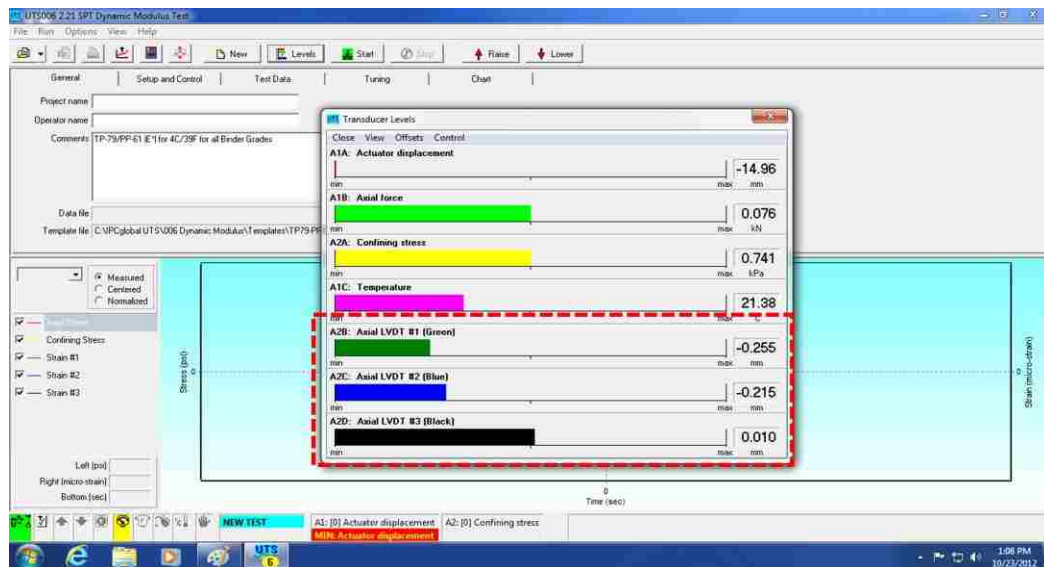


Figure 9 – LVDT Levels

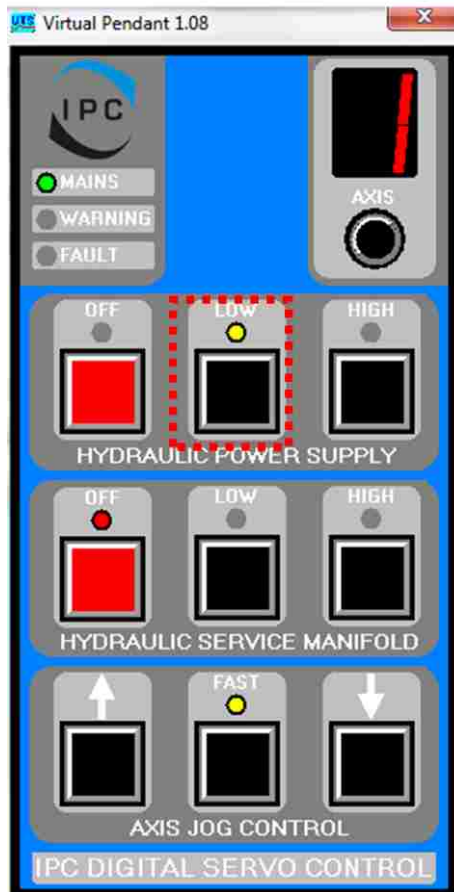


Figure 10 – Low Enabled

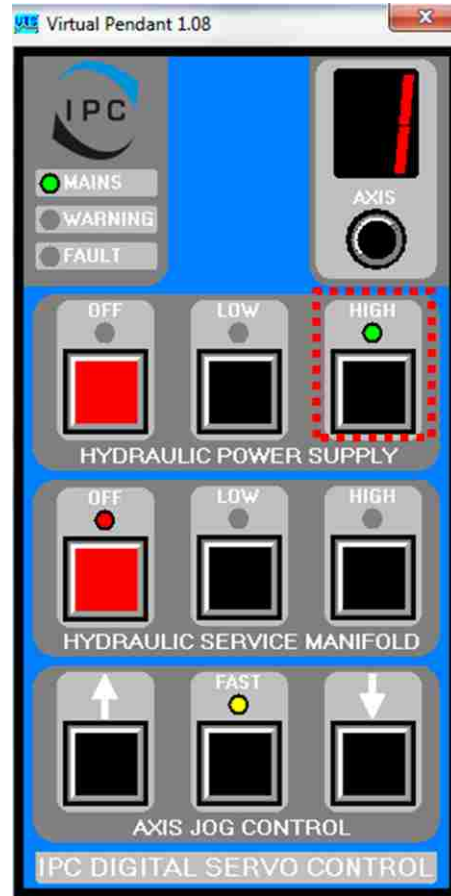


Figure 11 – High Enabled

19. When powering down both systems, proceed in this exact order. “Hydraulic Service Manifold” “High” to “Low” to “Off”, allowing several seconds in between each step. Then for the “Hydraulic Power Supply”, start with “High” to “Low” to “Off”, also allowing several seconds in between each step. This prevents any damage from occurring to either system.

### Procedure

1. Double Click on the Dynamic Modulus program icon (Figure 12)
2. When the program opens, the screen in Figure 13 will appear



Figure 12 – Dynamic Modulus Icon

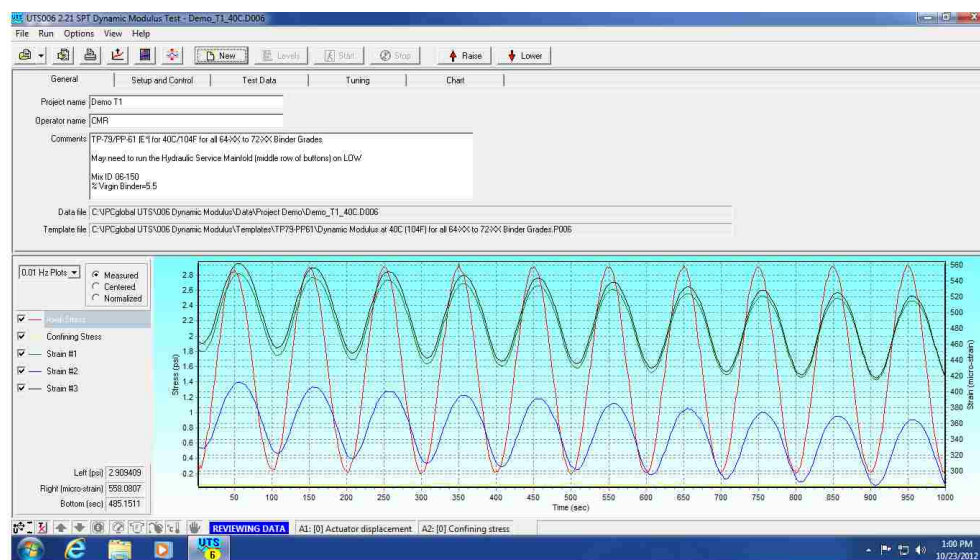


Figure 13 – Main Program Screen

3. First select a new template by clicking the “File” tab at the upper left corner of the window (Figure 14), scrolling down to the “Template” tab and choosing the “Open Template” button. After clicking on the “Open Template” button, a window will open with pre-made templates for running dynamic modulus tests at various temperatures (Figure 15). Choose appropriate temp for test desired

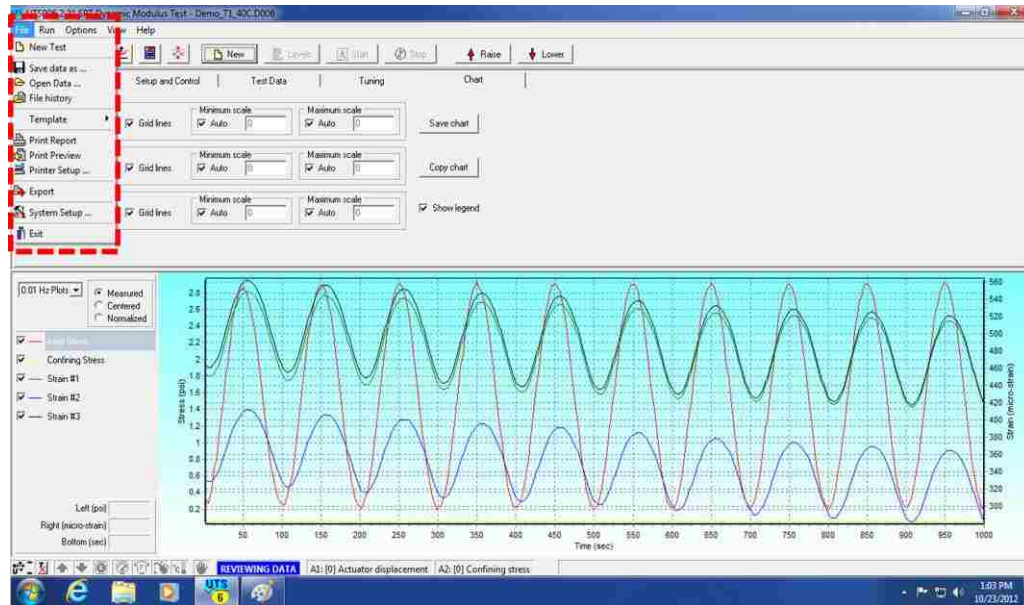


Figure 14 – File Tab

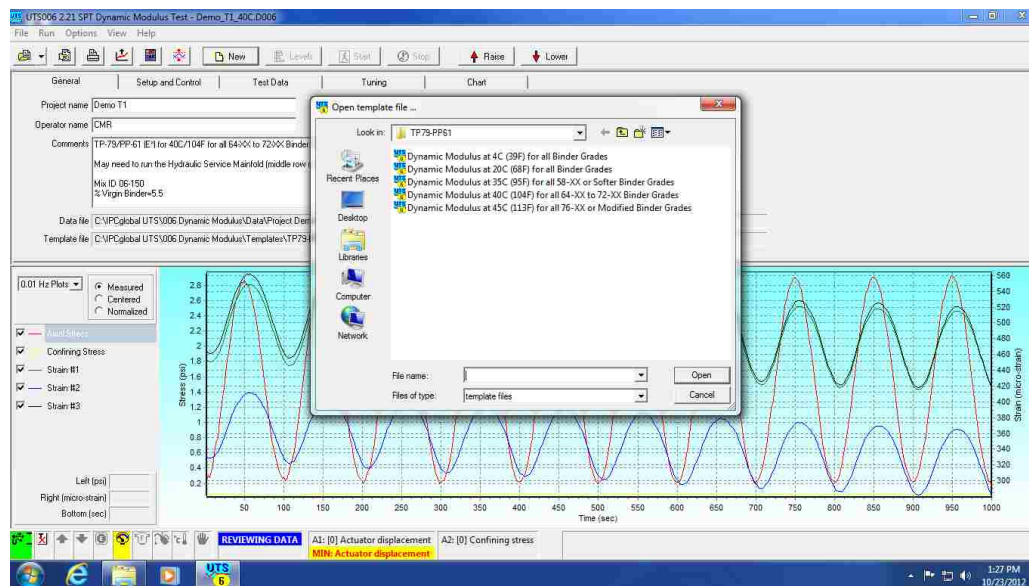


Figure 15 – New Template Window

- Once the temperature template has been chosen, click on the “New” Tab on the main tool bar on the top of the program window. This will allow the user to enter information in the following tabs. Starting with the “General” tab (Figure 16), the user will enter the project name, operator name, and comments regarding the

particular mix being tested at all three dynamic modulus temperatures. Next, under the “Setup and Control” tab (Figure 17), the user will enter the identification, conditioning time, and any properties/comments directly specific to the individual specimen being tested.

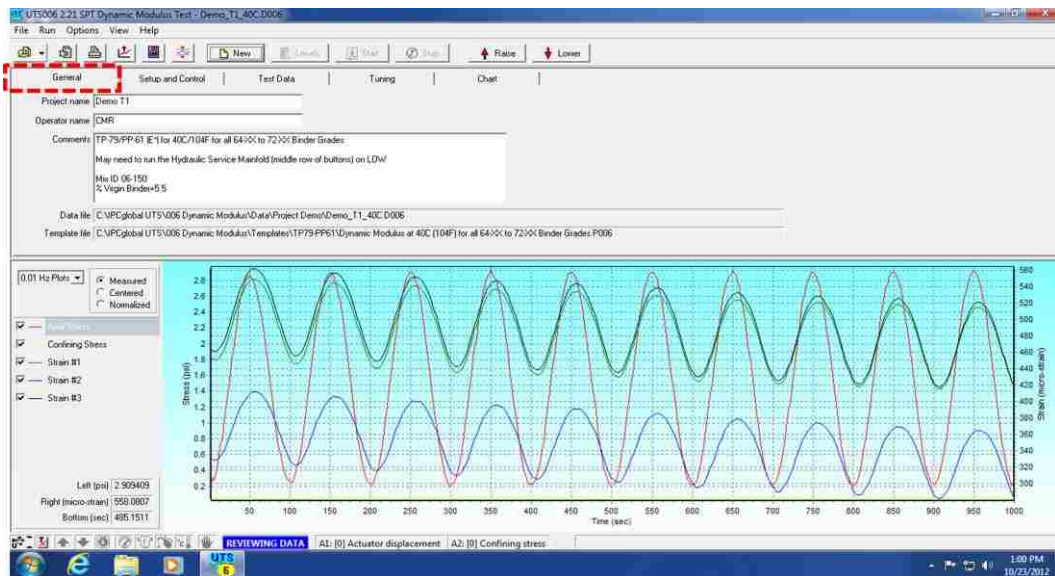


Figure 16 – General Tab

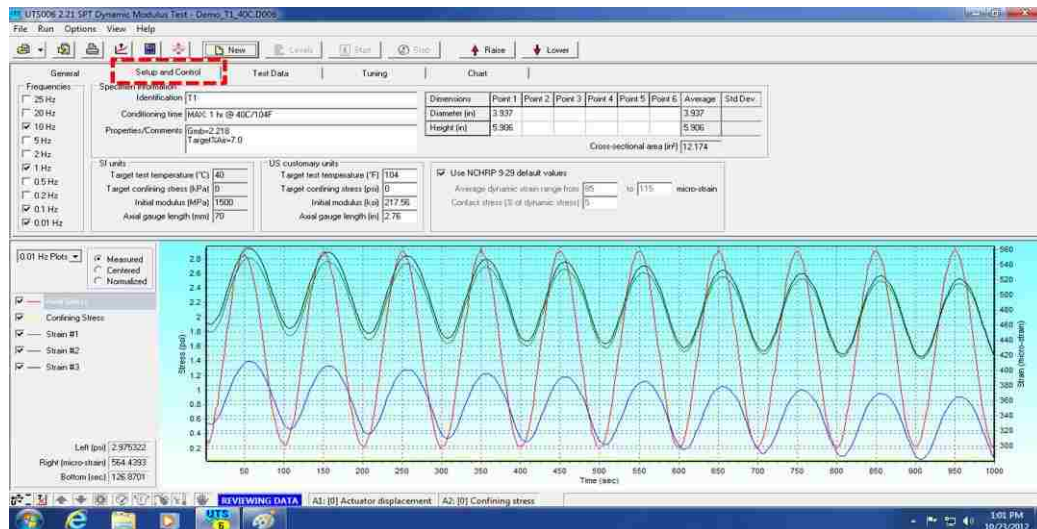


Figure 17 – Setup and Control Tab

- Now click on the “Test Data” tab (Figure 18). Under this tab the initial test start up and test progress can be monitored. To begin the test, click on the “Start”



button on the main tool bar. A window will pop up asking for the file to be saved. Save the file in the folder where all current and future test data will be saved for ease of access later. After saving the file, another window will pop up showing that the machine is applying confining and/or contact stress to the test specimen (Figure19). DO NOT IMMEDIATELY CLICK OK. Allow the contact stress applied to level out and become stable. Observe the contact stress box on the screen (Figure 20). Once the stress becomes stable, click “OK”. The dynamic modulus test will now begin.

- Under the “Test Data” tab, the progress of the test can be followed by watching the box in Figure 20

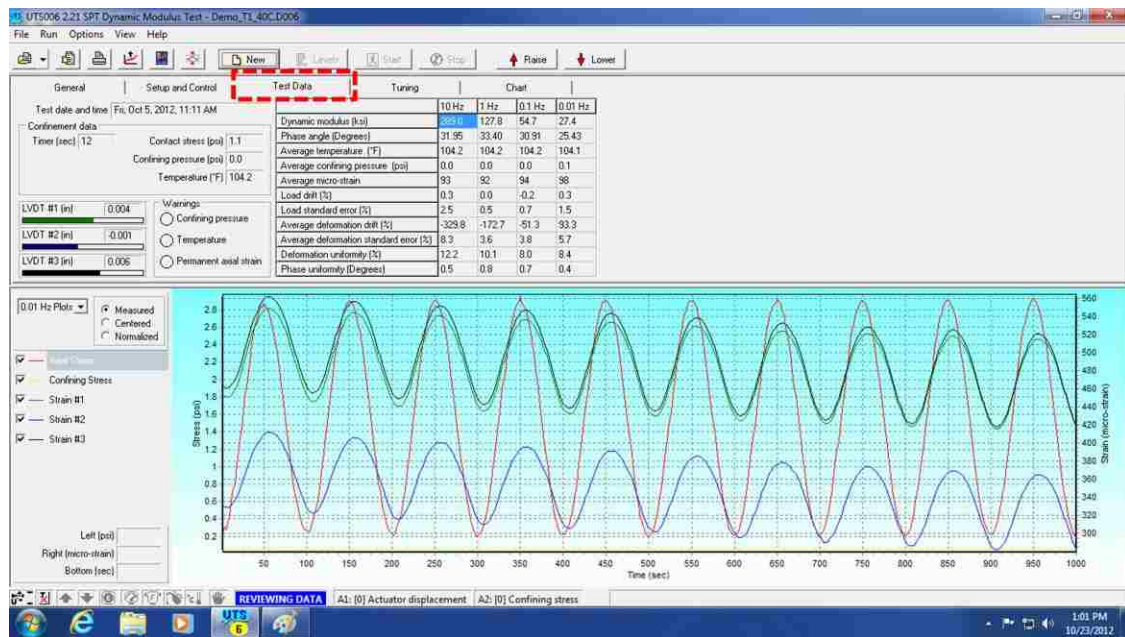


Figure 18 – Test Data Tab

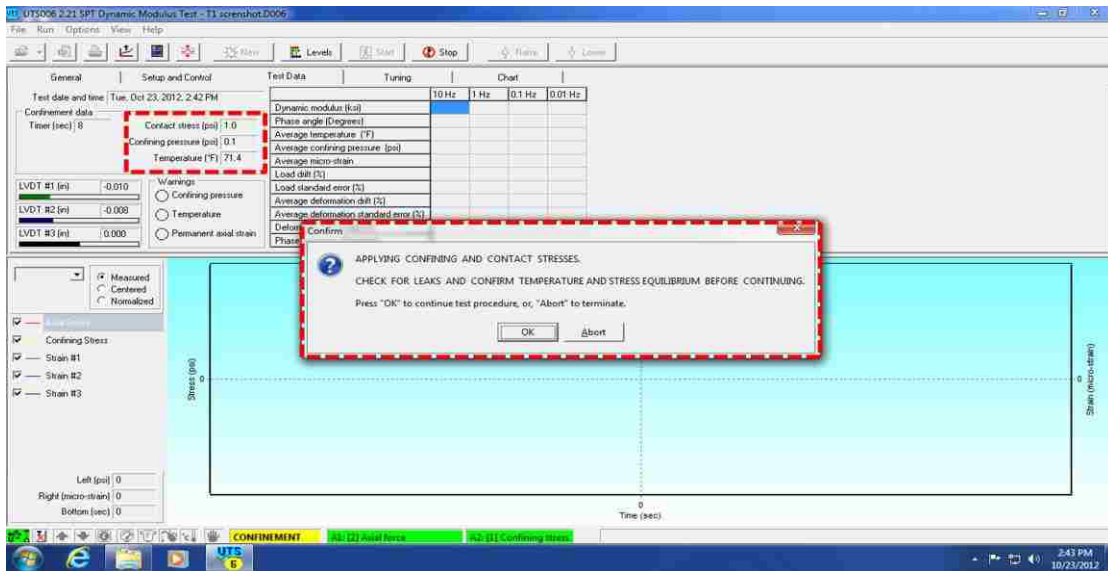


Figure 19 - Test Begin Warning – DO NOT IMMEDIATELY CLICK OK

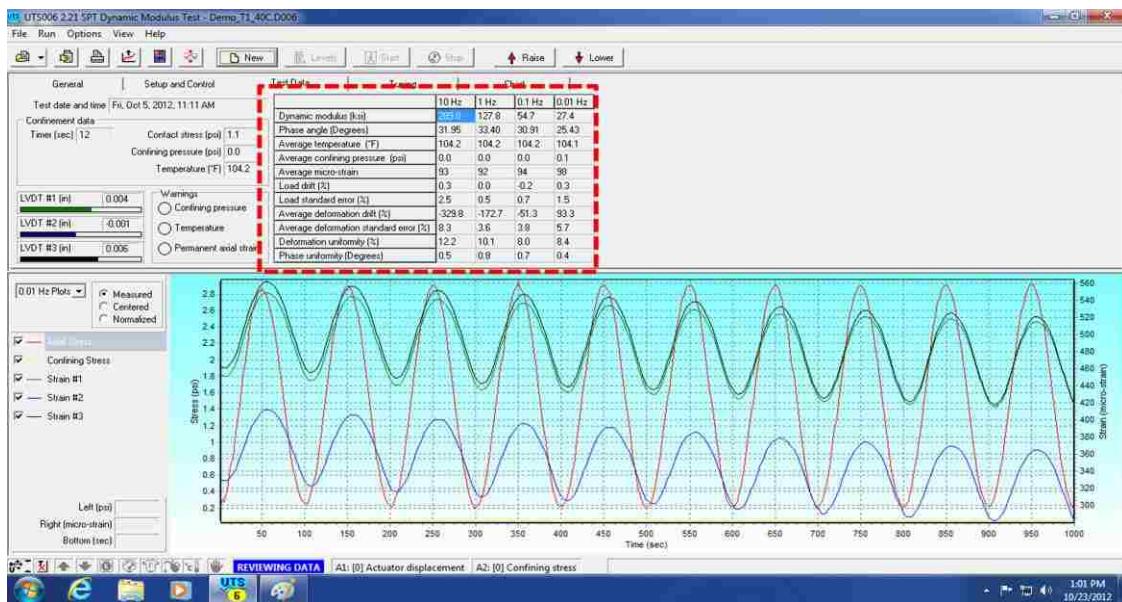


Figure 20 – Test Progress

- After test has completed, a box on the lower tool bar will show “Test Completed” in a green box. By clicking on the “Chart” tab, adjustments can be made to the output chart from the completed test (Figure 21).

8. Adjustments to data imputed under the “Tuning” tab are not required or needed. The default values are used for all dynamic modulus test templates (Figure 22)

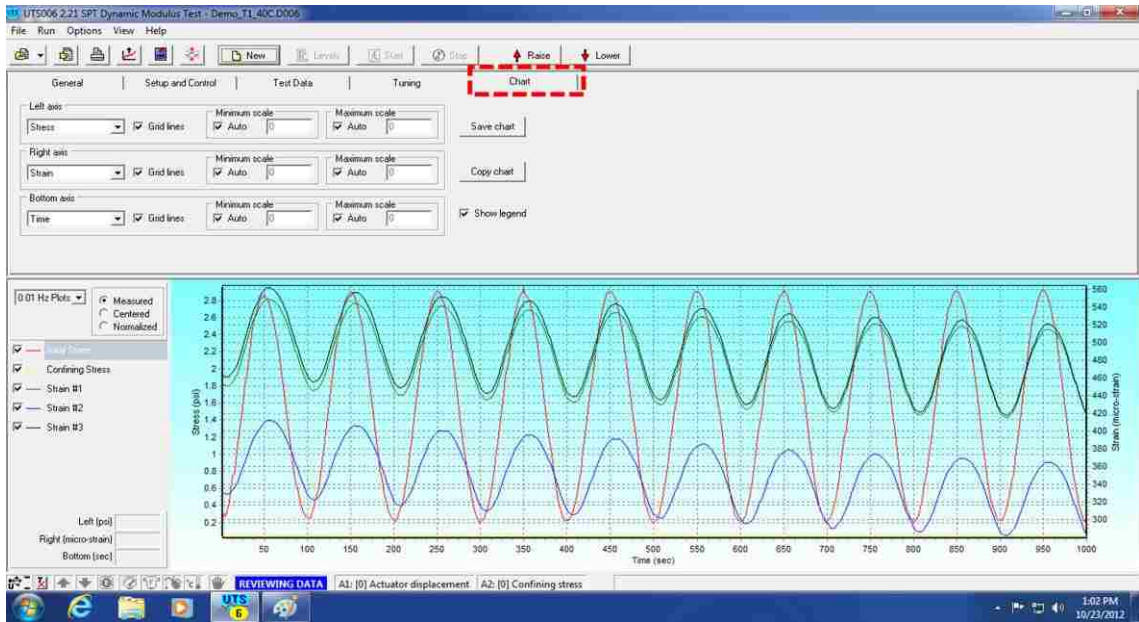


Figure 21 – Chart Tab

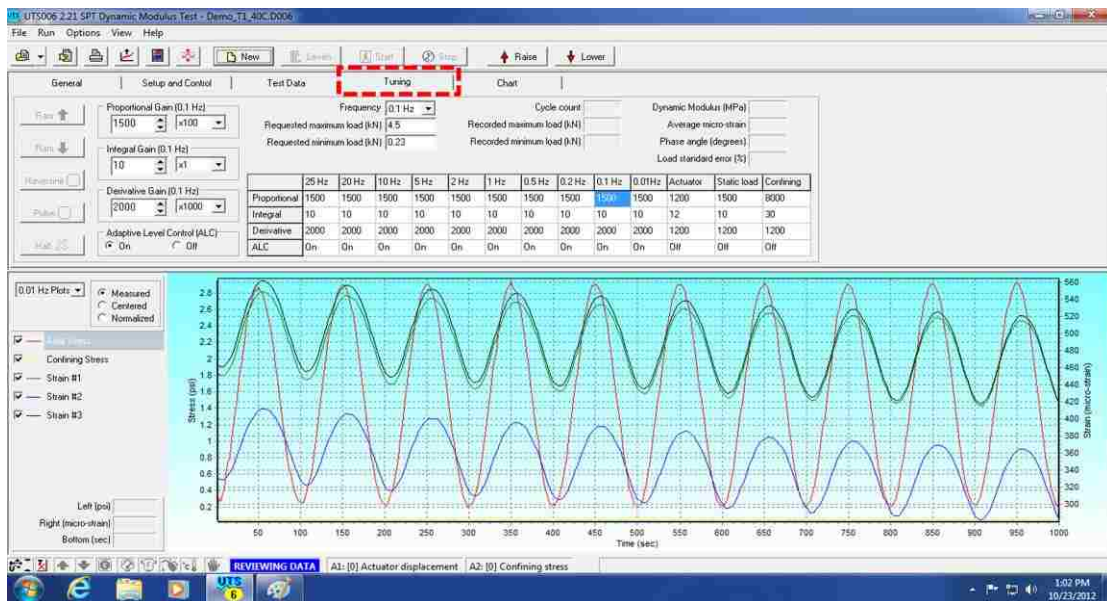


Figure 22 – Tuning Tab

9. In the example results plot above, the stress is held constant throughout the test while strain gradually decreases. This is expected because the rebound of the test specimen decreases as each additional loading is applied.

## Verification Procedure

It is recommended by InstronTek that the AMPT be verified weekly. The steps below outline the verification procedure:

1. Locate AMPT Dynamic Verification Device or “Proving Ring” (Figure 1)



Figure 1 – Dynamic Verification Device with Gauge Point Clips Attached

2. Attach gauge point clips to gauge points on Proving Ring (Figure 1)
3. Load the Proving Ring into in the test chamber and attach all three LVDTs to their respective colors. Make sure the steel ball is placed on top of the device (Figure 2)



Figure 2 – LVDTs Attached to Chamber Base

4. Lower test chamber shell until fully closed. Hold both lowering safety buttons to lower test chamber shell
5. Open verification template and check LVDT readings. The LVDT reading bars should approximately be within the first 1/3 and 2/3 third of the total measuring range (Figure 3)

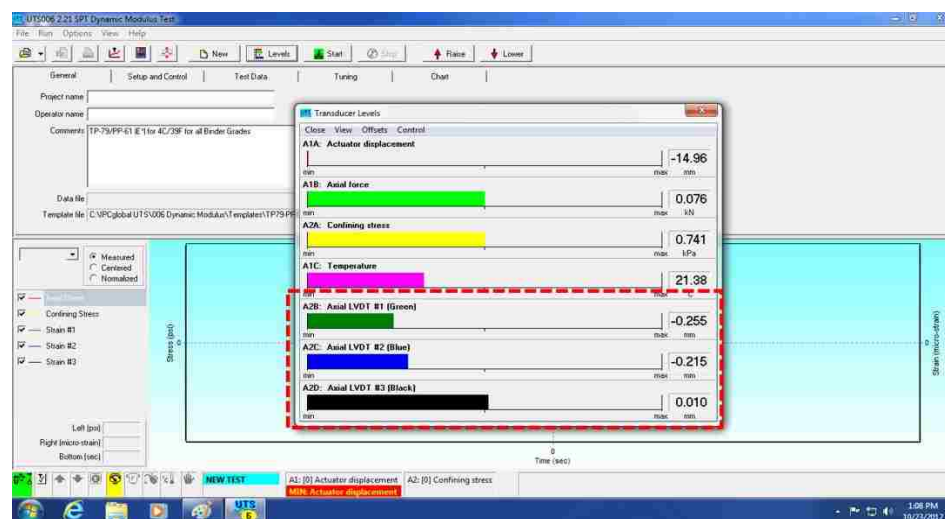


### Figure 3 – LVDT Reading Levels

6. Click “New” on the main upper tool bar and then click “Start”
7. The verification test will now run. Analyze results for any anomalies or false readings from the LVDTs

**Determining the Flow Number for Hot Mix Asphalt (HMA)  
Using the Asphalt Mixture Performance Tester (AMPT)  
AASHTO TP 79-11**

The Asphalt Mixture Performance Tester (AMPT) can be used to determine the dynamic modulus of a particular asphalt mixture as well as the flow number. The following steps outline procedures to obtain the Flow Number.

**Specimen Preparation**

1. The specimen shall be cored and sawed in accordance with the coring and sawing procedure previously outlined
2. The specimen shall be then prepared for the flow number test. A separate cored and sawed specimen can be used for this test, or the dynamic modulus test specimen. If using the dynamic modulus test specimen, remove all gauge points and recondition the test specimen to the appropriate test temperature for the flow test by using an environmental chamber
3. The flow number test is a confined pressure test. Therefore the specimen must be sealed from the confining pressure by using a latex membrane.
4. To install the membrane on the specimen, first stretch the membrane over the vacuum collar. Use the vacuum connection on the Gauge Point Fixing Jig to apply vacuum to the collar and suck the membrane against the sides of the collar. The end friction modifiers should be placed between the specimen and the bottom/top platens. Either a greased double latex modifier or latex modifier can be used. Slide the collar over the specimen while the specimen has the both the top and bottom plate in place (Figure 1)
5. Once in place, release the vacuum and slide the ends of the membrane off the collar and over both the top and bottom plate. Fold the excess membrane so that it rests on the top and bottom plate without resting on the sides of the specimen and not over the outside edge of the plates (Figures 2 and 3)



Figure 1 – Membrane Over Collar with Vacuum Applied



Figure 2 – Collar/Membrane Over Specimen with Vacuum Released





Figure 3 – Excess Membrane Folded Over Plates

6. Place the wrapped specimen gently into the test chamber and lower the outer chamber shell by clicking on the “Lower” button on the main tool bar and pressing both external green buttons on the front of the machine (Figure 4)



Figure 4 – External Lowering Safety Buttons

7. Allow the test specimen and chamber temperature to stabilize before beginning the test
8. Open the “Virtual Pendant” menu before beginning test. Click the “Low” button on the “Hydraulic Power Supply” row first, then click on the “High” button; allow several seconds to pass before switching from “Low” to “High”
9. Next click on the “Low” button on the “Hydraulic Service Manifold” row and allow the hydraulic oil to heat up for a minimum of 10 minutes before clicking on the “High” button (Figure 5 and 6).

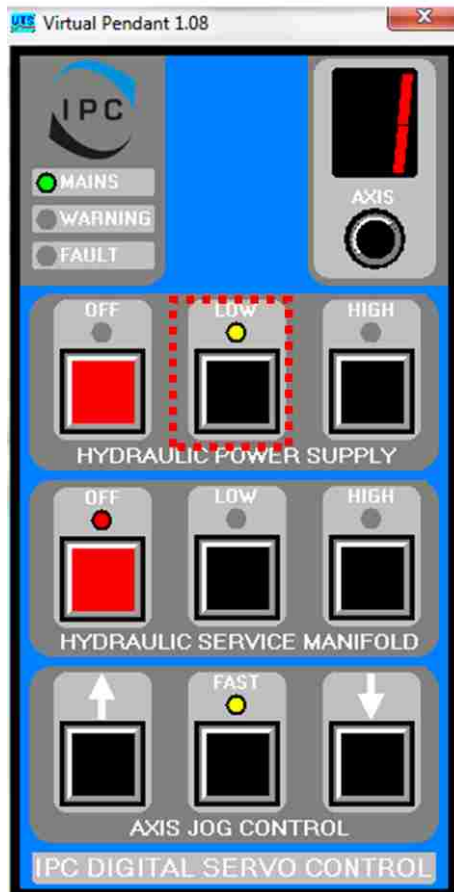


Figure 5 – Low Enabled

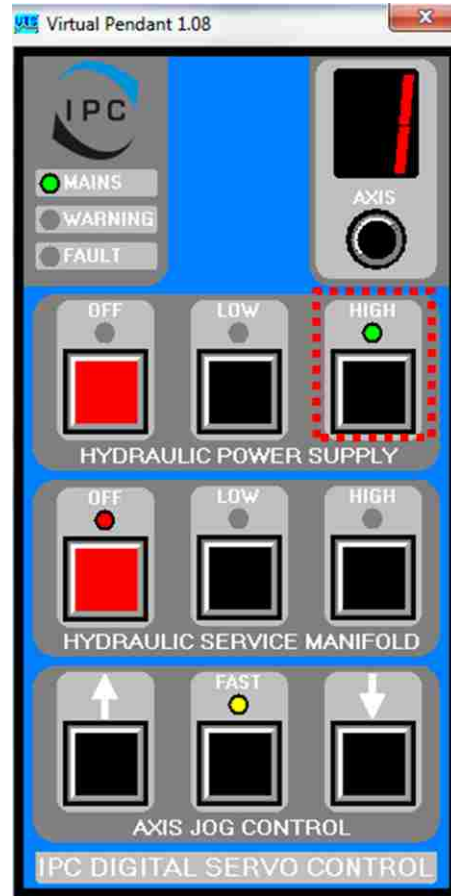


Figure 6 – High Enabled

10. When powering down both systems, proceed in this exact order. “Hydraulic Service Manifold” “High” to “Low” to “Off”, allowing several seconds in between each step. Then for the “Hydraulic Power Supply”, start with “High” to “Low” to “Off”, also allowing several seconds in between each step. This prevents any damage from occurring to either system.

### Procedure

1. Double Click on the Flow Number program icon (Figure 7)
2. When the program opens, the screen in Figure 8 will appear

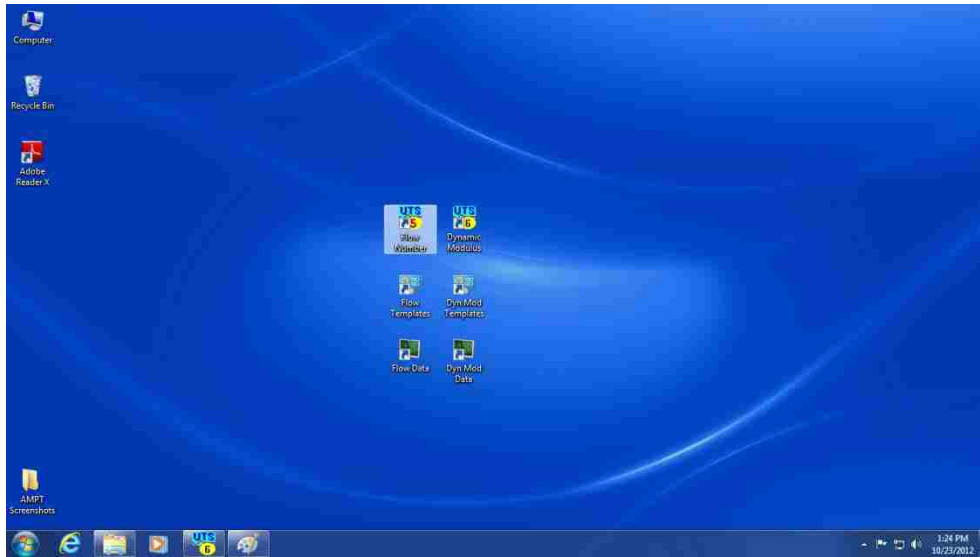


Figure 7 – Flow Number Icon

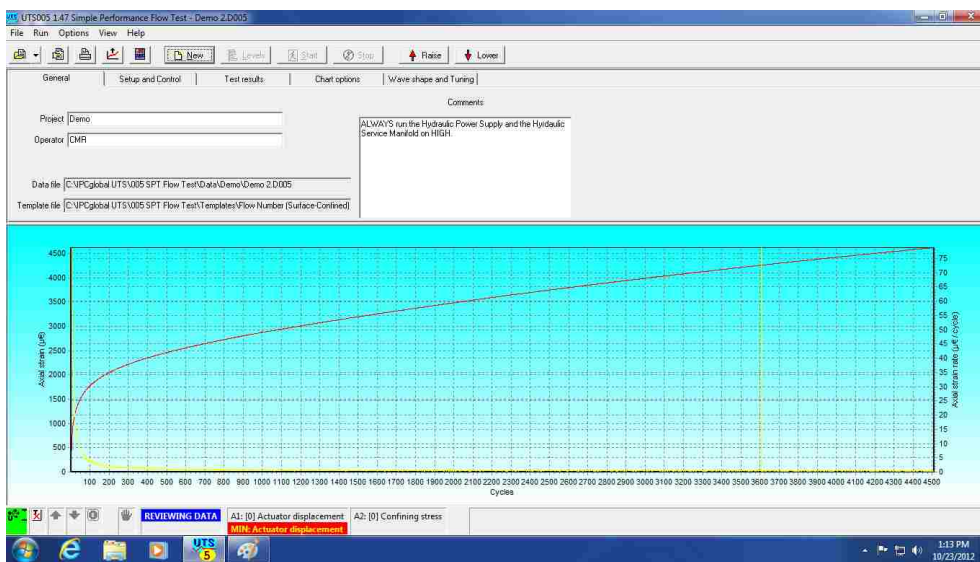


Figure 8 – Main Program Screen

3. First select a new template by clicking the “File” tab at the upper left corner of the window (Figure 9), scrolling down to the “Template” tab and choosing the “Open Template” button. After clicking on the “Open Template” button, a window will open with pre-made templates for running dynamic modulus tests at various temperatures (Figure 10). Choose appropriate temp for test desired

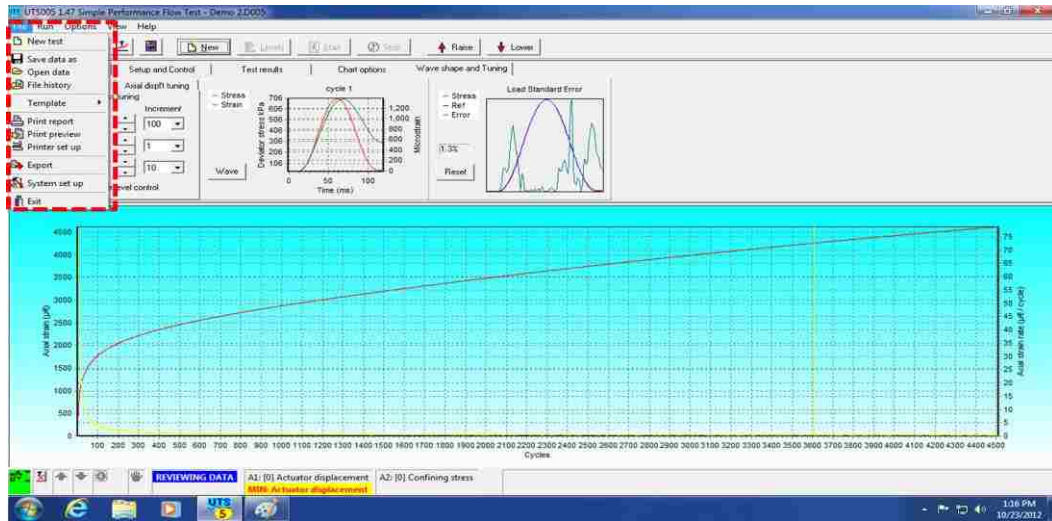


Figure 9 – File Tab

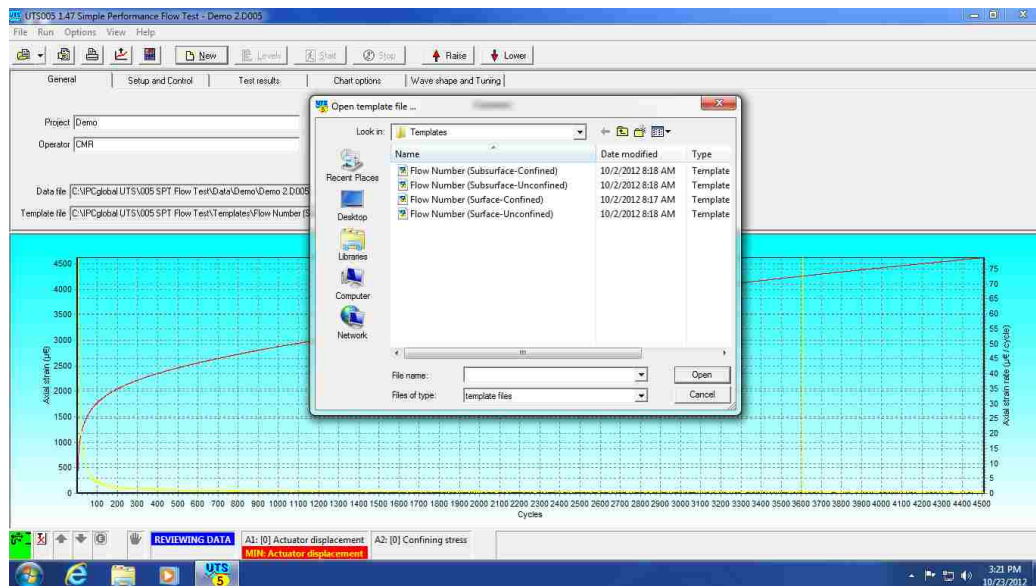


Figure 10 – New Template Window

4. Once the temperature template has been chosen, click on the “New” Tab on the main tool bar on the top of the program window. This will allow the user to enter information in the following tabs. Starting with the “General” tab (Figure 11), the user will enter the project name, operator name, and comments regarding the particular mix being tested at all three dynamic modulus temperatures. Next, under the “Setup and Control” tab (Figure 12), the user will enter the

identification, conditioning time, and any properties/remarks directly specific to the individual specimen being tested.

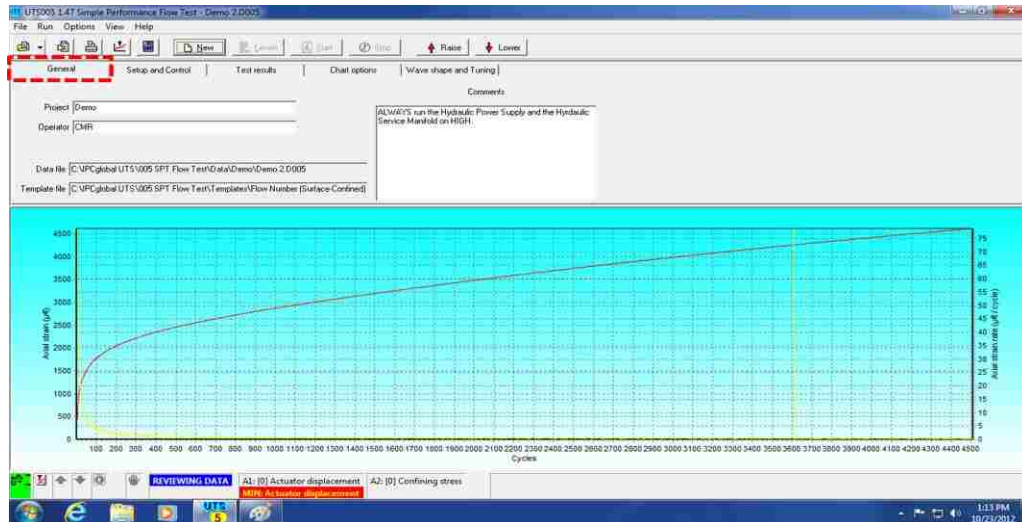


Figure 11 – General Tab

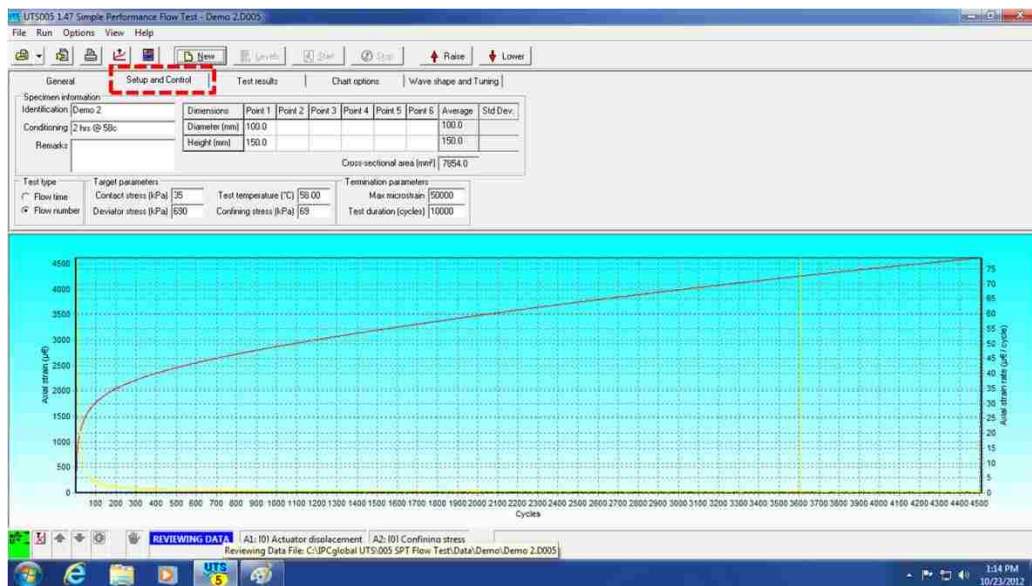


Figure 12 – Setup and Control Tab

5. Now click on the “Test Results” tab (Figure 13). Under this tab the initial test start up and test progress can be monitored. To begin the test, click on the “Start” button on the main tool bar. A window will pop up asking for the file to be saved. Save the file in the folder where all current and future test data will be saved for

ease of access later. After saving the file, another window will pop up showing that the machine is applying confining and/or contact stress to the test specimen (Figure 14). DO NOT IMMEDIATELY CLICK OK. Allow the contact stress applied to level out and become stable. Observe the contact stress box on the screen. Once the stress becomes stable, click “OK”. The dynamic modulus test will now begin.

- Under the “Test Results” tab, the progress of the test can be followed by watching the box in Figure 15

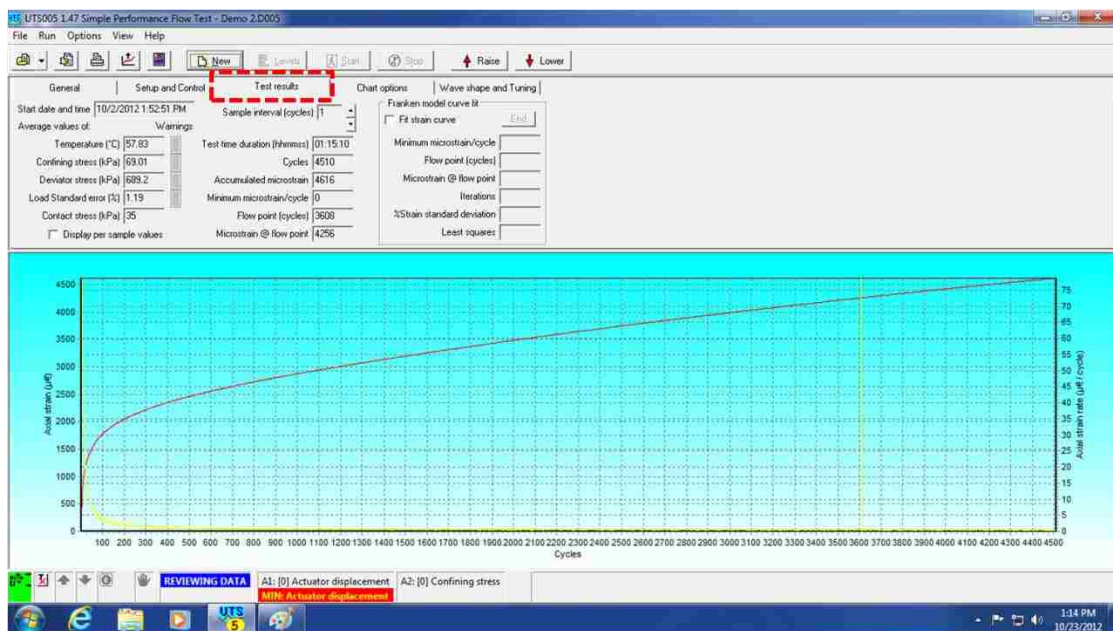


Figure 13 – Test Results Tab

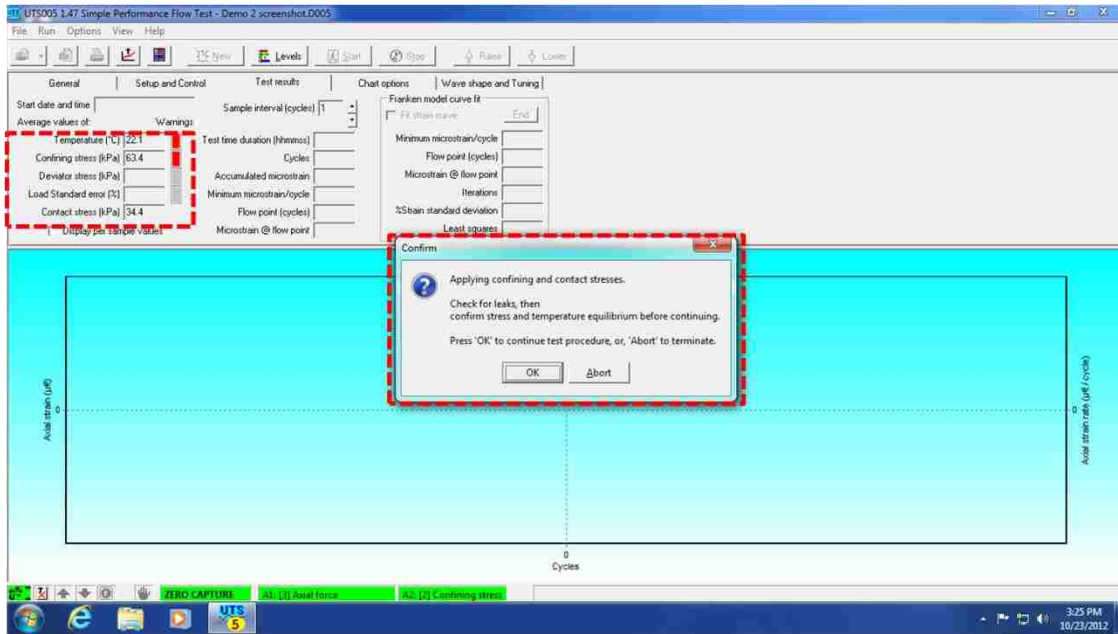


Figure 14 - Test Begin Warning – DO NOT IMMEDIATELY CLICK OK

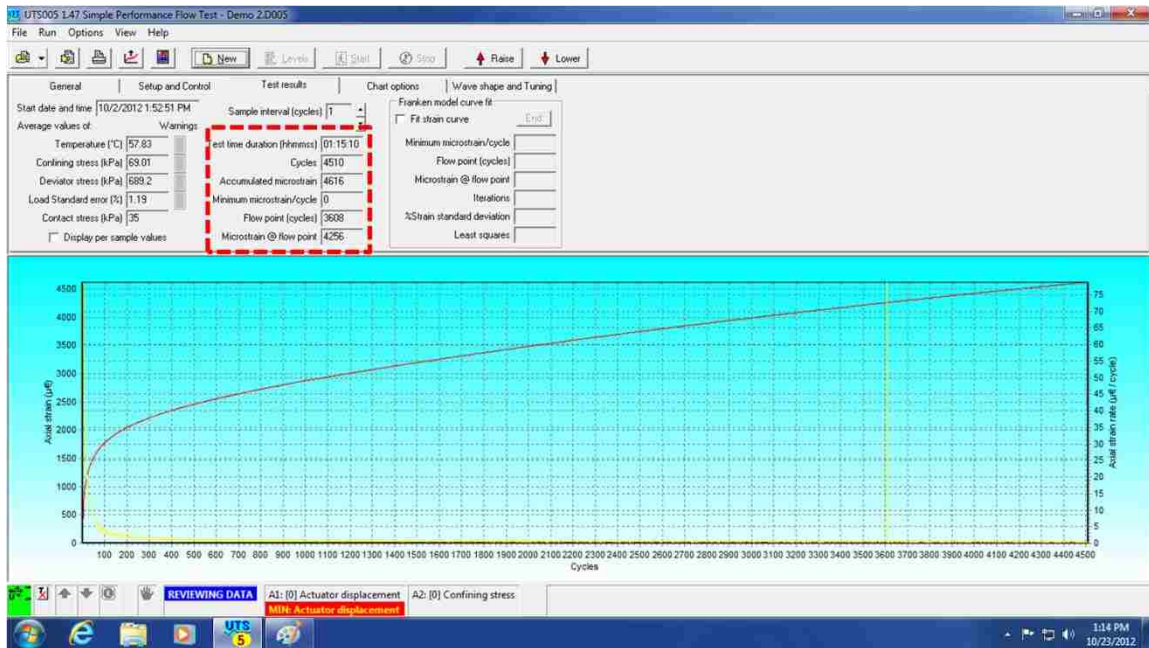


Figure 15 – Test Progress



7. After test has completed, a box on the lower tool bar will show “Test Completed” in a green box. By clicking on the “Chart Options” tab, adjustments can be made to the output chart from the completed test (Figure 16).
8. Adjustments to data imputed under the “Waveshape and Tuning” tab are not required or needed. The default values are used for all dynamic modulus test templates (Figure 17)

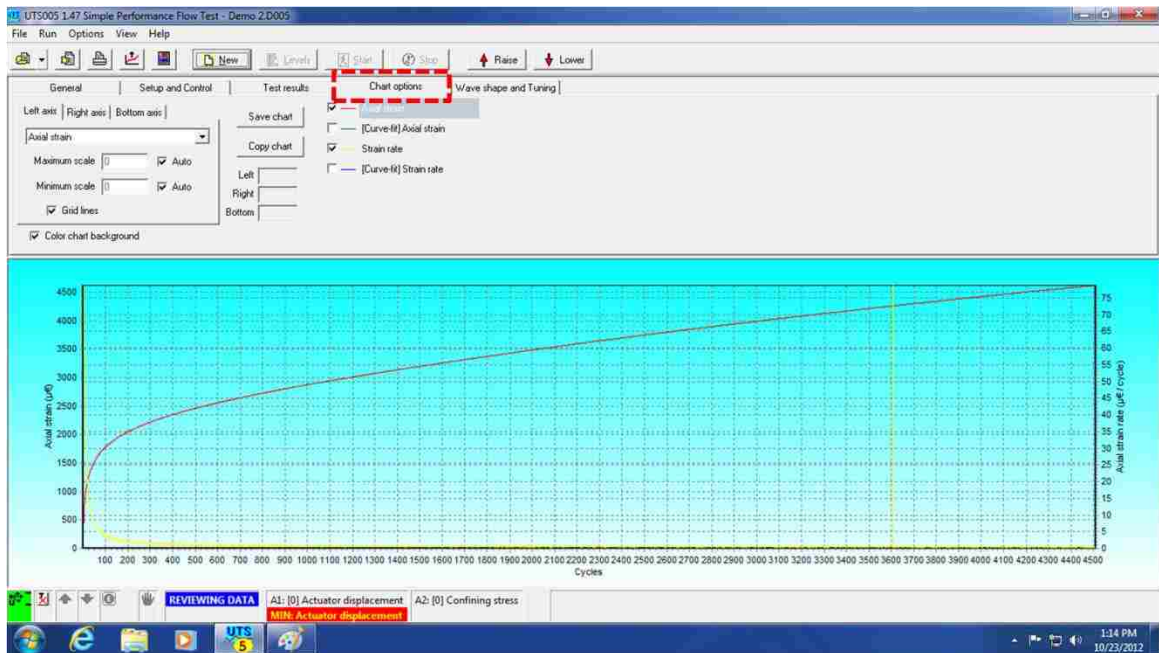


Figure 16 – Chart Options Tab

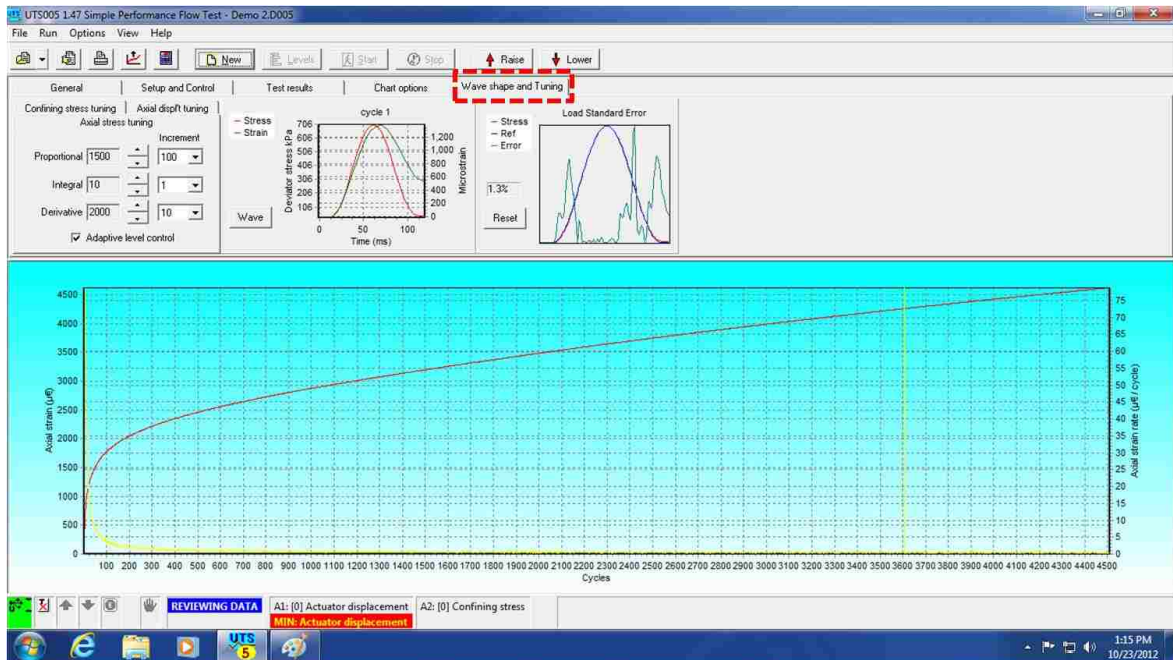


Figure 17 – Waveshape and Tuning Tab

## Verification Procedure

It is recommended by InstronTek that the AMPT is verified weekly. The steps below outline the verification procedure:

1. Locate AMPT Dynamic Verification Device or “Proving Ring” (Figure 1)



Figure 1 – Dynamic Verification Device with Gauge Point Clips Attached

2. Attach gauge point clips to gauge points on Proving Ring (Figure 1)
3. Load the Proving Ring into in the test chamber and attach all three LVDTs to their respective colors. Make sure the steel ball is placed on top of the device (Figure 2)



Figure 2 – LVDTs Attached to Chamber Base

4. Lower test chamber shell until fully closed. Hold both lowering safety buttons to lower test chamber shell
5. Open verification template and check LVDT readings. The LVDT reading bars should approximately be within the first 1/3 and 2/3 third of the total measuring range (Figure 3)

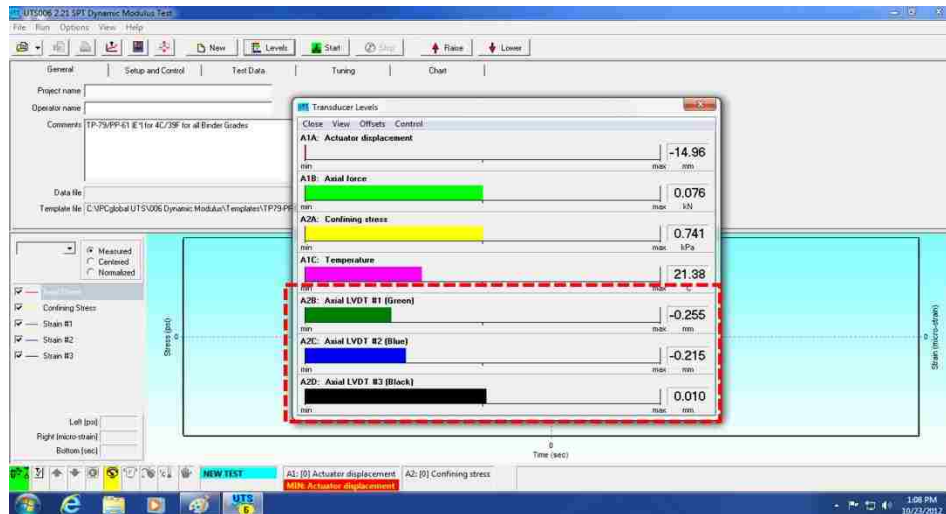


Figure 3 – LVDT Reading Levels

6. Click “New” on the main upper tool bar and then click “Start”
7. The verification test will now run. Analyze results for any anomalies or false readings from the LVDTs

## BIBLIOGRAPHY

- Azari, Haleh, Alaeddin Mohseni, and Nelson Gibson. "Verification of Rutting Predictions from Mechanistic-Empirical Pavement Design Guide by Use of Accelerated Loading Facility Data," *Transportation Research Record: Journal of the Transportation Research Board* (2008): 157-67. Print.
- Bari, Javed, and Matthew W. Witczak. "Development of a New Revised Version of the Witczak E\* Predictive Model for Hot Mix Asphalt Mixtures." *Journal of the Association of Asphalt Paving Technologists* 75 (2006): 381-423. Print.
- Brown, E. R., Prithvi S. Kandhal, Freddy L. Roberts, Y. Richard. Kim, Dah-Yinn Lee, and Thomas William Kennedy. *Hot Mix Asphalt Materials, Mixture Design, and Construction*. 3<sup>rd</sup> ed. Lanham, MD: NAPA Research and Education Foundation, 2009. Print.
- Chehab, Ghassan R., and Jo Sias Daniel. "Evaluating RAP Mixtures Using the Mechanistic Empirical Pavement Design Guide Level 3 Analysis," *Journal of the Transportation Research Board* (2006): 3-23 Print.
- Choubane, Bouzid, Gale C. Page, and James A. Musselman. *Investigation of the Suitability of the Asphalt Pavement Analyzer for Predicting Pavement Rutting*. FL/DOT/SMO/98-427. Gainesville: Florida Department of Transportation, State Materials Office, Oct. 1998. Web. 13 Oct. 2012.
- Cooper, Samuel B., III, Mostafa Elseifi, Louay N. Mohammed, and Marwa Hassan. "Performance and Cost-Effectiveness of Sustainable Technologies in Flexible Pavements Using the Mechanistic-Empirical Pavement Design Guide." *American Society of Civil Engineers* 24.2 (2012): 239-47. *American Society of Civil Engineers Library*. Web. 8 Apr. 2013.
- Diefenderfer, Stacey D., Ph.D. *Analysis of the Mechanistic-Empirical Pavement Design Guide Performance Predictions: Influence of Asphalt Material Input Properties*. FHWA/VTRC 11-R3. Virginia Transportation Research Council, Aug. 2011. Web. 17 Oct. 2012.
- Goh, Shu Wei, and Zhanping You. "Preliminary Study of Evaluating Asphalt Pavement Rutting Performance Using the Mechanistic-Empirical Pavement Design Guide," *Cold Regions Engineering 2009*. Proc. of 14th Conference on Cold Regions Engineering, Minnesota, Duluth. American Society of Civil Engineers, Aug. 2009. Web. 17 Oct. 2012.

- Grebenschikov, Sergey, and Jorge A. Prozzi, PhD. "Enhancing Mechanistic-Empirical Pavement Design Guide Rutting-Performance Predictions with Hamburg Wheel-Tracking Results," *Transportation Research Record: Journal of the Transportation Research Board* 2226 (2011): 111-18. Transportation Research Board of the National Academies, 14 Oct. 2011. Web. 16 Oct. 2012.
- Hall, Kevin D., and Stacy G. Williams. *Aquisition and Evaluation of Hamburg Wheel-Tracking Device*. Publication no. MBTC FR-1044: University of Arkansas, Mack-Blackwell National Rural Transportation Study Center, (1999): 1-15. NTIS No. 9917. Print.
- Hamburg Wheel Tracking Device - Bituminous Mixtures Laboratory (BML). *U.S. Department of Transportation - Federal Highway Administration - Pavements*. U.S. Department of Transportation - Federal Highway Administration, 7 Apr. 2011. Web. 08 Feb. 2013. <<http://www.fhwa.dot.gov/pavement/asphalt/labs/mixtures/hamburg.cfm>>.
- Hunter, Elizabeth R., and Khaled Ksaibati. *Evaluating Moisture Susceptibility of Asphalt Mixes*. MPC02-138. Washington D.C: Research and Innovative Technology Administration, 2002. *National Transportation Library*. Web. 13 Oct. 2012. <<http://ntl.bts.gov/lib/13000/13100/13132/MPC02-138.pdf>>.
- Kandhal, Prithvi S., and Rajib B. Mallick. "Potential of Asphalt Pavement Analyzer (APA) to Predict Rutting of Hot Mix Asphalt," *International Conference on Accelerated Pavement Testing*. Proc. of International Conference on Accelerated Pavement Testing, Nevada, Reno. Auburn: National Center for Asphalt Technology, (1999): 2-23. *Minnesota Department of Transportation - Research Services*. Web. 16 Oct. 2012. <<http://www.mrr.dot.state.mn.us/research/apt/DATA/CS06-02.PDF>>.
- Mallela, Jagannath, Leslie Titus-Glover, Harold Von Quintus, P.E., Michael I. Darter, Ph.D, P.E., Mark Stanley, and Chetana Rao, Ph.D. *Implementing the AASHTO Mechanistic-Empirical Pavement Design Guide in Missouri - Volume II: MEPDG Model Validation and Calibration*. Publication no. CM08.01: Applied Research Associates, 2009. Print.
- Putnam, Bradley J., and Serji N. Amirkhanian. *Laboratory Evaluation of Anti-Strip Additives in Hot Mix Asphalt*. FHWA-SC-06-07. Columbia: South Carolina Department of Transportation, 2006. Print.
- Rand, Dale A., P.E. *Technical Advisory - Hamburg Wheel Test*. Publication. Texas Department of Transportation - The Construction and Bridge Division (2006): 1-3 Print.
- Richardson, D.N. *Relative Durability of Shale*. PhD Dissertation, University of Missouri-Rolla, Rolla, Missouri (1984).

- Richardson, D.N. (2009), "Quick Test for Percent Deleterious Material," *Contract No. RI07-052, MoDOT*, Missouri University of Science and Technology, Rolla, Missouri, 166 p.
- Richardson, D.N. (2009), "Quick Test for Durability Factor Estimation," *Contract No. RI07-042, MoDOT*, Missouri University of Science and Technology, Rolla, Missouri, 113 p.
- Schwartz, Charles W., and Regis L. Carvalho. *Implementation of the NCHRP 1-37A Design Guide*. SP0077B41. Vol. 2. College Park: University of Maryland - Department of Civil and Environmental Engineering, 2007. 18-34, 100-103. Web.
- Shu Wei Goh, and Zhanping You. "Properties of Asphalt Mixtures with RAP in the Mechanistic-Empirical Pavement Design of Flexible Pavements: A Preliminary Investigation," *Efficient Pavements Supporting Transportation's Future*. Proc. of Airfield and Highway Pavements, California, Santa Barbara. American Society of Civil Engineers, 2009. 171-81. Web. 1 Jan. 2009
- Tarefder, Rafiqul A., and Musharraf Zaman. *Evaluation of Rutting Potential of Hot Mix Asphalt Using the Asphalt Pavement Analyzer*. ORA 125-6660. Norman: School of Civil Engineering and Environmental Science - The University of Oklahoma, 2002. *Oklahoma Department of Transportation - Planning and Research Division*. Oct. 2002. Web. 16 Oct. 2012.
- Tarefder, Rafiqul A., and Nasrin Sumea. "Evaluating Sensitivity of Pavement Performance to Mix Design Variable in MEPDG." *Road Materials and New Innovations in Pavement Engineering*. Proc. of GeoHunan International Conference 2011, China, Hunan. American Society of Civil Engineers, July 2011. 49-56. Web. 17 Oct. 2012.
- Tashman, Laith, and Muthukumar Elangovan. "Dynamic Modulus of HMA and Its Relationship to Actual and Predicted Field Performance Using MEPDG." *Journal of Performance of Constructed Facilities* (2012): 1-22. *ASCE Library*. Web. 16 Oct. 2012.
- Transportation Research Board, comp. "Test Methods to Predict Moisture Sensitivity of Hot-Mix Asphalt Pavements," *Characteristics of Bituminous-Aggregate Combinations to Meet Surface Requirements*. Proc. of Moisture Sensitivity of Asphalt Pavements - A National Seminar, California, San Diego. Washington D.C: Transportation Research Board. (2003): 3-20 . *Transportation Research Board - Online Publications*. Web. 13 Oct. 2012. <[http://onlinepubs.trb.org/onlinepubs/conf/reports/moisture\\_seminar.pdf](http://onlinepubs.trb.org/onlinepubs/conf/reports/moisture_seminar.pdf)>.

Velasquez, Raul, Kyle Hoegh, Iliya Yut, Nova Funk, George Cochran, Mihai Marasteanu, and Lev Khazanovich. *Implementation of the MEPDG for New and Rehabilitated Pavement Structures for Design of Concrete and Asphalt Pavements in Minnesota*. Tech. no. MN/RC 2009-06. St. Paul: Minnesota Department of Transportation Research Services Section, (2009): 33-60 Print.

Yildirim, Yetkin, and Kenneth H. Stokoe, II. *Analysis of Hamburg Wheel Tracking Device Results in Relation to Field Performance*. FHWA/TX-06/0-4185-5. Vol. 1. Austin: Center for Transportation Research - The University of Texas at Austin, (2006): 51-60 Print.



## VITA

Clayton Matthew Reichle was born in Florissant, Missouri to Paul and Cheryl Reichle. He has one sister, Christy Lucke. Clay was raised in Troy, Missouri and attended Troy Buchanan High School, where he graduated in 2006. Clay attended the Missouri University of Science and Technology, graduating in the 2010 with a Bachelors of Science in Civil Engineering. In August of 2013, he earned his Masters of Science in Civil Engineering from the Missouri University of Science and Technology.

While attending the Missouri University of Science and Technology, Clay was a member of the Missouri S&T Concrete Canoe Team and the Missouri S&T ACI Chapter. He worked as a graduate teaching assistant for an introductory construction materials course for two semesters, as well as working as a research assistant during his graduate studies.